2019

TOWARD AN UNDERSTANDING OF THE CLINICAL RELEVANCE OF NITRIC OXIDE (NO) MEASUREMENTS IN IN VITRO CELL CULTURE STUDIES

Maria Paula Kwesiga

TOWARD AN UNDERSTANDING OF THE CLINICAL RELEVANCE OF NITRIC OXIDE (NO) MEASUREMENTS IN IN VITRO CELL CULTURE STUDIES

By

Maria Paula Kwesiga

A DISSERTATION

Submitted in partial fulfillment of the requirements for the degree of

DOCTOR OF PHILOSOPHY

In Biomedical Engineering

MICHIGAN TECHNOLOGICAL UNIVERSITY

2019

This dissertation has been approved in partial fulfillment of the requirements for the Degree of DOCTOR OF PHILOSOPHY in Biomedical Engineering.

Department of Biomedical Engineering

Dissertation Advisor:	*Dr. Megan C. Frost*
Committee Member:	*Dr. Feng Zhao*
Committee Member:	*Dr. Jeremy Goldman*
Committee Member:	*Dr. Caryn Heldt*
Department Chair:	*Dr. Sean J. Kirkpatrick*

Dedication

I dedicate my dissertation to my family (Valerian Kwesigaho (May He's Soul Rest in Eternal Peace), Specioza Kwesigaho, Rodney Atuhaire, Patrick Kwesigaho, Frank Kwesigabo, Anita Asiimwe, Father William Ssozi) who have always supported me through the four years of preparing my PhD project, have encouraged me do my very best and always believe that anything is possible.

This dissertation is also dedicated to Madame Kanoun Akila (May Her Soul Rest in Eternal Peace) who inspired me to pursue a PhD in Biomedical Engineering.

I dedicate my work to my professors and advisor who took the time to teach and mentor me in the different projects that I worked on.

Finally, I dedicate my dissertation to all my friends from Uganda, Algeria and the United States who have constantly been there for me.

In closing, I thank God for all the Blessings that He has bestowed upon me and I pray that God will pour His abundant Blessings on everyone who has made the work presented in my dissertation possible.

Table of Contents

List of figures

List of tables

Preface

The research presented in this dissertation was done under the advisement and supervision of Dr. Megan C. Frost in the department of Biomedical Engineering, Michigan Technological University from May 2015 to October 2019.

The work described in chapter 2 was performed in collaboration from Emily Cook who helped with manuscript writing and western blot analysis, Jennifer Hannon and Sarah Wayward who assisted with the real-time NO measurements and cell proliferation assays, Dr. Smitha Rao, Dr. Caroline Gwaltney and Dr. Megan C. Frost who guided the project.

The biopsy sample and wound swabs used in chapter 3 were obtained by Dr. Wade Liston and Dr. Caroline Gwaltney. Sarah Wayward helped to make the CellNO trap devices and run some of the real-time NO experiments presented in this chapter. Eyerusalem Gebreyesus and Emily Cook assisted with the nitrite measurements.

Experiments in Chapter 4 were performed with help from Sarah Wayward who performed cell imaging and the cell count for normalizing the data.

The preliminary results on the applications of real-time NO measurements in cardiovascular calcification in chapter 5 was done with help from Dr. Jeremy Goldman who provided the aorta for cell isolation, Dr. Weilue He who assisted with the cell isolation procedure and Dr. Roger Guillory who assisted with cell imaging.

The preliminary results on the localized NO delivery systems for cell cultures presented in Chapter 5 was assisted by Murphy Mallow, Sarah Wayward and Eyerusalem Gebreyesus who prepared the devices, performed cell imaging and fabricated the polymer gradient targets respectively.

The work herein has not been submitted for a degree or diploma at Michigan Technological University or any other university/institution.

Chapter 2 was submitted for publication in *Medical Sciences* and part of the work presented in Chapter 3 and Chapter 4 is to be submitted for possible publication in the future.

Maria Paula Kwesiga

October 2019

Abstract

Diabetic foot ulcers (DFU) are one of the most challenging complications associated with diabetes mellitus (DM). Every 1 in 4 patients with DM are expected to develop an ulcer in their life time. The time course of healing is on average 90 to 120 days which increases the risks of infection, amputations and death. Nitric oxide (NO) is a signaling molecule produced in the body that has been established in the literature to serve many roles in the body, including as a vasodilator, neurotransmitter immune modulator and antimicrobial agent. Emerging evidence has shown that NO is indispensable in every stage of wound healing and its dysregulation is a major hinderance in the healing of DFU. The problem associated with harnessing the biological effects of NO is that it is very reactive and consequently it is extremely difficult to measure. As a result, majority of the studies in the literature measure its metabolic products (nitrate and nitrite) to correlate NO function. The challenge with relying on NO metabolites is that they can only be analyzed at static time points as an accumulation measure and they do not give any information about the dynamic NO changes taking place in the wound environment. Moreover, the NO dose produced by specific cells during the course of cell migration and proliferation varies depending on the stage of wound healing. The function of NO is very complex with its effects ranging from protective to deleterious depending on the dose and duration of the treatment and even the surrounding host environment. It is therefore of paramount importance to understand the real-time NO profile produced and exposed to the cells that are actively involved in the wound healing process and to analyze how the profile changes in physiological and pathological conditions. This dissertation presents the real-time NO levels produced from normal and chronic wound fibroblast cells cultured in normal and high glucose conditions when stimulated by inflammatory mediators that are commonly present in the wound environment. The results showed that the real-time NO levels produced by fibroblasts are higher in normal glucose compared to high glucose cell culture conditions (8.42±1.16 vs 3.26±0.79 nmols/10^5 cells). The real-time NO levels were significantly increased in normal glucose with stimulation compared to normal glucose without stimulation. High glucose conditions in the absence and presence of stimulation showed no statistical difference between the two groups. The NO levels produced by fibroblasts obtained from biopsy samples from patients treated at a chronic wound care clinic was suppressed. Overall there was no statistical difference within the experimental groups. The NO levels produced by the cells did not correlate with the nitrite and nitrate detected in the fluid obtained from the wound site (nanomolar vs micromolar concentration respectively). The results were compared with the well characterized macrophage cell line RAW 264.7 which also showed higher NO levels (161.80± 29.05 vs 46.30±12.9 nmols/10^6 cells) in normal glucose compared to high glucose conditions and no statistical difference in the nitrite levels in normal and high glucose conditions. The results clearly indicate the need for real-time NO monitoring to determine the level and duration of NO production by cells in the wound bed and that the use of nitrite and nitrate does not provide accurate information regarding NO dysregulation in chronic non-healing wounds. The work presented herein will facilitate the development of treatments that address not only the actual dose of NO treatment needed in the wound but also potentially indicate factors that may interfere with the NO function.

1 INTRODUCTION

Diabetes mellitus (DM) is by far the most prevalent and one of the most challenging non communicable disease[1] currently dealt in the world. In 2000, the estimated number of people living with DM worldwide was 151 million with costs of treatment greater than $44 billion in the United States alone [1]. The population affected was predicted to go up to 300 million in 2025[2]. However, as of 2017, the global prevalence of diabetes has already risen to 425 million with increased healthcare costs of US$ 727 billion. Currently, it is predicted to affect 629 million people by 2045[3]. DM encompasses a group of metabolic conditions that result in high glucose levels (> 7Mm) [4]. It exists in 4 main categories; DM type 1, DM type 2 , gestational DM and genetic defects in the beta cell function DM[5]. The most predominant being type 1 and type 2 DM. DM Type 1 is mainly an autoimmune disease of the younger population that causes destruction of pancreatic beta cells and reduced production of insulin that is necessary for glucose metabolism[6]. A common finding in patients is the presence of the histocompatibility antigen HLA-DR3/DR4. Other risk factors include; environmental exposures, gender differences, ethnicity, infections, seasonal variation and location[2]. DM Type 2 is characterized by the inability to maintain fuel hemostasis due to hyperglycemia and altered lipid metabolism. There is no destruction of the islet cells. However, there is inadequate insulin production and negative body responses resulting from over nutrition, obesity and inactivity[7]. In contrast, it mainly affects the older population although the risk factors remain similar to type 1 DM. More recently it has become more prevalent among the younger population especially in North America (10-14 years) [8]. In almost all DM patients, the high circulating blood glucose levels (hyperglycemia) causes a multi organ effect that can lead to complications on a micro (neuropathy, retinopathy and nephropathy) and macro vascular scale (coronary artery disease, stroke and peripheral vascular disease). The prevalence and mechanisms of each of these complications can be found elsewhere[9-13]. This dissertation focuses on peripheral vascular disease with emphasis on diabetic foot ulcers (DFU).

It is reported that every 1 in 4 people living with DM will develop a foot ulcer. In the US, 1 million cases of diabetic foot ulcer complications were recorded in various emergency departments from 2006-2010. The costs of treatment for both in care and out care patients in 2014 surpassed 10 billion dollars[14]. Unfortunately, the clinical outcomes of DFU are very grim. The main reason is the prolonged healing time which on average is about 90-120 days [15]. This increases the risk of infection resulting in sepsis, amputation and death [16]. (**Figure 1-1)**. Additionally, these non-healing wounds have a significant negative impact on a patient's lifestyle [17].

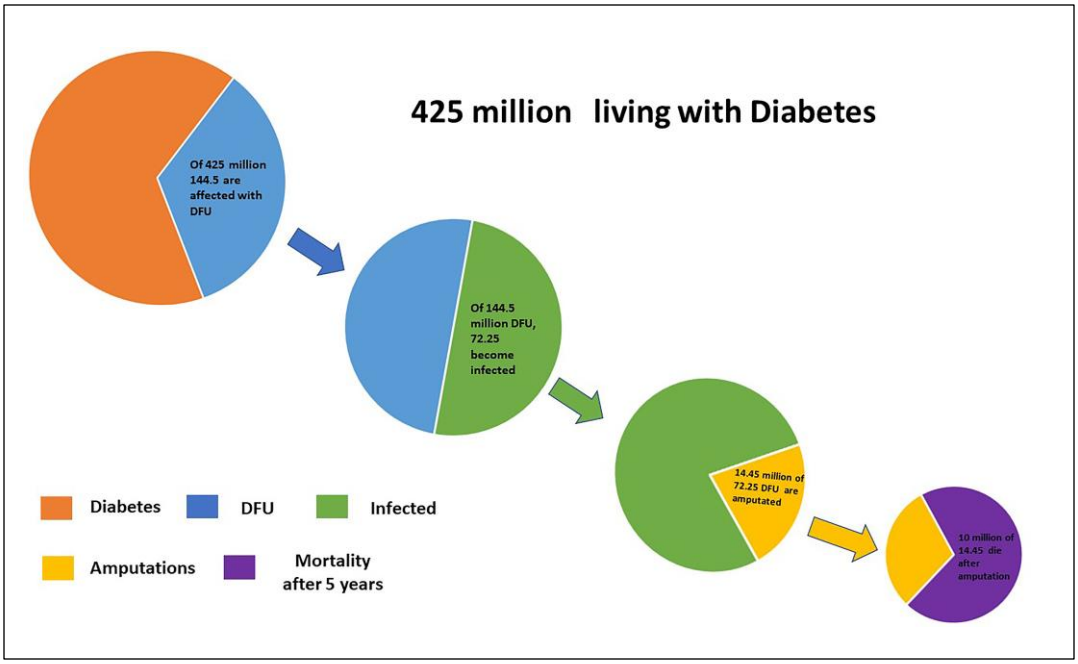

Figure 1-1 The prevalence and clinical outcomes of DFU

1.1 The physiological wound healing process and alterations in DFU

Wound healing proceeds in 4 complex and overlapping stages; hemostasis, inflammation, proliferation and remodeling [18-21](**Figure 1-2**). The duration can vary depending on the injury, age, genetic makeup and co morbidities of the individual[21]. However, in majority of cases, it is approximately 3 weeks[22].

During the first 24 hours following injury, platelets are released at the wound site, and in the presence of a number of extrinsic and intrinsic factors, a fibrin plug is formed preventing blood loss and infection. The fibrin plug provides a provisional matrix scaffold for the migration of immune cells[22]. The platelets also release growth factors such as platelet derived growth factor (PDGF), insulin like growth factor (IGF), epidermal growth factor (EGF) and transforming growth factor-Beta (TGF-ß) that are essential for recruiting inflammatory cells at the wound site[23].

The arrival of immune cells, marks the beginning of the acute inflammatory phase, which peaks at 24 hours and lasts 3-4 days[24]. The capillaries dilate and become more permeable through mediation by prostaglandins (PG) specifically; PGI_2, PGD2 and PGE_2. Vasodilation will slow down the blood flow in the post capillary venules allowing transmigration to take place. Circulating neutrophils align on the basement membrane, selectins P and E are upregulated on the endothelial cells that line the blood

vessels, which makes it possible for the neutrophils to slow down and cross the basement membrane into the affected tissue space. Other neutrophil chemotactic agents such as; leukotriene B_4 (LTB_4), complement component 5a (C5a), Tumor necrotic factor-alpha (TNF-α), TGF-ß, platelet factor 4 (PF4), interleukin1 (IL1), interleukine 8 (IL8), and bacterial products further facilitate neutrophil recruitment at the wound site[24, 25]. Neutrophils produce hypochlorous acid (HClO) through the myeloperoxidase pathway to sterilize the wound[26]. In addition, neutrophils cleanse the wound of necrotic debris by forming a phagolysosome. To modulate the acute immune response, platelets will adhere to neutrophils and through the 5-lipoxygenase pathway, the association will lead to the formation of lipoxins A_4 and B_4 that act as a checkpoint to stop the infiltration of neutrophils.[26, 27]Circulating blood monocytes will migrate to the wound and differentiate into macrophage cells. Macrophages co-ordinate host defense, immune response and direct the wound healing process by taking on two opposite polarized forms, both of which can be lethal if overly expressed; M1 (*kill* function) and M2 (*heal* function)[28, 29]. The granulocyte macrophage and macrophage colony stimulating factors (GM-CSF and M-CSF) are key players that initiate macrophage polarization into classically (M1) and alternatively (M2) activated macrophages respectively [29, 30]. In the next 2-3 days following hemostasis, the predominant phenotype is M1. The function of M1 is enhanced in the presence of inflammatory mediators' interferon-Y (IFN-Y), TNF-α and bacterial products lipopolysaccharide (LPS). M1 produce large amounts of superoxide and express the inducible nitric oxide synthase enzyme (iNOS), which generate nitric oxide (NO) from the conversion of the amino acid L-arginine into L- citrulline [31, 32].NO and superoxide are responsible for the antimicrobial properties of M1 and will be discussed later in this project. Other roles of M1 include clearing the wound bed of necrotic tissue and microbial products by phagocytosis[33].M1 also recruit Th1 cells which are involved in the adoptive immune response. TH1 are responsible for the destruction of intracellular parasites and produce high levels of the proinflammatory cytokine IFN-Y[34]. When the wound is sterile, macrophages switch to M2 that counteract the pro-inflammatory effects of M1 cells through activation of Th2 cells[33]. Th2 secrete the anti-inflammatory cytokines IL-4, 5, IL-10 and IL-13[34]. M2 are further activated by IL-4 produced by TH2 cells, eosinophils and basophils. Glucocorticoids secreted from the adrenal gland also activate M2 cells[33]. Interestingly, M2 also utilize the amino acid arginine to produce ornithine via the enzyme arginase-1. Ornithine promotes cell growth, collagen production and tissue repair[29, 30]. In a rat model, M2 macrophages appeared on day 7 of healing in healthy rats, and it also marked the beginning of the proliferation stage of wound healing[35]. Growth factors PDGF and EGF produced by both macrophages and platelets attract the migration and proliferation of fibroblast cells from the wound edge[25]. Fibroblast cells deposit extracellular matrix (ECM) that is indispensable for re-epithelialization and tissue remodeling to take place. The initial components of the matrix produced are collagen type 3, glycosaminoglycans (GAGs), specifically chondroitin sulphate, tenascin and fibronectin [36, 37]. Fibronectin promotes adhesion of the cells to the fibrin scaffold deposited by the platelets[37]. The hydration capacity of chondroitin sulphate increases the mechanical strength and serves as a temporary matrix during the first two weeks of healing[36]. Tenascin regulates

the cell shape and therefore function of the cell. In addition, tenascin plays a role in maintaining the tissue hemostasis [36, 38]. Ploeger et al[39] demonstrated that like macrophages, fibroblasts also exhibit an element of plasticity depending on the polarized form of macrophages. In this study, human dermal fibroblasts cultured in M1 conditioned media upregulated inflammatory cytokines in fibroblasts and increased their ability to degrade the ECM while fibroblasts cultured in M2 conditioned media had the inverse effect. This strongly suggests that in the early phases of wound healing, a more compliant matrix is necessary to allow the free movement of cells to their destinations as well as sprouting of vessels to ensure adequate nutrition for the growth, maintenance and function of the cells. Matrix metalloprotease enzymes (MMPS) secreted by macrophages, fibroblasts (collagenases, gelatinases, stromelysin) and plasmin present in the serum are responsible for the breakdown of the ECM[40]. In addition, MMPS modulate the inflammatory response through the degradation and activation of chemokines[41]. The activity of MMPS is in turn also regulated by tissue inhibitors of matrix metalloprotease enzymes (TIMPS) produced from fibroblasts that are stimulated by TGF-ß and IL-6. Studies also show that fibroblast cells produce low levels of NO [42-44]. However, the specific role of the NO produced still needs to be determined.

The proliferation and migration of fibroblasts initiates the granulation/remodeling stage. The former flexible matrix is gradually replaced by a stiffer and more permanent scaffold. This is the most important phase of the healing process because it determines the risk of recurrent injury depending on the matrix that is deposited. Several factors are involved and the concentration of each one needs to be precisely controlled to facilitate the formation of an appropriately organized and mechanically sound tissue. The benefit is to maintain isometric tension which prevents the shortening and lengthening of cells during the remodeling process. The switch from M1 to M2 macrophages promotes the production of ECM by fibroblasts. TGF-ß produced from M2 stimulates the production of collagen type 1 [25, 45]. The permanent matrix that is formed is composed mainly of type 1 (80-90%) which increases the wound breaking strength. Moreover, TGF-ß mediates the transformation of fibroblasts into myofibroblasts that are responsible for wound contracture[46]. Other formed elements of the ECM include elastin which adds resilience and elasticity to the wound. In addition, the cleavage of elastin by MMPS releases tropoelastin that helps in the attachment, spreading and proliferation of fibroblasts[47]. The granulation/remodeling stage can last about a year and the scar that is formed will only achieve 80% strength of the uninjured skin tissue under physiological wound healing conditions[25].

A key feature in wound healing is epithelialization. This is the process of covering a denuded epithelial surface and is critical to achieve wound closure [48] Epithelialization starts as early as day 4 during wound healing. The cytokines IL-1 and TNF-α stimulate fibroblasts to produce keratinocyte growth factors (KGF) 1, 2 and IL-6 which attract the keratinocyte cells at the wound edge[25]. Epithelialization is a layer by layer process that requires keratinocyte cells to detach from the basal layer, migrate and proliferate across the newly formed matrix of the wound bed to allow a sufficient

cell density to close off the wound[49] (**Figure 1-2**). The degradation of the ECM by MMPs releases and activates growth factors that promote proliferation of keratinocyte cells. These growth factors include: EGF, TGF-α, KGF and heparin-binding EGF-like growth factor[50]. The keratinocytes also promote angiogenesis by secreting vascular endothelial growth factor (VEGF) and IL4. When the migrating/proliferating keratinocytes from both ends of the wound meet, they cease to proliferate (contact inhibition)[51]. In addition, growth factors like TGF-ß synthesized by the fibroblast cells, stop the proliferation of keratinocytes by causing a switch from activated to basal keratinocyte phenotypes [49, 52]. Thereafter, cornification begins in the supra basal layer. Cornification is an elegant form of cell death. It proceeds with keratinocyte cells switching to a terminally differentiating phenotype accompanied by the synthesis of cornified envelope structural proteins and lipids that are covalently bonded by specific transglutaminases to form a spinous, granular and desquamous layer that acts as a barrier against the hostile external environment [52]. Epithelialization usually lasts approximately 2 weeks [53].

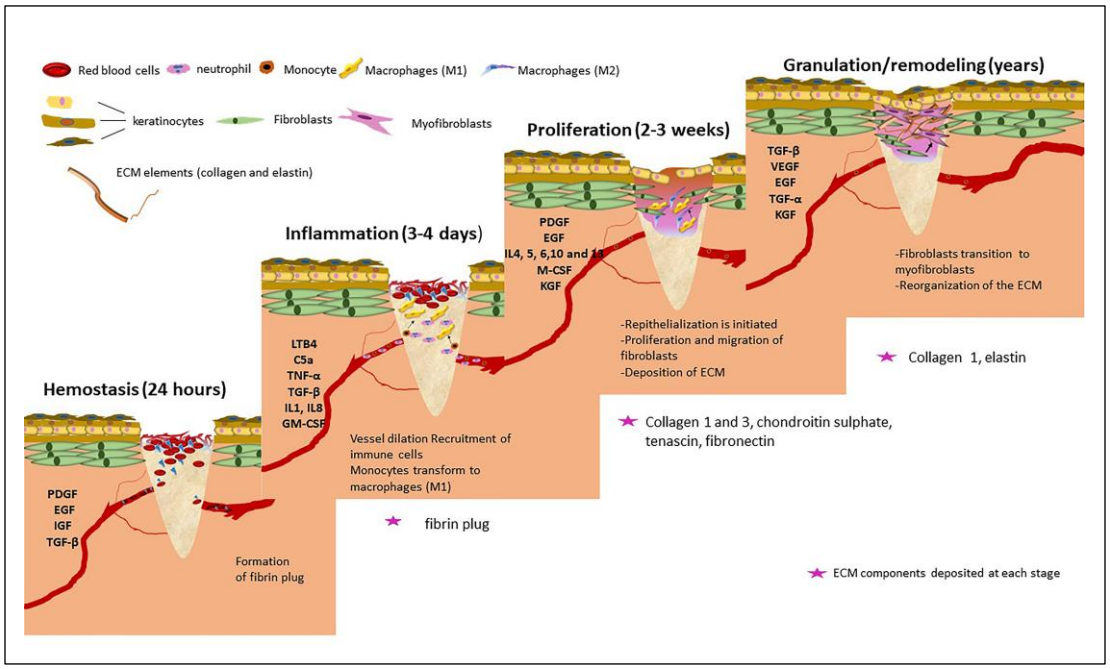

Figure 1-2. The physiology of wound healing

The successful closure of a wound involves an intricately coordinated cross talk between immune cells and resident cells such as the keratinocyte and fibroblasts that allows temporal and spatial control over the production and function of the different elements required for the formation of healthy tissue. The harmony of this wound environment relies greatly on metabolic, chemical, and mechanical cues that are significantly altered in DFU that leads to impaired healing.

The diabetic foot is a metabolic disorder characterized by a pathological triad; neuropathy ischemia, and infection that results in the development of a chronic

ulcer[54], which is a breakdown in the skin that extends from the surface to the subcutaneous tissue, muscle and bone[55]. It is termed chronic when it does not heal in an orderly or timely manner and does not result in structural integrity[56].

In the mitochondria, hyperglycemia causes an abnormally high membrane potential. Above the threshold, electron transport at complex III of the electron transport chain is inhibited with an increase in the half-life of the co- enzyme Q that reduces oxygen to superoxide. Superoxide inhibits the glycolytic enzyme glyceraldehyde-3-phosphate dehydrogenase (GAPDH) causing an increase in the glucose flux and enhancement of the polyol pathway[57]. The result is the consumption of NADPH that is needed for the regeneration of antioxidant molecules such as glutathione. In the absence of antioxidants, there is an accumulation of reactive oxygen and nitrogen species (ROS and RNS) which activate the master transcription factor of inflammation, nuclear factor kappa beta (NF-kβ) [58, 59]. NF-kβ influences gene expression and the production of number of chemokines namely IL-1, IL-6 and TNF-α [60]. The latter proteins lead to insulin resistance further aggravating hyperglycemia[61]. The increase in oxidative stress induces nerve damage, impairs vascular reflexes, peripheral vasodilation and bone resorption. All these factors augment the likelihood of a bone fracture and foot deformity consequently increasing the risk of foot trauma. Moreover, the loss of sensation that accompanies neuropathy also increases susceptibility to injury for the patient. Glucose binds to residue amino groups on polypeptides and lipids to form advanced glycation end products (AGEs)[62]. AGEs bind to the receptor of advanced glycation end products (RAGE) on endothelial cells, vascular smooth muscle cells and macrophages, which in turn also activate NF-kβ[61, 63]. Glycation of the structural proteins collagen and laminin found in the basement membrane of the blood vessels impairs the electric charge and leads to increased membrane permeability and stiffening of the vessel wall[64]. The effect is most pronounced in the microcirculation where it leads to an increase in hydrostatic pressure and shear forces resulting in the injury of the endothelium lining. There is a release of extravascular matrix proteins that leads to basement membrane thickening[65]. In the event of a foot injury, the thickened vessel makes it difficult for immune cells to migrate to the affected area and also increases the risk of infection that hinders the healing of the ulcer. Neuropathy also reduces the formation of neuropeptide proteins (nerve growth factor, calcitonin, substance p that are involved in recruiting cells to the wound site[66]. Poor cell infiltration is accompanied by a deficiency in growth factors and molecules that are required for the ideal symphony of events that lead to wound regression.

Advanced treatments have been developed that take advantage of the different factors (Mechanical, chemical and biological cues) involved in the physiological wound healing process. These include; Silver impregnated dressing (Aquacel Ag®) which effectively cleanses the wound of infection while absorbing excess exudate and maintaining a moist environment ideal for wound healing[67]. Medihoney® gel dressing that acts as debridement agent and lowers the pH at the wound site[68]. Polyurethane foam (Allevyn®) facilitates gaseous exchange and absorbs excess exudate which facilitates the healing process[69]. Hydrogels also provide a moist

environment ideal for healing and lowers the temperature at the wound site[69]. Other dressings incorporate collagen and growth factors (PDGF and EGF)[70, 71] consequently providing a suitable milieu for the formation of granulation tissue. Unfortunately, none of these dressing have resulted in an adequate response or healing time for diabetic foot ulcers[72].

1.2 The role of NO in wound healing and its alterations in DFU

Nitric oxide is a gaseous molecule that was first characterized by Joseph Priestly in 1772 and before 1980 was viewed mainly as an air pollutant present in automobile exhaust and cigarette smoke. However, as a result of the work done by Robert Furchgott, Louis Ignarro, Marek Radomski and Ferid Murad, it is now well known in the literature for its myriad of roles in maintaining vascular homeostasis, inhibition of inflammation and bacterial invasion, facilitating wound healing and as an intercellular signaling molecule involved in neurotransmission [73-76]. In the body, NO is primarily produced via a metabolic pathway involving L-arginine, Ca2+/calmodulin, oxygen, nicotinamide adenine dinucleotide phosphate (NADPH), tetrahydrobiopterin (BH4) and one of three nitric oxide synthase (NOS) isoform enzymes depending on the tissue and cell type. The NOS enzyme aids in the transfer of electrons from NADPH in its carboxyl terminal reductase domain to the heme in the amino-terminal oxygenase domain. This domain binds oxygen and BH4. The heme reduces oxygen and oxidizes L-arginine into L-citrulline and NO. Calmodulin is required to facilitate the flow of electrons (**Figure 1-3**). All the isoforms can bind calmodulin at different affinities depending on the intracellular calcium levels and binding site structure on the enzyme. There are 3 NOS isoforms that have been identified so far. NOS -1 (neuronal) and NOS-3(endothelial) are constitutively expressed in the cells of origin and require increased calcium concentration to bind calmodulin (200-400 nM) while NOS-2 (inducible) expression is induced by inflammatory mediators and is referred to as calcium independent because it strongly binds calmodulin at very low calcium levels (<40 nM)[77] [78].

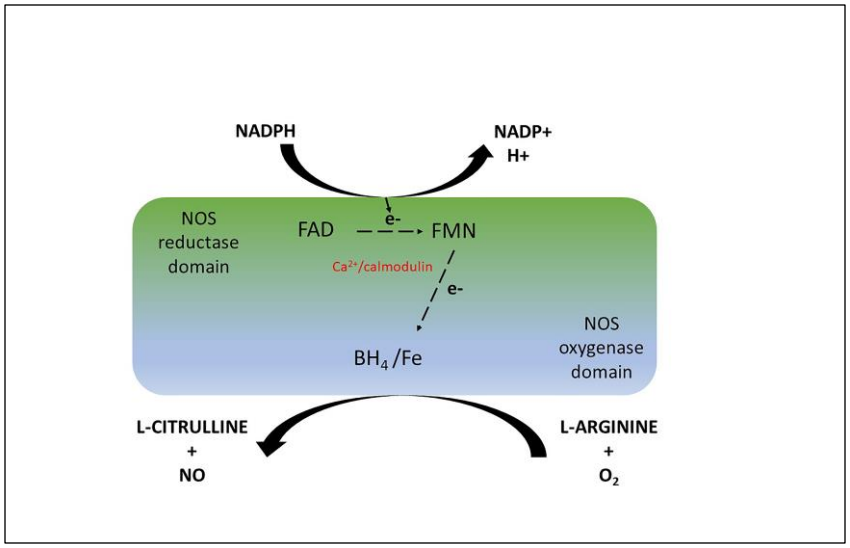

Figure 1-3. The metabolic pathway of NO generation

In 1992, Heck et al reported the first production of NO in the skin by keratinocyte cells when stimulated by inflammatory mediators[79]. The cells expressed NOS confirmed by an enzyme activity assay. The maximal activity required both ca and calmodulin showing probable dependence on constitutively expressed NOS isoforms. The production of NO was observed to regulate the proliferation of keratinocyte cells. It was later confirmed that keratinocytes constitutively express NOS-1 and can be induced to express NOS-2 as well[80-82]. Since then, there have been several studies reporting NO production in the skin when exposed to various stimulating factors as well as expression of the different NOS isoforms in cells that are actively involved in the wound healing process (**Table 1.1**). During hemostasis, NO produced from endothelial cells activates the enzyme guanylate cyclase which initiates the cyclic c-GMP pathway to inhibit platelet aggregation and enhance vasodilation. Endothelial cells express NOS-3 responsible for NO production. In the inflammatory phase, M1 produce significant amounts of NO (>0.5mM) that acts to destroy microbes and prevent infection of the wound. In fact, the highest NOS activity occurs in the early phases of wound healing [31] and is predominantly produced from macrophages. The NO levels are drastically reduced (0.01-0.25mM) when the wound transitions to the proliferation stage [80, 83-85]. M1 convert to M2 macrophage cells that do not produce NO. However, fibroblast cells produce low levels of NO (nanomolar range) and express both NOS-1 and NOS-3 isoform enzymes[42, 43]. The low concentrations of NO have a more anti-inflammatory effect on wound healing. A prime example is the inhibitory effect on NF-κβ signaling. NO acts directly through S-nitrosylation of the p50 subunit of NF-κβ and inhibits its binding to DNA[86]. The NO produced in fibroblasts has been shown to regulate collagen production[44]. It is also speculated that these low NO levels produced from fibroblasts act as the first response before the immune cells arrive at the wound site [43, 80]. The NO role in the proliferation of fibroblasts has not been well established and its impact on their migration still needs to be determined. Low NO levels also play a role in extracellular matrix remodeling/turnover. Ridnour et al demonstrated the effect of NO treatment on modulating the activities of MMPS-1,9 and 13[87]. NO promotes

angiogenesis through the activation of the growth factors VEGF, TGF and bFGF [88]. In keratinocytes, the production of VEGF is controlled by NO production [89]. In addition, NO has been shown to exert antiapoptotic effects through regulating the activity of antiapoptotic markers such as HIF-1α [90] and inhibition of caspase activity [91]. It is therefore conceivable that the doses of NO produced at the wound site change gradually over the time course of healing to ensure that the production and regulation of growth factors proceeds as expected to maintain the phenotype and the function of the cells at each stage. (**Figure 1-4**).

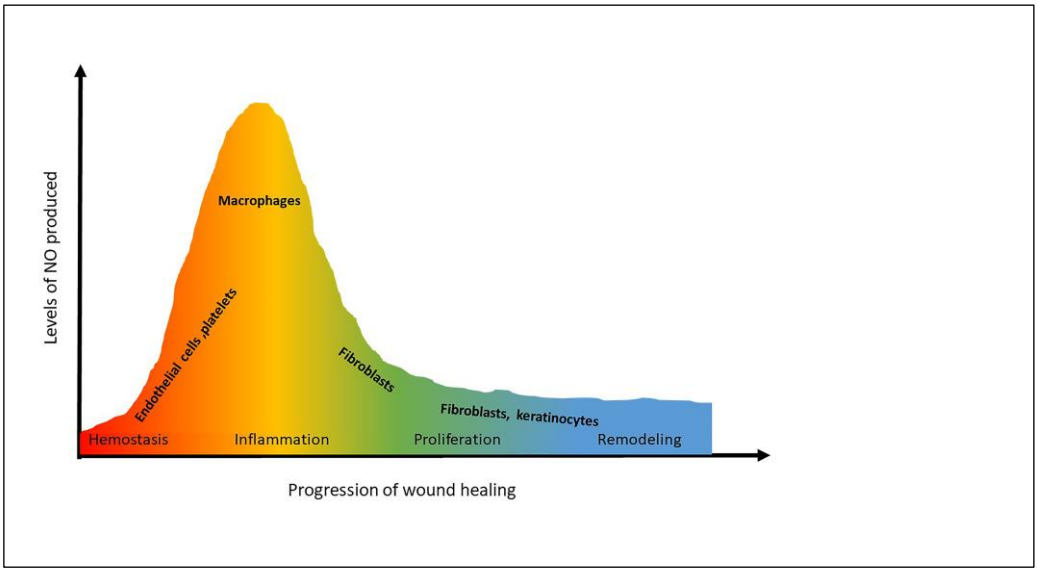

Figure 1-4. The predicted nitric oxide levels produced from cells in the different stages of wound healing

NO is highly reactive and very short lived and this dictates its overall effect on the cells. In the presence of aggravating factors, there are mechanisms in place to maximize the biological effect of NO in order to produce an appropriate host response. The most important is the maintenance of nitroso-redox balance. If the stimulus persists or in case of inadequate feedback, it alters the equilibrium of the wound environment, which is the hallmark of dysregulated healing in DFU.

Table 1-1. The different NOS isoforms and their functions in cells types found in the skin

TYPE	CELL	FUNCTION	REFERENCES
Neuronal/brain (nNOS) 150-160kD	Melanocytes, keratinocytes (basal epidermal layer)	Vasodilation in response to mechanical stimulation, Melanogenesis	[92-95]
Inducible (iNOS) 130kD	Keratinocytes, melanocytes Fibroblasts, macrophages, Langerhans	Angiogenesis, collagen production, wound breaking strength, immune response, antimicrobial effects, antiapoptotic effect	[80, 92]
Endothelial (eNOS) 135-140kD	Endothelial cells Keratinocytes, melanocytes, fibroblasts	Angiogenesis, Melanogenesis	[80, 92]

1.2.1 Nitroso-redox balance in the pathophysiology of diabetic foot ulcers

Redox balance is determined by the change in the oxidative state of an atom[96]. An addition of electrons results in reduction and a loss in electrons leads to oxidation[97]. An imbalance between these two states causes oxidative stress that has deleterious effects on the healing process. Reactive oxygen and nitrogen species (ROS and RNS) as well as antioxidants are the major players in maintaining redox balance. Examples of ROS and RNS include; superoxide ($O^{\cdot}$), hydrogen peroxide (H_2O_2), hydroxyl radical, hypochlorous acid (HClO), nitric oxide (NO), and peroxynitrite ($ONOO^{\cdot}$).

1.2.1.1 Sources of ROS and RNS

Hydrogen peroxide formation

The spontaneous transfer of an electron to superoxide at low pH or by an enzyme reaction (superoxide dismutase) produces hydrogen peroxide (H_2O_2)[98, 99]. H_2O_2 readily diffuses across intra and intercellular membranes where it is involved in either cell signal transduction or cytotoxic effects [99]. Hydrogen peroxide is a potent antimicrobial agent at high concentrations (500 μM)[100]. In the inflammatory phase, H_2O_2 augments the phosphorylating capacity of the enzyme tyrosine kinase which downstream amplifies the signal at the antigen receptor site of the cell[101].

Hydroxyl radical formation

The hydroxyl radical ($^{\cdot}OH$) can be formed from the reaction of H_2O_2 with superoxide (Haber weiss reaction) or via the breakdown of H_2O_2 by metal ions; Fe^{2+} or Cu^{2+}(Fenton reaction) [102]. $^{\cdot}OH$ is highly reactive, it interacts with DNA, lipids, proteins and carbohydrates causing severe cell damage [103]. Although, a study has shown a dose dependent effect of $^{\cdot}OH$ on fibroblast function. The authors used an ascorbate-copper ion system to generate hydroxyl radicals. Low levels (<10mumol/l) increased collagen polymerization and high levels (>100mumol/l) evoked degradation of collagen showing a possible role of $^{\cdot}OH$ in remodeling of the ECM[104].

Hypochlorous acid formation

Hypochlorous acid is mainly produced by leuckocyte cells from the reaction of H_2O_2 with chloride anions that originate from the uptake of extracellular fluid by the cell[105]. The reaction is catalyzed by the enzyme myeloperoxidase (MPO) [24, 105]. HClO has very strong antimicrobial effects and facilitates the removal of foreign particles and damaged tissue. However, because of its cytotoxic effects it also affects the surrounding host environment.

NO and peroxynitrite

Nitric oxide readily diffuses rapidly in water and lipids which makes its functions very diverse. Its effects can be direct and indirect depending on the redox state. NO reacts with metal ions such as ferrous heme to form a nitrosyl-heme complex. This mechanism is used to activate the enzyme guanylate cyclase consequently converting GTP to cGMP which downstream dictates majority of NO function especially in hemostasis[106]. NO also reacts with the thiol groups in proteins through covalent post translational modification of proteins[92] (s-nitrosylation). An example is the NO effect on transglutaminases by s-nitrosylation of the cysteine residues on their protein structure. Transglutaminases facilitate the cross linking of the proteins in the ECM during epithelialization, proliferation and remodeling[107]. The rate constant of both mechanisms is approximately 10^5-10^6 M^{-1} $S^{-1.}$ In the presence of ROS specifically superoxide, indirect effects of NO manifest because it rapidly reacts with superoxide at a rate that is faster than its reactions with proteins/metal ions (1.9×10^{10} M^{-1} S^{-1}) or the reaction of superoxide with the scavenger superoxide dismutase (SOD) (2×10^{9} M^{-1} S^{-1}) [92] to form the more reactive and toxic compound peroxynitrite[108] [58, 96]. At low concentrations, peroxynitrite acts as a signaling molecule through activation of 3 tyrosine phosphorylation and the mitogen activated protein kinases (MAPK) pathway which activates glycolysis and controls cell proliferation respectively [58, 96] . In one study, it was shown to have antiapoptotic effects by inhibiting caspase-3 activity through s nitrosylation in adhesion fibroblasts.[109]. Unfortunately, the majority of peroxynitrite effects are cytotoxic. It modifies protein molecules by reacting with the amino acids tyrosine and tryptophan to form nitrotyrosine and nitrotryptophan

respectively. It also nitrates lipids and nucleic acids resulting in DNA damage. The damage to DNA structure over activates the enzyme poly (ADP-ribose) polymerase-1 (PARP-1) which consumes NAD+, ATP and eventually leads to cell dysfunction and death. At physiological pH, peroxynitrite decomposes into more toxic species; nitrogendioxide and hydroxyl radical [92].

1.2.1.2 Antioxidant mechanisms

To maximize the biological functions and reduce the accumulation and deleterious effects of ROS and RNS, the body produces a variety of antioxidants. The toxic effects of superoxide are controlled through dismutation by antioxidant enzymes SOD[58, 97]. Under physiological conditions, H_2O_2 levels are controlled through inactivation by the enzyme glutathione peroxidase in the presence of the amino acid glutathione or the enzyme catalase which convert H_2O_2 into oxygen and water [97]. Evidence shows that NO its self-acts as a substrate for MPO through the reaction with its end product $NO2^-$ which reduces and inactivates the MPO compound 1[110]. Whether this could be a mechanism for regulating HClO still needs to be investigated. Peroxynitrite accumulation can be controlled by glutathione peroxidase in the presence of glutathione (GSH) which regulates its cytotoxic effects[111]. Studies have shown an aggravated effect of hypovolemic shock in case of increased toxicity by peroxynitrite and low GSH levels[112]. At high doses, NO can also be toxic. In vivo, the detoxification of NO is achieved mainly through its reaction with hemoglobin. [58, 113]. NO also reacts rapidly with oxygen to form nontoxic compounds nitrate/nitrite[114]. SOD also regulates NO and the production of peroxynitrite by scavenging superoxide[115].

1.2.1.3 Oxidative and nitrosative stress in diabetic foot ulcers

In the diabetic state, persistent hyperglycemia leads to an over production of superoxide by activating different pathways; polyol pathway, xanthine and NADPH oxidases, cyclooxygenases, uncoupled nitric oxide synthase, glucose auto-oxidation, mitochondrial respiratory chain[57]. The result is high ROS levels and low antioxidants, a state defined as oxidative stress. The high levels of superoxide surpasses the body's antioxidant mechanisms. Superoxide activates the NF-κβ transcription factor which upregulates expression of NOS-2 and consequently NO production. In the presence of high superoxide and low levels of the super oxide scavenger molecules, NO will react very rapidly with superoxide to produce peroxynitrite consequently reducing the bioavailability of NO. Moreover, high ROS and peroxynitrite levels in the hyperglycemic state limits the production of BH_4 (an indispensable co factor for NO production) and causes the uncoupling of NOS to generate superoxide instead of NO [96, 116, 117]. The concentration of arginase is another mechanism that interferes with NOS activity. Arginase competes with NOS enzymes for the substrate arginine and reduces NO availability favoring superoxide production. A diabetic induced state was found to increase arginase activity levels in the wounds of diabetic mice and this correlated to delayed healing observed in the study [35]. The deficiency of NO alters endothelial vascular function causing vessel

constriction. Moreover, in diabetic patients with high cholesterol levels, the presence of peroxynitrite favors lipid peroxidation and induces an inflammatory response, activating platelet aggregation[96]. These effects are mostly pronounced in the small blood vessels and plays a role in the progression of neuropathy[118]. Vascular impairment can result in persistent ischemia. Wounds are often associated with low oxygen tension[119]. In physiological conditions cells express HIF-1 α, a key transcription factor that allows the cells to adopt to hypoxic conditions. HIF-1α promotes angiogenesis, cell proliferation, cell survival and energy metabolism. NO is a key regulator in the expression of HIF-1α. The effect of NO on regulation of HIF-1 α is very complex and yet indispensable to cell survival and function under external insult. It is reported that the effect of NO on HIF-1 α is primarily mediated by S-nitrosylation.[120]. In normoxia (1-10mmHg) and hypoxia, high levels of NO (> 1μM) stabilize the HIF-1 α transcription factor while low NO levels (<400 nM) in hypoxia destabilize it[121]. During the early phases of wound healing when M1 are predominant, it is possible that the high NO production from the cells facilitate the stabilization of the protein in order to produce an adequate adoptive response to injury and when this is resolved the low NO levels produced from the other cells promote resolution in the wound environment to restore its normal state. In fact, Pena and O'Neil[122] report a possible link of HIF-1α protein in the polarization of macrophages which might be regulated by NO concentration. The association of ischemia in the presence of hyperglycemia has devastating effects on the redox and metabolic state in the wound bed by altering NO function and consequently adoptive response to the hypoxic environment. Catrina et al showed that HIF-1 α protein levels were low in human endothelial and dermal fibroblast cells cultured simultaneously in hyperglycemic and hypoxic conditions[123]. In the same study, biopsy samples obtained from patients with DFU showed lower HIF-1 α staining in the nucleus and cytoplasm compared to non-diabetic patients with chronic wounds. Jazayeri et al [124] also showed increased expression of proapoptotic marker p53 as well as ischemia induced apoptosis in diabetic mice and dermal fibroblasts cultured in hyperglycemic conditions. It is interesting that NO in a dose dependent manner also regulates both HIF-1α and p53 expression. Thomas et al[90] showed that a single high dose of NO (>2000 nM) increased the P53 P-Ser-15 protein levels while the same dose delivered over a longer period of time increased HIF-1α protein levels instead. A contrasting study showed inhibition of HIF-1 α accumulation by NO in liver and cancer cells (50 μM). However, addition of peroxynitrite scavengers alleviated this effect [125]. Patients with diabetes have been found to have high levels of nitrotyrosine in plasma[126]. Another study showed increased peroxynitrite production in diabetic platelets [115] and other researchers have found high levels of nitrotyrosine levels in rat and mice diabetic skin which correlated to the dysregulation in the wound healing process[127, 128].

The number of factors that affect wound healing are intertwined and very diverse. It is further complicated in an altered metabolic and redox environment where the absence or malfunction of one factor affects a cascade of events downstream. This is clearly demonstrated in the key signaling molecule NO. The complexity of NO makes its interpretation in vivo and invitro studies very sensitive to concentration, duration of NO delivery and redox environment. These are all very important factors to consider in terms of the response and efficiency to a given treatment plan for DFU.

1.3 Current methods used to measure NO in diabetic conditions and their limitations

The high reactivity and very short half-life of NO makes it extremely difficult to measure directly under physiologically relevant conditions. As a result, the majority of studies in the literature rely on its metabolic decomposition products nitrite/nitrate, enzyme activity assays and protein levels. However, because of the complex chemistry of NO in an altered cell or tissue environment, it is very difficult to interpret results from different studies and draw a conclusion on the actual role of NO in a given pathology. In addition, the decomposition of its toxic species such as peroxynitrite can also generate nitrite/nitrate in vivo and invitro[112, 129]. It is therefore not surprising that NO studies in diabetic states show contradicting results in the levels of NO determined as well as the outcome based on these methods of analysis (**Table 1-2**).

Table 1-2. Experiments and analysis methods and outcomes on the effect of NO in diabetic states

SAMPLE	SPECIES	NO ANALYSIS	OUTCOME	MODEL	TREATMENT	REFERENCE
Aortic endothelial cells	Human	Griess assay (nitrite) PCR Western blot	High nitrite accumulation ,high superoxide levels, High NOS-3 levels	High glucose 22.2mmol/l	High glucose 22.2mmol/l	[130]
Skin	Mouse	Immunofluorescent staining, PCR and western blot	Low NOS-2 expression and levels	Diabetes	Streptozotocin	[35]
Glomerular endothelial cells	Human	Griess assay (nitrite) Western blot	Low nitrite levels, increased NOS-3 levels	High glucose (15,30,60 mM)	High glucose (15,30,60 mM)	[131]

Macrophages (RAW 264.7 and primary peritoneal macrophages)	Mouse	Griess assay (nitrite) Western blot PCR	High nitrite levels, Increased NOS-2 expression and levels	High glucose (25mM)	LPS treatment	[132]
Skin fibroblasts	Human	Griess assay (nitrite)	High nitrite levels	High glucose (22.5/42 mM)	Irradiation 830 nm	[133]
Umbilical endothelial cells	Human	Immunoblotting	Low nitrosylation NOS-3	High glucose (30mM)	High glucose (30mM)	[134]
Skin	Mouse	NOS-3 deficiency angiogenesis assays	Delayed wound closure	NOS-3 knock out	N/A	[135]
HUVEC	Human	Griess assay, gene expression	High nitrite levels, high NOS-2 AND 3	High glucose (100mM)	High glucose (100mM)	[136]
Blood serum	Mouse	Griess assay	High nitrite levels	Diabetes	Streptozotocin	[136]
Blood serum	Human	Griess assay	High nitrite levels	DM type 2	N/A	[136]
HUVEC	Human	Griess assay	Low nitrite levels	High glucose (30mM	A23187 (2.5uM)	[137]

Skin	Mouse	Immunohistochemistry, Griess assay	Low NOS-3 expression, low nitrite levels, delayed wound closure	Diabetes	A23187 (2.5uM)	[137]
Skin	Mouse	Immunofluorescent staining	High iNOS expression, delayed wound closure	Diabetes	Streptozotocin	[138]
Urine	Human	Griess assay (nitrite)	Low nitrite levels	DM Type 2	Arginine intravenous infusion	[139]

In a diabetic mouse model, Miao et al found that M1 cells were deficient at the wound site by staining for iNOS/cd68 macrophage marker. These cells mainly appeared early on in the wound healing process and the levels of iNOS staining cells was low in diabetic mice compared to controls. The low levels of iNOS were correlated to low NO levels and delayed wound healing. The upregulation of the iNOS enzyme shows a causal relationship with NO however it does not always translate to the actual levels of NO produced or how it relates to cell function. For example, the islet cells in the pancreas stained positive for nitrotyrosine an indicator of peroxynitrite destruction in another diabetic mouse model. The formation of this protein was decreased in the presence of iNOS inhibitors or superoxide scavengers[140]. In another study, high glucose increased NOS-3 expression in vascular endothelial cells, although nitrite levels measured in the media was low. When the superoxide scavenger SOD was added, nitrite levels were restored[131]. Another indicator of this inconsistency is in Hwang's study, the researchers looked at the effect of high glucose on NO production in macrophage cells. The results showed that macrophages produced more NO compared to cells cultured in normal glucose conditions and the NO was reduced when an anti-inflammatory compound glucosamine was added[132]. The nitrite accumulation in the media was taken as an indicator of NO production. In addition to NO, macrophages also release significant amounts of superoxide which would greatly have an effect on the bioavailability of NO released.

The majority of NO treatments in physiological cell culture conditions have shown a positive effect on the function of cells involved in wound healing. For example, the NO

donors sodium nitroprusside, Diethylenetriamine NONOate (DETANO) and S-nitroso-N-acetylpenicillamine (SNAP) in a dose dependent manner improved migration in keratinocyte cells [141]. In other study, the migration and re-epithelialization of epidermal stem cells was accelerated in the presence of NO donor SNAP[142]. Similarly, normal and diabetic wound animal models have shown success which supports the theory that NO levels are low in diabetic conditions and when integrated back into the system, these NO levels are restored. (**Table 1-3**).

Table 1-3 The effects of NO treatments *in vitro* and *in vivo* experimental studies

MODEL	SPECIES/CELL TYPE	TREATMENT	EFFECT	REFERENCES
Cell culture	Keratinocytes	SNP/DETANO/ SNAP, GSNO	Improved cell migration and proliferation	[141, 143]
Cell culture	Fibroblasts	SNAP, NO releasing hydrogel and particles	Improved cell migration, proliferation, ECM deposition	[143-145]
Cell culture	Epidermal stem cells	SNAP	Improved cell migration and re-epithelialization	[142]
Animal	Non-diabetic mice	PCL/CS-NO/NO releasing ointment	Re-epithelialization, improved granulation tissue,collagen deposition and angiogenesis	[146, 147]
Animal	Diabetic mice	NO releasing hydrogel and nanoparticles	Reduced inflammation, increased collagen deposition, angionesis and granulation tissue	[144, 148]

S-Nitrosoglutathione (GSNO), polycaprolactone (PCL), chitosan-based NO-releasing biomaterials (CS-NO)

However, the translation of NO treatments in patients affected with DFU has yielded insufficient results despite the fact that most of these clinical trials were completed (**Table 1-4**).

Table 1-4 Reports on clinical trials that applied NO treatments to patients with DFU

STUDY	REGISTRATION #	STATUS	OUTCOME	REFERENCES
Advanced plasma therapy 001plasma/NO therapy for the treatment of diabetic foot ulcers	NCT03078933	Recruiting (2017)	N/A	https://clinicaltrials.gov
Nitric Oxide Generating Gel Dressing in Patients with Diabetic Foot Ulcers (ProNOx1)	NCT01982565	Completed (2016)	Reduced wound size, improved healing and minimal adverse effects	[149]
PT001 Plasma/NO Generator to Treat Diabetic Foot Ulcer in Adults (APT-14-002	NCT02356835	Completed (2016)	No results posted	https://clinicaltrials.gov
Electrical Stimulation and Expression of VEGF and NO in Diabetic Foot Ulcer	NCT02019082	Completed (2013)	No results posted	https://clinicaltrials.gov
Clinical Trial for the Treatment of Diabetic Foot Ulcers Using a Nitric Oxide Releasing Patch: PATHON	NCT00428727	Completed (2012)	No results posted	[150]

This shows the problem of relying only on biproducts or enzyme activity to dictate NO function. The assumption in the Griess assay is that all the NO produced is converted to nitrite in the presence of an enzyme nitrate reductase. This method is not quantitatively accurate and is susceptible to variations depending on the media or buffer used[151]. The sensitivity of the assay is also quite low with a detection limit of approximately (0.1-0.5μM). With NOS activity, it is inferred that the presence of the NOS enzyme represents NO levels and function which is also grossly inaccurate since the enzyme can uncouple to

generate other reactive oxygen species [116]. Most importantly, they are all accumulation assays and the means of determining the rate of production of NO or how this rate changes over time in different pathological states is practically impossible. He and Frost[152] developed a novel measurement system (the CellNO trap) that allows the direct, real-time, continuous measurement of NO produced or exposed to cells under conventional culturing conditions using chemiluminescence, one of the most sensitive and specific methods for detecting NO through its reaction with ozone[74]. This device has previously been validated and used to characterize the rate and amount of NO produced in macrophage cells as well as the actual levels of NO that cells are exposed to when treated with soluble NO donors[153]. The authors proved that the average or maximum NO measured is not an indicator of the dynamic character of NO. In addition, they showed how adding of different NO mediators commonly used in the literature affects the NO release in real-time. For example, adding arginine, the NO substrate that is frequently used to increase NO production in various studies had different effects on the NO release profile in stimulated macrophage cells depending on the time that it was added. The results from the same study also showed that the Griess assay recorded significantly lower NO levels compared to the real-time NO measured. He and Frost [153] further demonstrated that various conditions such as the pH, CO_2, reaction volume and redox environment affect the ultimate NO levels that cells in culture are exposed to. The soluble NO donor DETANO at different pH levels in the presence and absence of CO2 showed different NO release profiles. At physiological pH, there was an increase in NO release which stayed constant for 24 hours. In the presence of CO_2, there was higher peak of NO which gradually reduced over 24 hours and at pH 6 the NO level had the highest peak but by 15 hours the NO treatment was depleted [153]. In a study, that included 50 patients with chronic and acute wounds, the baseline pH levels of most wounds was approximately 8.5[154]. The evidence that the NO release from NO donors alters with changes in pH further proves that without the knowledge of the dynamic changes in the NO released from NO donors, the outcome of these treatments is unpredictable. Moreover, the soluble NO donor SNAP showed large variation in its NO release profile for different replicates measured[153]. Three studies (**Table 1-3)** showed that both SNAP and DETANO accelerated migration, improved proliferation and re epithelialization of keratinocytes, epidermal stem cells and fibroblasts in invitro wound healing models. However, the NO release kinetics of these two NO donors were not determined. The authors relied only on the overall analytical concentration of the NO donors which might prove to be a challenge in reproducing these effects in NO treatments for DFU. On the bright side, two clinical studies have shown promising results. In patients with diabetic neuropathy, isosorbide dinitrate alleviated pain but did not show an effect in improving other sensory symptoms[155]. The use of this organic nitrate compound has been very successful in patients with heart failure when administered with an antioxidant[156] which might equally show better results for diabetic patients with peripheral vascular disease if the same mode of administration is employed. The second study was in a randomized clinical trial in which patients were given an NO release wound dressing sustained for 12 weeks. There was significant reduction in wound area, improved healing and minimal adverse effects compared to patients treated with standard wound dressings. The study was also superior to others because they included patients with ischemic and infected ulcers. While it showed a positive response in wound healing, the

absolute effects of NO could not be measured and the NO levels at the wound site of the patients was also unknown[149] [157].

1.4 Statement of purpose

Brüne and Zhou used an interesting analogy to define the role of NO and hypoxia. They described this relationship as one ranging from courting to matrimony and divorce[121]. In essence this same analogy can be used to describe the overall NO function in the physiological wound healing process and its alteration in DFU. Wound healing is very dynamic and complex with different yet overlapping stages that are controlled from the molecular to the cellular and tissue level. It's clear that NO is needed in each of these stages. However, the timing, dose and duration of NO produced is very distinct and its function at a given time relies greatly on the redox environment. This harmony is severely altered in an unstable metabolic state like diabetes and consequently it plays a major role in the improper and delayed healing of DFU. Therefore, understanding how the direct NO levels produced from the cells actively involved in healing changes over time in both physiological and pathological conditions is extremely critical in developing NO treatments to reestablish skin integrity. The work herein mainly focuses on using the device that was previously developed to determine the real- time NO levels produced from cells involved in wound healing under physiological and diabetic conditions. Chapter 2 shows the real- time NO produced from normal human skin fibroblasts cultured in normal glucose conditions and how the levels of NO change in high glucose conditions in the presence and absence of inflammatory mediators. This study reports the first ever assessment of real-time NO produced from human dermal fibroblast cells. Chapter 3 adopts these culture conditions to determine the real- time NO produced in human wound dermal fibroblast cells isolated from a patient with a chronic ulcer. In addition, a highly sensitive method of analysis is validated to determine the nitrite and nitrate levels present in wound fluid obtained from patients with chronic ulcers. Chapter 4 reports the changes in NO levels produced from the macrophage cell line RAW 264.7 cultured in normal and high glucose conditions and finally chapter 5 looks at the potential applications of real-time NO measurements in localized NO delivery systems and in the determination of the role of NO in the progress of cardiovascular calcification.

2 INVESTIGATIVE STUDY OF REAL-TIME NO MEASUREMENTS IN NORMAL FIBROBLAST CELLS IN NORMAL AND HIGH GLUCOSE CONDITIONS[1]

Fibroblasts are the most prevalent cell type in the dermis layer of the skin. The main function of fibroblasts is to secrete the extracellular matrix (ECM) scaffold, for all cells residing in the skin tissue [158]. They are the most important mesenchymal cells and are defined as the architects of the wound healing process. The main component of the ECM is collagen which replaces the fibrin provisional matrix. Other elements include proteoglycans, glycoaminoglycans (GAGS), heparin sulfate and elastin that facilitate the aggregation of collagen fibrils, direct cells, cytokines and growth factors within the ECM as well as providing flexibility to the skin [159]. Fibroblasts also regulate the growth and function of other cells involved in wound healing through the production of growth factors and secretion of MMPS. **Table 2-1** shows the components produced by fibroblasts and their roles during healing. A few studies have emerged that provide evidence of NO production from fibroblast cells. Wang et al showed that human skin fibroblasts produced low levels of NO and express both constitutive and inducible forms of NOS[43]. The NO produced was hypothesized to be involved in the inflammatory process before the arrival of the immune cells. In a follow up study that consisted of cells isolated from hypertrophic burn tissue and site marked normal skin tissue, NO levels, enzyme activity and expression were reduced in cells isolated from hypertrophic scar tissue compared to normal skin tissue. The authors drew the conclusion that NO helps to control the proliferation of cells and its deficiency was evidence to explain hypertrophic scar formation in patients. During the same period, Schaffer et al also showed NO production from mouse wound dermal fibroblasts played a role in collagen deposition and wound mechanical strength. In the same study, the group demonstrated that wound fibroblast cells produce NO while normal fibroblasts do not produce NO. Furthermore, the NO levels were reduced in subsequent cell passages. Other authors have reported increased NO production from human skin fibroblasts when irradiated with UV light and showing potential in regulating the proliferation of the cells[160]. The NO production in fibroblasts is altered in diabetes. In Schaffer et al's study,[161] the wound breaking strength and collagen deposition was low in wounded diabetic induced mice compared to normal mice and this correlated with the low nitrite levels in the wound fluid and cells isolated from these wounds. Another group of researchers showed that the NO production was low in fibroblast cells cultured in diabetic conditions and it was significantly increased when the cells were irradiated with a light source. Moreover, cell migration and proliferation in diabetic conditions was improved when the cells were irradiated with light[162]. It's interesting that none of these studies looked at the direct NO levels or how the production of NO would change or alter the effect observed depending on the culture conditions. The researchers only looked at

[1] The majority of the work presented in this chapter was submitted and published in *Medical Sciences* and the rights to use this content is presented in appendix C and licensed under Creative Commons Attribution 4.0 International License

nitrite or enzyme activity to correlate the function and production of NO in fibroblast cells which might not be an accurate assessment.

Table 2-1 Elements produced by fibroblasts and their function in wound healing

Elements	Function	References
Collagen, proteoglycans, hyaluronic acid, tropoelastin and elastin	Strength, cell movement, aggregation of collagen fibrils, direct and regulate function of cells and growth factors, resilience and elasticity	[26, 158, 163]
Cytokines (IL-1, IFN-γ, TNF-α)	Stimulate production of growth factors, regulate inflammatory response	[26, 163]
Cysteine-rich angiogenic inducer 61(Cyr61)	Regulate inflammation, angiogenesis,cell matrix interaction, matrix remodeling	[164-167]
Growth factors (NGF, TGF-β, PDGF, FGF.EGF)	Nerve growth, keratinocyte proliferation, angiogenesis, cell proliferation, chemotaxis	[26, 163, 168]
MMPS and TIMPS	ECM remodeling, activation and regulation of growth factors	[26, 66]

In this chapter, we specifically elucidated the temporal aspects (both rate and amount) of NO produced by human dermal fibroblasts under normal glucose (5.5mM) and high glucose (25mM) conditions. For the first time, we report the actual levels of NO that human dermal fibroblast cells produced in real-time both with and without stimulation. The rate of cell proliferation and the expression of the iNOS enzyme responsible for the production of NO when the cells are stimulated by inflammatory cytokines was also assessed. The real- time NO and nitrite accumulation were measured in the cells and cell culture media,

respectively, and compared. By understanding the levels of NO produced and how it compares to the nitrite and the protein expression in these cells under both normal and diabetic conditions, we will begin to clearly understand the levels and timing of NO delivery necessary to promote appropriate fibroblast proliferation, migration and deposition of the extracellular matrix in order to reduce the healing time in chronic DFUs.

2.1 Materials and Methods

2.1.1 Cell culture and chemical supplies

Primary human adult dermal fibroblasts (HDFa, ATCC® PCS-201-012™,), mouse macrophages (RAW 264.7), penicillin streptomycin, fetal bovine serum (FBS), phosphate buffered saline (PBS), MTT proliferation assay kit and Dulbecco's modified eagle medium (DMEM high glucose 4500mg/l) were all purchased from ATCC (Manassas, VA). DMEM (no glucose), sodium pyruvate and Hoescht dye were obtained from Fischersci (Hanover Park, IL). D-(+)-Glucose, Lipopolysaccharide *pseudomonas aeroguinosa* (LPS), Calcein-AM, protease inhibitor cocktail, mouse nitric oxide synthase and dopamine-HCl were purchased from Sigma-Aldrich (St. Louis, MO). Ethidium bromide was acquired from Invitrogen (Grand Island, NY). Human recombinant Interferon gamma (hrIFN-Y) was purchased from GenScript (Piscataway, NJ). The primary and secondary antibodies against CD90/Thy1 (ab23894) protein and inducible nitric oxide synthase (iNOS) (ab136918) were purchased from Abcam (Cambridge, MA). The 7.5% SDS polyacrylamide gels and gelatin were acquired from Bio-Rad (Hercules, CA). The Odyssey western blot starter kit 2 was obtained from *LI-COR* (Lincoln, NE). Silicone elastomer base and curing agent (Dow Corning Sylgard®184) were obtained from ML Solar LLC (Campbell, California).

2.1.2 Real time NO measurements from Primary human adult dermal fibroblasts

Primary adult dermal fibroblasts at passage 1 were cultured and expanded in conventional cell culture plates (100mm) in DMEM (high or normal glucose levels), 10% FBS and 1 % penicillin/streptomycin (complete growth media). At confluency, the cells were reseeded in CellNO trap devices at a density of 0.25-1 $\times 10^4$ cells/cm^2. Previously, we have reported the detailed fabrication and characterization of the device [152]. Briefly, silicone elastomer base and curing agent were dissolved in hexanes, manually cast onto 5×5 square polyvinylidene fluoride (PVDF) membranes and left to cure in a 50ºC oven for 24 hours. The modified membrane was cut into a circle to fit into a 60mm diameter cell culture plate with the bottom removed forming the upper chamber. The upper chamber was sealed by applying toluene to the edges of the membrane and the plate. A second 60mm plate with drilled holes and plastic outlets attached was affixed to the upper chamber using toluene and reinforced with epoxy adhesive. The upper chamber was used for cell culture and the lower chamber was used for gaseous transfer. To make the device suitable for cell culture,

freshly prepared dopamine solution in Tris-HCl buffer (2mg/ml) was added to the device and incubated for 12 hours. The device was rinsed several times and sterilized using 70% ethanol and ultraviolet light (1 hour). Prior to cell culture, the device was coated with gelatin solution (2mg/ml). After 24-72 hours, the cell culture media was changed and substituted with media containing 40µg/ml of LPS and 200 U/ml of hrIFN-Ɣ or complete growth media (control) under normal glucose (5.5mM) and high glucose (25mM) conditions. The device was placed in a standard incubator (37°C, 65% humidity, 5% CO_2) and was connected to a calibrated nitric oxide analyzer (NOA) and the real-time NO release profile was measured for 24 hours.

2.1.3 Cell viability assay in the CellNO trap device

After 24 hours, the live-dead assay was carried out using 2µM calcein AM, 2µg/ml ethidium bromide and 10µg/ml Hoescht dye in DMEM media for 10-15 minutes. The cells were imaged and analyzed using an Olympus fluorescent microscope (model BX51) and Image J1 respectively[169].

2.1.4 Cell proliferation assays (MTT assay)

The fibroblast cells were cultured in 96 well plates at a density of 10,000 cells per well in normal and high glucose cell culture conditions and stimulated with 40µg/ml and 200U/ml of LPS and IFN respectively. At the end of 24, 48 and 72 hours, MTT assay was performed according to the manufacturer's instructions (Trevigen, 4890-025-K) with minor modifications. Briefly, the cell culture media was replaced with 25µl of the MTT reagent and incubated for 4 hours to allow the intracellular reduction of soluble yellow MTT to insoluble formazan dye. The MTT reagent was discarded and 100µl of Isopropyl alcohol was added to solubilize the dye. The absorbance was read at a wave length of 570nm using a Beckman Coulter microplate reader model DTX880.

2.1.5 Nitrite assay

After 24 hours of measurement in the CellNO trap device, the cell culture media from the cell samples under normal and high glucose conditions were collected. The triiodide assay was used to measure the nitrite accumulation in the media[74]. Briefly, 50µl of the media was added to a vial containing a stirring solution of 300µl of glacial acetic acid and 120µl of potassium iodide. The vial was connected to a calibrated Sievers Nitric Oxide Analyzer 280i (Zysense, LLC, Boulder, CO, USA) and the NO produced from the nitrite present in the media was measured and normalized to the number of live cells.

2.1.6 Cell characterization

Fibroblast cells at passage 2 were cultured in 12 well plates at a cell density of $1 \times 10^4/cm^2$ in normal and high glucose conditions. At confluency, the cells were fixed in 4% paraformaldehyde for 10 minutes, rinsed 3 times in phosphate buffered saline, incubated in blocking buffer for 90 minutes followed by the primary antibody for 18 hours at 4°C. The cells were rinsed 3 times in blocking buffer and incubated for 1 hour at room temperature with the secondary antibody, stained with 4', 6-diamidino-2-phenylindole (DAPI) and viewed under a fluorescent microscope.

2.1.7 Western blot analysis

Confluent HDFa cells were cultured in 100mm diameter tissue culture dishes, stimulated with 40µg/ml of LPS and 200U/ml IFN-Ɣ in normal and high glucose conditions and incubated for 72 hours. Mouse macrophage cells RAW 264.7 were grown to confluency and stimulated with 100ng/ml of LPS for 18 hours and served as the positive control. The cells were quickly washed in ice cold PBS, trypsinized, centrifuged and re-suspended in 200µl of RIPA buffer in the presence of protease cocktail inhibitors. The cell lysates were incubated for 30 minutes on ice on a plate shaker and centrifuged at 12,000 rpm for 20 minutes at 4°C. The supernatant was collected, and the protein concentration determined for each sample using Bradford assay[170]. An equal amount of loading buffer containing dithiothreitol was added to each sample, boiled at 100°C for 5 mins and immediately placed on ice for 2 mins. About 5.63-9.37µg of protein was loaded in a 7.5% SDS-PAGE gel and separated by electrophoresis at 100V for approximately 70 minutes. The proteins were transferred to immobilon®-FL PVDF membrane using the Trans-Blot® Turbo™ Transfer System (Bio-Rad) for 7 minutes. The membrane was incubated in Odyssey blocking buffer (TBS) for 60 minutes to block nonspecific binding sites followed by incubation in TBS containing 0.2% of tween20 (TBS-T) and the iNOS antibody (1:1000 dilution) for 18 hours at 4°C. After that, the membrane was washed 4 times with TBS (0.1% tween20) and incubated in TBS-T with the secondary antibody (1:20000 dilution) for 1 hour then extensively washed in TBS, visualized by *LI-COR* Odyssey infrared imager and analyzed using Image Studio Lite Software Version 5.2.

Statistical analysis was performed in Microsoft Excel using one-way ANOVA followed by a benferroni corrected t-test with statistical significance set at a 95% confidence level ($P<0.05$).

2.2 Results

2.2.1 Real-time NO detected under normal and high glucose conditions

HDFa were cultured in the CellNO trap in either normal (5.5mM) or high glucose (25mM) media with and without stimulation by the inflammatory cytokine interferon gamma (IFN-Y) and bacterial endotoxin lipolysaccharide (LPS). The NO production was measured for 24 hours (**Figure 2-1**)[42].

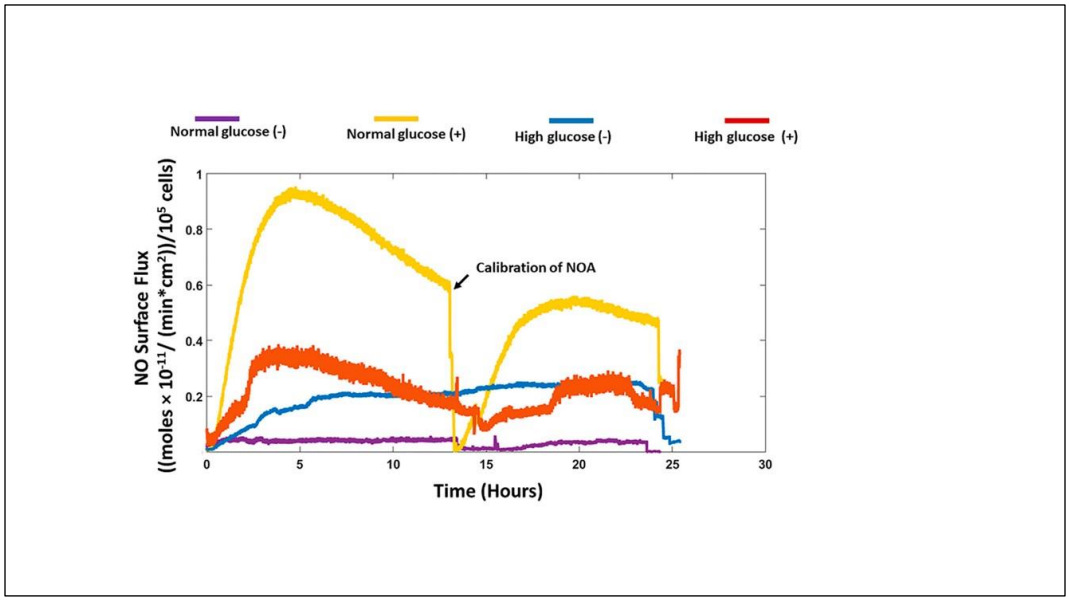

Figure 2-1. The real-time NO release from HDFa with (+) and without (-) stimulation cultured under normal (5.5mM) and high glucose (25mM) conditions. Arrow represents calibration of NOA. Image copied from [42]. The right to use this material is licensed under Creative Commons Attribution 4.0 International License.

The cells cultured in normal glucose media in the absence of stimulation showed a slight increase in NO release in the first 1 hour which peaked at 0.25×10^{-12} moles/min·cm^2 and gradually went down to undetectable NO production up to 24 hours. HDFa cultured in high glucose media without stimulation showed an increase in NO production which peaked at 0.56×10^{-12} moles/min·cm^2 and remained constant for 24 hours. With stimulation, there was an increase in the NO production for cells cultured in normal glucose media, which peaked at 2.03×10^{-12} moles/min·cm^2 and gradually dropped to 0.76×10^{-12} moles/min·cm^2. At 12 hours, the NOA was disconnected and recalibrated to confirm the validity of the signal obtained (Arrow denoting the sudden drop in curve in Figure 1). The NO detected remained

constant at 0.44×10^{-12} moles/min·cm^2 from 15 to 24 hours. The NO release for cells cultured in high glucose media followed a similar trend but with lower NO detected, which peaked at 0.93×10^{-12} moles/min·cm^2 at 5 hours and gradually dropped to 0.23×10^{-12} moles/min·cm^2 at the end of 24 hours. The viability of the cells cultured in the CellNO trap device in normal and high glucose culture conditions with and without stimulation by IFN-Ɣ and LPS was analyzed by the live/dead assay at the end of the real-time NO measurements. The cells maintained over 95% cell viability in all the treatment groups (**Figure 2-2**).

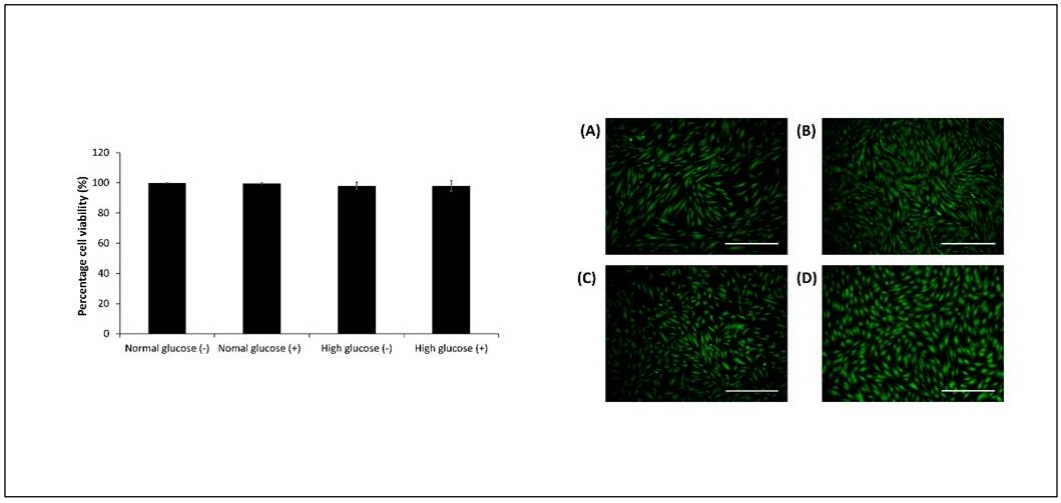

Figure 2-2. Cell viability detected by calcein AM and ethidium bromide for HDFa cultured in normal (5.5mM) glucose condition without and with stimulation, A and B respectively and high glucose (25mM) condition without and with stimulation C and D respectively. **S**cale bar 500µm. The results are presented as the mean ± standard deviation for n=3, *p<0.05. Image copied from [42]. The right to use this material is licensed under Creative Commons Attribution 4.0 International License.

2.2.2 Nitric oxide detected from nitrite accumulation in the absence and presence of stimulation

After the real-time NO measurements, the nitrite accumulated in the cell culture media was collected and analyzed for NO release using the triiodide assay (**Figure 2-3**). The nitrite present in the media is reduced in the presence of an acid and nucleophile to produce NO that is measured via chemiluminescence detection.[25] Normal glucose conditions without stimulation had significantly lower NO levels produced from nitrite compared to normal glucose conditions with stimulation (0.73±0.05 versus 3.68±0.98 nmol/10^5 cells, $p<0.05$ for n=3). In high glucose conditions, there was no statistical difference in the levels of NO detected without stimulation compared to stimulation with LPS/IFN (0.91±0.70 versus

4.26±2.11 nmol/10^5 cells). In the absence of stimulation, the NO detected from nitrite in normal glucose conditions compared to high glucose were not significantly different (0.73±0.05 vs 0.91±0.70 nmol/10^5 cells). Similarly, with stimulation, the NO detected from nitrite was not statistically different in normal glucose compared to high glucose (3.68±0.98 vs 4.26±2.11 nmol/10^5 cells).

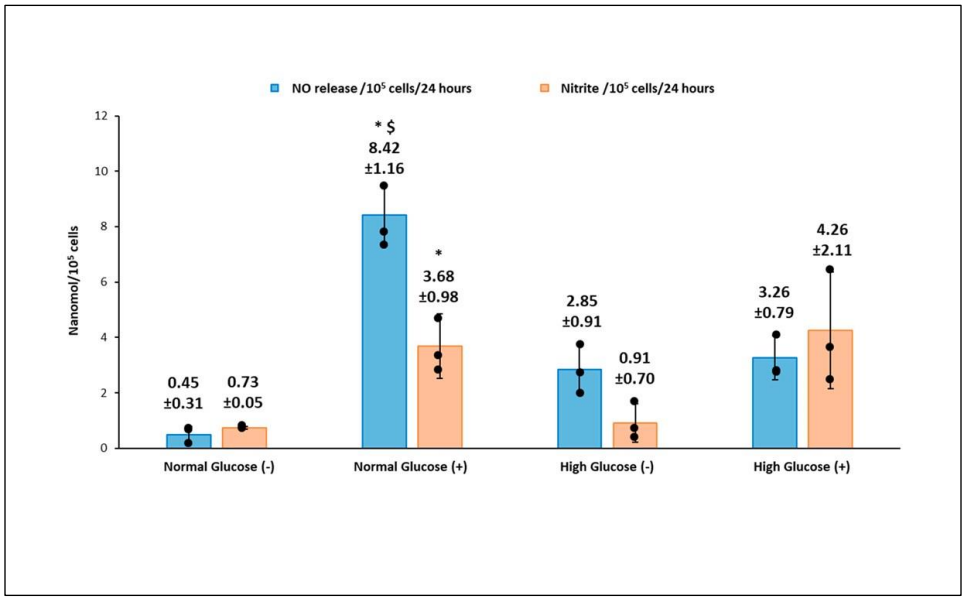

Figure 2-3, Total NO compared to nitrite accumulation determined for HDFa with and without stimulation under normal and high glucose conditions. (for n=3, there is statistically significant difference at $p<0.05$: ***** Normal glucose (LPS/IFN) vs Normal glucose (without stimulation); **$** Normal glucose (LPS/IFN) vs High glucose (LPS/IFN). Image copied from [42]. The right to use this material is licensed under Creative Commons Attribution 4.0 International License.

2.2.3 Comparison of real-time NO measurements and nitrite accumulation

The total NO detected in real-time for the HDFa was integrated as the area under the curve (**Figure 2-3**) and was compared to the NO inferred from nitrite present in the cell culture media for the 4 treatments groups (Figure 3, N=3). lists the total amount of NO and nitrite produced by each test group. The results showed that the levels of real-time NO detected in nmol/10^5 was significantly higher for cells in normal glucose conditions with stimulation (8.42±1.16 $p<0.05$ for n=3) compared to without stimulation (0.48±0.31 for n=3 $p<0.05$). Similarly, under identical conditions, nitrite accumulation was significantly higher in normal glucose with stimulation (3.68±0.98) compared to absence of stimulation

(0.73±0.05 for n=3 $p<0.05$). It is interesting to note that there was a higher direct NO measured compared to nitrite. However, high glucose conditions did not show the same trend. The levels of real-time NO detected with stimulation were not statistically different from levels of real-time NO without stimulation (3.26±0.79 and 2.85±0.91 nmol/10^5cells respectively). The NO levels obtained from nitrite measurement depicted a similar trend as the real-time NO measured, with no statistical difference in high glucose conditions with stimulation compared to high glucose without stimulation (4.26±2.11 and 0.91±0.70 nmol/10^5 cells). The real-time levels of NO and nitrite detected in normal glucose conditions without stimulation was also not statistically different from the real time NO detected from the cells in high glucose conditions without stimulation (0.48±0.31 and 3.26±0.79 vs 0.73±0.05 and 0.91±0.70 nmol/10^5cells respectively for n=3 $p<0.05$). Moreover, in normal glucose conditions with stimulation, the levels of real-time NO detected was significantly higher compared to high glucose conditions with stimulation. The nitrite levels were not statistically different. (8.42±1.16 and 3.26±0.79 versus 3.68±0.98 and 4.26±2.11 nmol/10^5cells respectively).

2.2.4 Cell characterization of HDFa cultured in normal and high glucose conditions

HDFa cultured in normal and high glucose media were assessed for the presence of CD90 (Thy-1), which is a reliable molecular marker used to identify fibroblast cells in culture[171]. HDFa maintained uniform staining for CD90 (Thy-1) protein in normal (Figure 2-4**a**) and high glucose conditions (Figure 2-4**b**) as well as the elongated and spindle shape that is characteristic of confluent fibroblast cells.

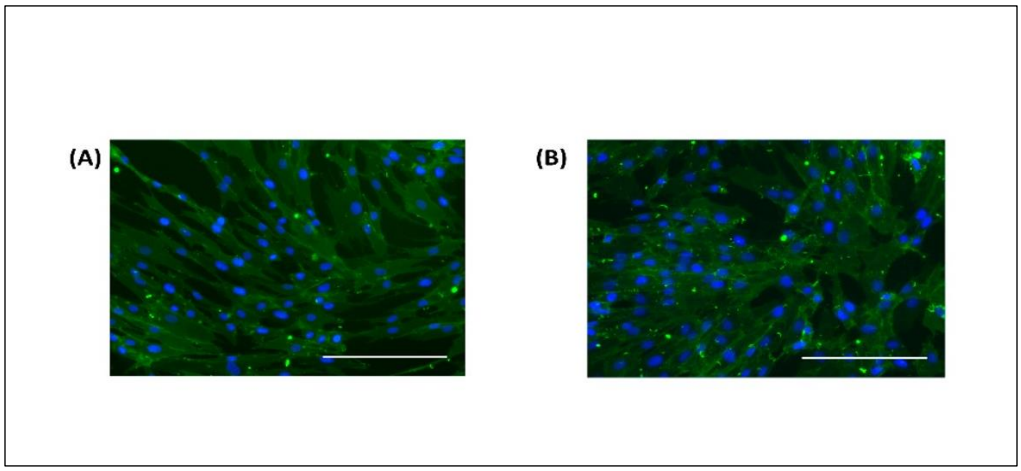

Figure 2-4. Immunofluorescent staining of CD90 (Thy-1) (green) in HDFa cultured in (**A**) Normal and (**B**) High glucose conditions. Cell nuclei (blue). Scale bar 200µm. Image copied from [42]. The right to use this material is licensed under Creative Commons Attribution 4.0 International License.

2.2.5 Expression of iNOS protein in HDFa cultured in normal and high glucose conditions

Stimulation of fibroblasts by inflammatory cytokines and bacterial endotoxins has been reported to upregulate the enzyme iNOS, which is directly responsible for the production of NO in the cells. We assessed the levels of iNOS in HDFa cultured in normal and high glucose conditions with and without stimulation by western blot technique. The results show that overall the iNOS enzyme was present in all treatment groups and the protein level was very low. Macrophage cell lysates (RAW 264.7) that are known to express iNOS when stimulated with LPS and the mouse iNOS enzyme protein were used as positive controls. Faint iNOS bands can be seen in the human fibroblast cells, which appear at the same molecular weight as the iNOS in macrophage cells and the mouse iNOS enzyme (**Figure 2-5**). There was no statistical difference in intensity found between the groups at $P<0.05$ for n=3.

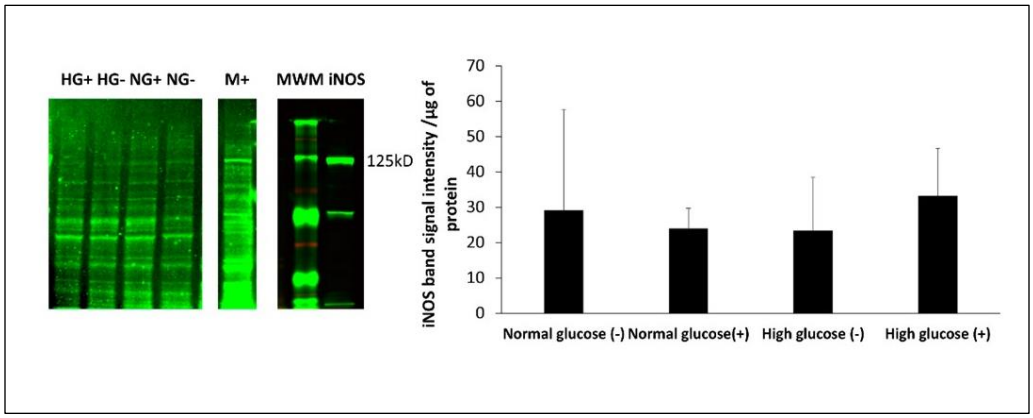

Figure 2-5. Detection of iNOS expression by western blot analysis of HDFa cultured in normal (**NG**) and high glucose (**HG**) conditions with (+) and without (**-**) stimulation. Predicted band size for iNOS 131 kD and observed band size 125kD with **iNOS** and RAW 264.7 (**M+)** as positive controls. Image copied from [42]. The right to use this material is licensed under Creative Commons Attribution 4.0 International License.

2.2.6 Effect of normal and high glucose conditions with and without stimulation on the proliferation of HDFa cells.

The proliferation rate of HDFa cells cultured in normal and high glucose conditions with and without stimulation by IFN-Y and LPS was assessed by the MTT proliferation assay for 24 to 72 hours. The cells that are metabolically active reduce the tetrazolium salts in the MTT reagent to intracellular purple formazan crystals, which when solubilized can be read at an absorbance of 570nm and correlated to the proliferation of the cells[172]. In normal glucose conditions in the absence and presence of stimulation there was an increase in cell proliferation from 24 to 72 hours (0.08 to 0.14 and 0.08 to 0.12 respectively). High glucose conditions with no stimulation showed a slight drop in absorbance from 24 to 48

hours (0.07 to 0.06) and an increase to 0.15 at 72 hours. High glucose conditions with stimulation also showed an increase in absorbance; 0.06 at 24 hours to 0.09 at 72 hours. Overall, there was no statistical difference between the treatment groups at 24, 48 and 72 hours (n=3 $P<0.05$ (**Figure 2-6**)[2]

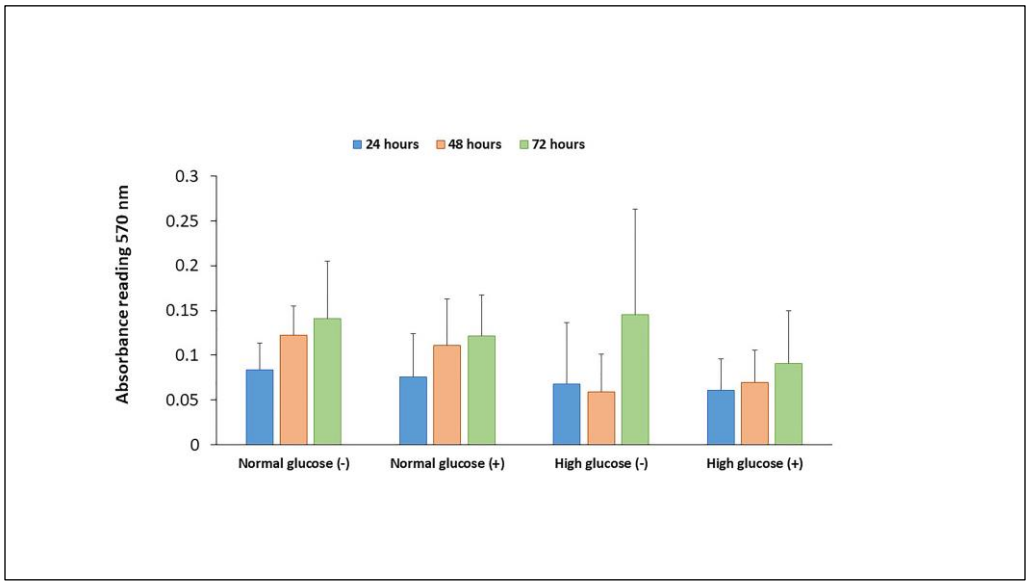

Figure 2-6. The rate of proliferation observed in HDFa cultured in normal (5.5 mM) and high glucose (25mM) conditions with (+) and without (-) stimulation from 24 to 72 hours. Three independent experiments were performed in triplicates (n=3). P value <0.05 was considered statistically significant. Image adopted from [42]. The right to use this material is licensed under Creative Commons Attribution 4.0 International License.

2.3 Discussion

Diabetic foot ulcers remain an immense challenge with debilitating consequences and no adequate treatment. One of the major problems in the delayed healing of these wounds is the senescent nature of fibroblasts and their inability to proliferate and produce extracellular matrix that will aid in the migration of keratinocytes across the wound bed [18, 19, 168, 173, 174]. NO is widely implicated as a major player in the wound healing process and studies have shown that fibroblast cells produce NO [43, 44, 175, 176]. Whether or not this NO production is consistent even in the absence of stimulation is still a matter of debate. Moreover, the spatial and temporal NO production and levels that

[2] The color to the bar graphs was changed from the original image to match the theme of the dissertation.

fibroblast cells experience is not known. The Griess assay used by previous authors only looks at the accumulated NO release at single point in time and this method of analysis measures nitrite, the stable end product of NO, not NO itself. The availability of NO to regulate biological functions greatly relies on various factors such as the dose, duration, location of NO production as well as the surrounding environment [90, 177, 178]. Therefore, the presence of nitrite in the cell culture media might not automatically translate to the level of NO generated and therefore cast doubt on the causal relationship NO may or may not actually have in the physiological environment [177, 178]. Wound healing is a dynamic process and understanding how the levels of NO production in the cells at the wound site changes over time is of utmost importance in exploring the possible use of NO to treat DFUs.

We recorded the real-time production of NO from fibroblast cells under normal and high glucose conditions with and without stimulation by the bacterial endotoxin LPS and inflammatory cytokine IFN-Y. The results obtained were then compared to the nitrite accumulation in the cell culture media. HDFa cells in normal glucose conditions with stimulation showed that significantly higher NO was detected compared to HDFa cultured in normal glucose conditions without stimulation (8.42±1.16 vs 0.48±0.31 nmol/10^5cells, $p<0.05$ for n=3). Stimulation by LPS and IFN-Y is thought to upregulate the expression of iNOS and consequently NO production in a variety of cells including human and rodent fibroblasts[43, 179]. In cells such as macrophages, the production of NO acts as a host defense mechanism to fight off infection [29, 176]. In the normal wound healing process, the production of NO in fibroblast cells could act to regulate the inflammatory response at the wound site[43]. Alternatively, and/or additionally the production of NO could be associated with regulation of cell proliferation, collagen deposition or angiogenesis, which would show its possible role in the proliferation stage [43, 44, 176]. The NO detected from the cells cultured in high glucose media with stimulation was not significantly different from the NO detected in non-stimulated cells cultured in the same media. Interestingly, cells cultured in normal glucose conditions in the absence of stimulation showed barely detectable levels of NO while NO levels in high glucose conditions without stimulation was significantly higher (Figure 2-1 and 2-3). Schaffer et al. showed that fibroblast cells do not produce NO unless they are phenotypically altered to produce NO (wound fibroblasts)[44]. However, Wang et al showed that fibroblast cells spontaneously produce NO even in the absence of stimulation[43]. The levels of glucose used in the cell culture media were not specified in Wang's study. High glucose DMEM media that is routinely used in culture of a variety of mammalian cells contains 25mM of glucose, which is four times greater than clinically relevant glucose levels (5.5-7mM)[4]. Therefore, the levels of glucose in the cell culture media could possibly explain the discrepancy reported in the literature. Cells cultured in normal glucose conditions with stimulation had significantly higher levels of NO detected compared to stimulated cells cultured in high glucose conditions (Figure 2-3). Low levels of NO and reduced nitric oxide synthase levels in the diabetic state has been strongly associated with the development of DFU and impaired wound healing [85, 133, 180]. Schaffer et al found that low NO levels correlated with reduced collagen deposition and wound strength in wounded diabetic mice compared to healthy mice[44]. The mechanism of low NO levels in the diabetic state is still unclear but

evidence points toward the increased production of reactive oxygen species, such as superoxide, that rapidly inactivate NO, reducing its bioavailability in the cells[176, 178]. It is worthwhile to note that all of these studies only looked at nitrite accumulated in the cell culture media and not NO levels directly exposed to the surface of the cells. Our work has shown that the NO and nitrite levels are different under normal and high glucose conditions and the variability is further compounded when stimulated by NO inducing factors such as LPS and IFN-Y. The real-time NO measurements were compared to the nitrite accumulated in the cell culture media. The levels of real-time NO in normal glucose conditions directly correlated with the nitrite levels in the presence and absence of stimulation. However, high glucose conditions showed a discrepancy in real-time NO and nitrite levels detected (in both cases, the results were not statistically different, but the difference observed suggests further study is warranted). Human aortic endothelial cells cultured in high glucose media has been shown to have higher levels of nitrite compared to cells cultured in normal glucose conditions in the absence of stimulation[181]. In another study, nitrite levels were suppressed in human renal endothelial and mouse schwan cells cultured in high glucose media compared to normal glucose media[131, 182]. The contradicting results obtained from these studies further illustrates that measuring only nitrite in the media is not sufficient to assess actual NO production and thereby attribute specific effects of NO on different cellular processes especially under a pathological state such as diabetes.

The iNOS enzyme is thought to be upregulated when cells are stimulated by inflammatory mediators. We analyzed the expression of iNOS in fibroblast cells in normal and high glucose levels with and without stimulation by LPS AND IFN-Y. The iNOS enzyme was found in both normal and high glucose conditions in the absence and presence of stimulation. Although, the expression was very low with no statistical difference between the 4 treatment groups. Fibroblast cells produce low amounts of NO, which could explain why the enzyme expression in the cells was low. To support this view, Wang showed that with immunocytochemical staining, only few stimulated fibroblast cells stained intensely for iNOS, while majority of the cells showed weak staining. Some unstimulated fibroblast cells also showed weak expression of iNOS. Interestingly, histological staining on the dermal tissue was negative for iNOS[43]. There are various factors in the cell culture system that could potentially affect cell response. An example of rat hepatocytes was reported by Halliwell; Isolation of the cells from the tissue was found to activate iNOS in the absence of stimulation. The author also reported that the oxygen levels in in vitro cell culture systems (150mmHg) was found to be much higher than the physiological levels of oxygen that the cells are exposed to in vivo (1-10mmHg)[183]. These high levels of oxygen are associated with increased production of reactive oxygen species (ROS). Reactive oxygen species activate the Nuclear factor-kappa B (NF-KB) signaling pathway that leads to transcription of iNOS mRNA and increased expression of the iNOS enzyme[184]. Moreover, ROS such as superoxide rapidly react with NO forming peroxynitrite. The NO deficiency in the cell environment is hypothesized to activate a feedback mechanism that upregulates iNOS expression[185]. In regards to these findings, we speculate that other factors including the levels of glucose present in the cell culture environment might explain the differences of nitrite levels compared to the real-time levels of NO observed.

Nitric oxide has been shown to regulate the proliferation of cells and production of extracellular matrix[186, 187]. In the diabetic wound, fibroblast cells do not proliferate adequately and there is reduced secretion of extracellular matrix, which is a key component for the migration and differentiation of keratinocyte cells [18, 19, 31]. Xuan et al have explored the effect of high glucose on human foreskin fibroblast proliferation with no significant difference at up to 60mM of glucose concentration (media supplemented with 10% FBS)[188]. In Schaffer's study inhibition of endogenous iNOS production in mouse wound fibroblasts did not affect proliferation[44]. While Shi et al showed reduced proliferation of dermal fibroblast cells isolated from iNOS knock out mice compared to wild type mice[189]. The correlation between glucose levels in the presence of inflammatory mediators that stimulate NO production and its effect on human dermal fibroblast cell proliferation has not been previously reported. We looked at the effect of normal and high glucose conditions with and without stimulation of NO production on the proliferation of fibroblast cells. The results show that overall there was no statistical difference between normal and high glucose conditions in the absence and presence of stimulation from 24 to 72 hours (Figure 6). However, the proliferation was lower in high glucose condition with stimulation at 48 and 72 hours compared to normal glucose with and without stimulation at the same time points, which prompts further investigation.

2.4 Conclusion

Our study showed that human dermal fibroblast cells cultured in normal glucose conditions with stimulation show significantly higher levels of NO compared to cells cultured in high glucose conditions with stimulation (8.42±1.16 and 3.26±0.79 nmols/10^5 cells $p<0.05$ for n=3). The nitrite levels in normal glucose conditions showed consistency with the real-time NO levels in normal glucose conditions with low nitrite levels in the absence of stimulation and a significant increase when the cells were stimulated. In contrast, there was no significant difference between the real-time NO measured and the nitrite levels that accumulated in the media in high glucose conditions with and without stimulation (Figure 3). The nitrite level in the media is not a reliable proxy for the actual level of NO produced by the cell. The iNOS enzyme that produces NO when cells are stimulated with inflammatory mediators was expressed at a low level in all the treatment groups and the proliferation of fibroblast cells from 24 to 72 hours showed no statistical difference between normal and high glucose conditions in the absence or presence of LPS and INF-ɣ (Figure 5 and 6 respectively). The results presented here clearly illustrate why nitrite accumulation should not be used to predict NO production in cells and clearly indicates that real-time NO measurement is essential in providing information that will allow a more complete understanding of how NO may affect the proliferation, migration and formation of extracellular matrix in fibroblast cells as well as the NO production in other cells present at the wound site. If we accurately measure the actual levels of NO produced by cells cultured under specific conditions, including the temporal NO release profile, we can understand and mimic the physiological NO release at different stages of wound healing and different pathological states, which will facilitate a smooth transition of the wound

from its chronic state into resolution, consequently, shortening the time to complete healing of DFU.

3 INVESTIGATIVE STUDY OF REAL-TIME NO MEASUREMENTS IN WOUND FIBROBLAST CELLS IN NORMAL AND HIGH GLUCOSE CONDITIONS[3]

Nitric oxide plays a key role in cardiovascular, immunology and respiratory physiopathology. In patients affected with coronary artery disease who were undergoing surgical procedures, the continuous administration of the NO drug nitroglycerin significantly reduced the risk of myocardial infarction compared to control patients[190]. Another study reported a very impressive reduction in mortality for patients with advanced heart failure treated with another NO drug isosorbide dinitrate[156]. For pediatric patients, exhaled NO is a non-invasive diagnostic tool to identify the severity of asthmatic episodes and control the administration of corticoid treatments[191]. However, its role in wound healing is not as well defined. Several studies have shown the beneficial effect of NO treatments in invitro models of migration ad cell proliferation as well as accelerated healing in mouse models (**Table 1-3**). In addition, the previous chapter and other researchers have demonstrated NO levels and iNOS protein expression or activity from normal human skin fibroblasts[43, 192]. Unfortunately, the translation of the results obtained in vivo and invitro have not been as straight forward in clinical application. Only one study so far has shown a positive effect of NO treatment in patients affected with DFU but even in this study, the major criticisms was that the absolute effect of NO on improved healing in these patients compared to patients treated with the control could not be determined [149, 193]. Moreover, the NO levels at the wound site was also not known [193]. A number of studies have reported the nitrite and nitrate levels in the wound fluid of acute and chronic wounds which could be an indicator to estimate correlation of NO to the healing of wounds in the patient[194-196]. However, it does not provide information on the timing/dose of NO required or which cells are responsible for the NO production at the time the samples are collected or when the measurements are taken. The majority of these studies also rely on the Griess assay which has been proven to have a wide range of variability and low sensitivity [151, 152]. Cells produce varying NO levels at different stages of the wound healing process. The unpredictable and delicate environment of chronic wounds further complicates this NO production in the cells. Without precisely comparing the levels of nitrite/nitrate in the wound fluid to the actual levels of NO produced from the cells present at the wound site, it is inaccurate if not impossible to determine the effect of NO on the wound healing cascade even when the NO treatment is applied. In this chapter, the NO levels produced from wound fibroblasts isolated from a patient with a chronic ulcer is determined. In addition, using highly sensitive chemiluminescence detection the nitrite levels in the cell culture media and at the wound site are also measured and compared to the real-time NO levels detected from the cells.

[3] Part of the work in this chapter will be submitted to a journal for future publication

3.1 Materials and Methods[4]

3.1.1 Cell culture and chemical supplies

Primary human adult dermal fibroblasts (HDFa, ATCC® PCS-201-012™,), mouse macrophages (RAW 264.7), penicillin streptomycin, fetal bovine serum (FBS), phosphate buffered saline (PBS), and Dulbecco's modified eagle medium (DMEM high glucose 4500mg/l) were all purchased from ATCC (Manassas, VA). Human aortic endothelial cells were purchased from Gibco life technologies (Carlsbad, CA). DMEM (no glucose), sodium pyruvate and Hoescht dye were obtained from Fischersci (Hanover Park, IL). D-(+)-Glucose, Lipopolysaccharide *pseudomonas aeroguinosa* (LPS), Calcein-AM, protease inhibitor cocktail, mouse nitric oxide synthase and dopamine-HCl were purchased from Sigma-Aldrich (St. Louis, MO). Ethidium bromide was acquired from Invitrogen (Grand Island, NY). Human recombinant Interferon gamma (hrIFN-Y) was purchased from GenScript (Piscataway, NJ). The primary and secondary antibodies against CD90/Thy1 (ab23894) protein and nitric oxide synthase (PAN 2977) were purchased from Abcam (Cambridge, MA) and cell signaling technology (Danvers, MA) respectively. The 7.5% SDS polyacrylamide gels and gelatin were acquired from Bio-Rad (Hercules, CA). The Odyssey western blot starter kit 2 was obtained from *LI-COR* (Lincoln, NE). Silicone elastomer base and curing agent (Dow Corning Sylgard®184) were obtained from ML Solar LLC (Campbell, California). Sodium nitrite and nitrate, potassium iodide, Aspergillus nitrate reductase, nicotinamide adenine dinucleotide phosphate hydrogen (NADPH), flavine adenine dinucleotide (FAD) potassium mono and dibasic phosphate (KHPO4) were all purchased from Millipore sigma (St. Louis, MO, USA). Glacial acetic acid was obtained from BDH analytical chemicals VWR (Batavia, IL, USA).

3.1.2 Biopsy tissue and wound fluid collection

A biopsy sample and wound fluid were obtained from a patient in an ongoing clinical study (IRB Number 1146644-4)) following procedures approved by the institutional review board of Michigan Technological University. The sample was immediately processed for cell isolation by a procedure adopted from Vangipuram et al [197].

3.1.3 Cell characterization

The wound cells at passage 3 were cultured in 12 well plates at a cell density of $1 \times 10^4/cm^2$ in normal (5.5 mM) and high glucose (25 mM) conditions. At confluency, the cells were fixed in 4% paraformaldehyde for 10 minutes, rinsed 3 times in phosphate buffered saline, incubated in blocking buffer for 90 minutes followed by the primary antibody for 18 hours at 4°C. The cells were rinsed 3 times in blocking buffer and incubated for 1 hour at room

[4] The materials and methods were adopted from chapter 2 [42]. The rights to use the content is presented in appendix C and licensed under Creative Commons Attribution 4.0 International License.

temperature with the secondary antibody, stained with 4', 6-diamidino-2-phenylindole (DAPI) and viewed under an Olympus fluorescent microscope (model BX51).

3.1.4 Real time NO measurements from wound fibroblasts

Primary wound dermal fibroblasts from passage 2-5 were cultured and expanded in conventional cell culture plates (100mm) in DMEM (high or normal glucose levels), 10% FBS and 1 % penicillin/streptomycin (complete growth media). At confluency, the cells were reseeded in the CellNO trap devices at a density of 0.25-1 $\times 10^4$ cells/cm^2. The devices were made using the procedure that was previously described[152]. After 24-72 hours, the cell culture media was changed and substituted with media containing 40µg/ml of LPS and 200 U/ml of hrIFN-Ɣ or complete growth media (control) under normal glucose (5.5mM) and high glucose (25mM) conditions. The device was placed in a standard incubator (37°C, 65% humidity, 5% CO_2) and was connected to a calibrated nitric oxide analyzer (NOA) and the real-time NO release profile was measured for 24 hours.

3.1.5 Cell viability assay in the CellNO trap device

After 24 hours, the live-dead assay was carried out using 2µM calcein AM, 2µg/ml ethidium bromide and 10µg/ml Hoescht dye in DMEM media for 10-15 minutes. The cells were imaged and analyzed using an Olympus fluorescent microscope (model BX51) and Image J1 respectively[169].

3.1.6 Nitrite assay

After 24 hours of measurement in the CellNO trap device, the cell culture media from the cell samples under normal and high glucose conditions were collected. The triiodide assay was used to measure the nitrite accumulation in the media[74]. Briefly, 50µl of the media was added to a vial containing a stirring solution of 300µl of glacial acetic acid and 120µl of potassium iodide. The vial was connected to a calibrated Sievers Nitric Oxide Analyzer 280i (Zysense, LLC, Boulder, CO, USA) and the NO produced from the nitrite present in the media was measured and normalized to the number of live cells.

3.1.7 Western blot analysis

Confluent wound fibroblast cells cultured in 100mm diameter tissue culture dishes were, stimulated with 40µg/ml of LPS and 200U/ml IFN-Ɣ in normal and high glucose conditions and incubated for 72 hours. Mouse macrophage cells RAW 264.7 grown to confluency and stimulated with 1ug/ml of LPS for 18 hours and human aortic endothelial cells served as positive controls for iNOS and eNOS respectively. The cells were quickly washed in ice cold PBS, trypsinized, centrifuged and re-suspended in 200µl of RIPA buffer in the presence of protease cocktail inhibitors. The cell lysates were incubated for 30

minutes on ice on a plate shaker and centrifuged at 12,000 rpm for 20 minutes at 4°C. The supernatant was collected, and the protein concentration determined for each sample using Bradford assay[170]. An equal amount of loading buffer containing dithiothreitol was added to each sample, boiled at 100°C for 5 mins and immediately placed on ice for 2 mins. Approximately 10-14µg of protein was loaded in a 7.5% SDS-PAGE gel and separated by electrophoresis at 100V for approximately 70 minutes. The proteins were transferred to immobilon®-FL PVDF membrane using the Trans-Blot® Turbo™ Transfer System (Bio-Rad) for 7 minutes. The membrane was incubated in Odyssey blocking buffer (TBS) for 60 minutes to block nonspecific binding sites followed by incubation in TBS containing 0.2% of tween20 (TBS-T) and the iNOS antibody (1:1000 dilution) for 18 hours at 4°C. After that, the membrane was washed 4 times with TBS (0.1% tween20) and incubated in TBS-T with the secondary antibody (1:20000 dilution) for 1 hour then extensively washed in TBS, visualized by *LI-COR* Odyssey infrared imager and analyzed using Image Studio Lite Software Version 5.2.

3.1.8 Nitrite and nitrate measurements from wound fluid

Swabs containing wound fluid were sterilized under ultraviolet light for 1 hour prior to experiments performed. The swabs were soaked in 500 µl of deionized water and sonicated for 10 minutes. These samples were prepared for nitrite and nitrate measurements using a procedure adopted from Gilliam et al with minor modifications[198]. Briefly for each nitrite standard solution, final reaction volume containing 40 µl of 0.14M of potassium phosphate buffer pH 7.5, 35 µl of deionized water and 25 µl nitrite standard was prepared. For the nitrate standards, a final reaction volume containing 40µl of 0.14M $KHPO_4$ buffer (pH 7.5), 26.8µl of deionized water, and 2.5 µl OF 100 µM FAD, 4µl OF 2.5mM NADPH, 25 µl of standard and 1.7 µl of 3.5U/ml of nitrate reductase was prepared. The samples were left to incubate for 24 hours at room temperature to convert all nitrate into nitrite.

3.1.9 Nitrite and nitrate standards preparation

Stock solutions of nitrite and nitrate standards were prepared to a final concentration of 10 mM in deionized water. The stock solutions were diluted in deionized water to make standard solutions ranging from 0- 50 µM and 0-150µM. The solutions were prepared as previously described.

3.1.10 Blinded concentrations of nitrite and nitrate

Three standard samples containing different ratios of nitrite and nitrate concentrations were prepared using the same procedure for the nitrite and nitrate calibration standards. Another researcher was blinded to the concentrations of these standards during measurements.

3.1.11 Chemiluminescence detection method for nitrite measurements

50 µl of each of the standards and samples, was injected into a vial containing a bubbling solution of 300 µl of glacial acetic acid and 120 µl potassium iodide in order to reduce all the nitrite into nitric oxide (NO). The vial was connected to a calibrated Sievers nitric oxide analyzer 280i (NOA) (Zysense, LLC, Boulder, CO, USA) to measure the total NO released. The background signal from the NOA before injecting the standards and samples was averaged for 1 minute and subtracted from each data point measured prior to integrating the area under the curve. Two calibration curves were determined for nitrite and nitrate standards. The nitrite calibration curve was used to calculate the concentration in the blinded standards and clinical samples. The concentration of nitrate was determined as the difference in the nitrite and the total nitrite measured from the nitrate samples. The experiments were performed as 3-5 replicates and the data obtained was analyzed in Microsoft Excel.

3.2 Results

3.2.1 Characterization of cells isolated from biopsy sample cultured in normal and high glucose conditions

The migration of the cells from the biopsy tissue took approximately 3 weeks. The cells appeared to grow well and different cell populations could be observed within the cell culture (**Figure 2-1**).

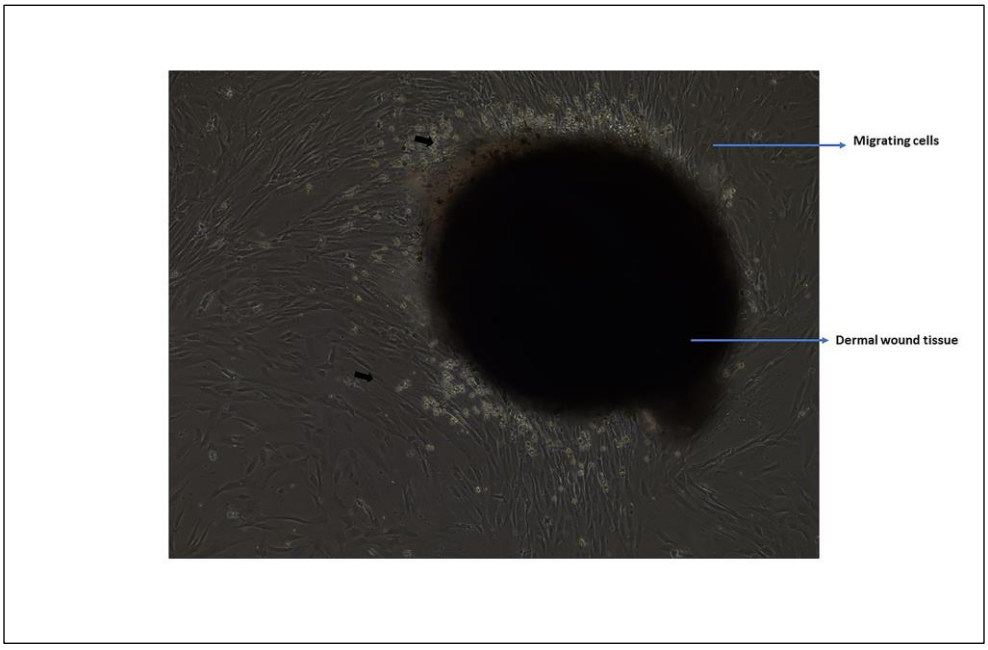

Figure 3-1. The cell isolation from a human skin biopsy sample. Arrows represent different cell populations observed

Cells at passage 3 cultured in 12 well plates in normal and high glucose conditions for 24 hours were elongated and spindle shaped which is commonly associated with confluent fibroblast cells (Figure 3-2**A** and 3-2**B**). In addition, the cells showed uniform staining of CD90, a characteristic marker frequently used to identify fibroblasts in primary cultures (Figure 3-2 **C** and 3-4 **D**).

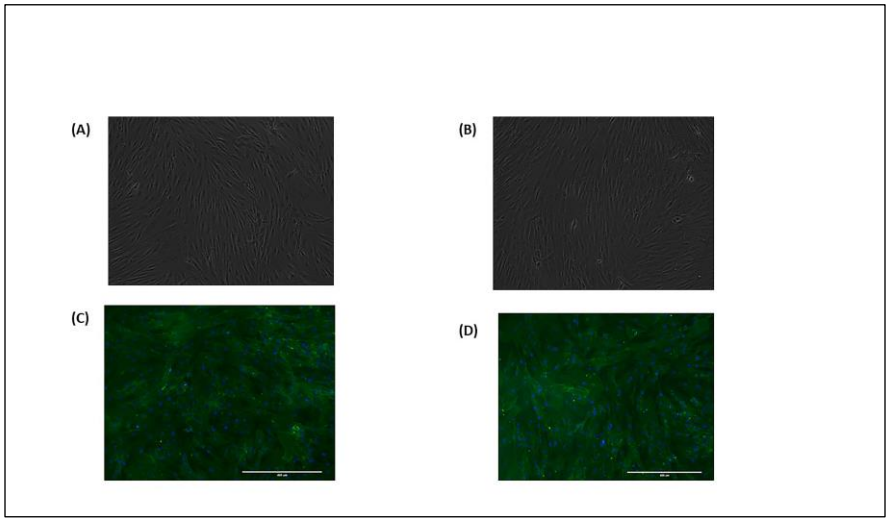

Figure 3-2. The characterization of cells isolated from the biopsy tissue. Phase contrast images showing morphological appearance of isolated cells cultured in (**A)** normal (5.5mM) and (**B)** high glucose (25mM) conditions. Immunofluorescent staining of Green (CD90) and Blue (cell nuclei) for the cells cultured in (**C)** normal and (**D)** high glucose conditions. Scale bar 400μM

3.2.2 Real- time NO measurements of wound fibroblasts cultured in normal and high glucose conditions

The real-time NO release in wound fibroblasts cultured in normal and high glucose conditions was measured for 24 hours with and without stimulation (**Figure 3-3**).

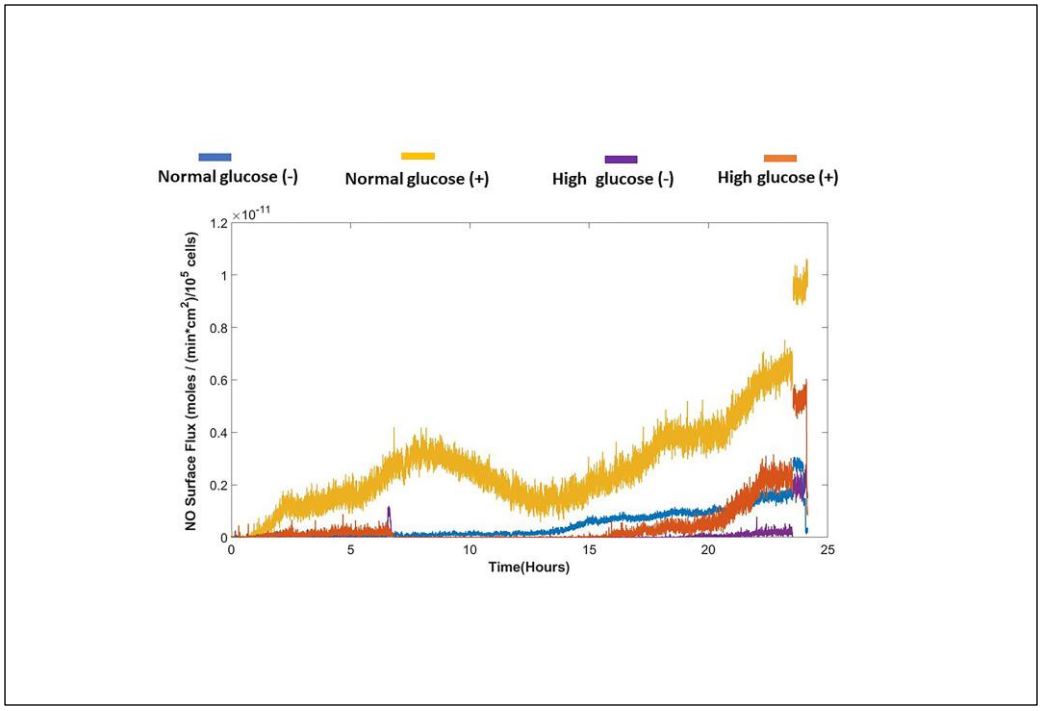

Figure 3-3. The real-time NO profile detected in wound fibroblasts cultured in normal (5.5mM) and high (25mM) glucose conditions with (+) and without (-) stimulation.

Cells cultured in normal glucose media without stimulation did not show any detectable NO measurements. When the cells were stimulated with inflammatory mediators, there was an increase in NO detected after 1 hour that peaked at 24 hours (1.03×10^{-11} (moles/(min·cm^2))/10^5cells). The cells cultured in high glucose without stimulation showed very low NO levels which also peaked at 24 hours (2.59×10^{-12}(moles/(min·cm^2))/10^5cells). When stimulated there was no detectable NO measured up to 20 hours. At this time point, there was an increase in NO detected which peaked at 24 hours but still lower than normal glucose with stimulation (5.27×10^{-12}(moles/(min·cm^2))/10^5cells). The wound fibroblasts maintained over 95% cell viability in all the treatment groups (**Figure 3-4**)

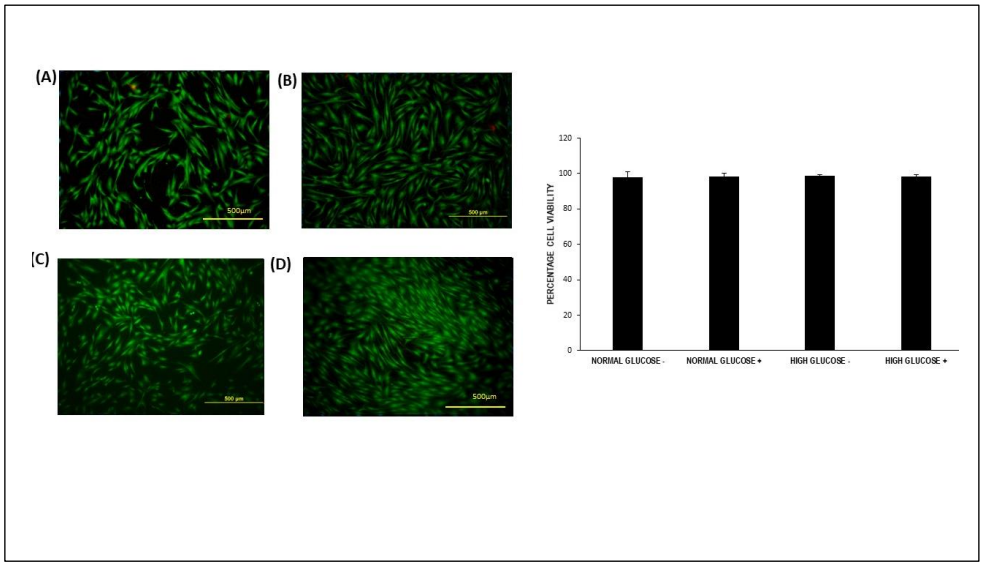

Figure 3-4. Cell viability detected by calcein AM and ethidium bromide for wound fibroblasts cultured in normal (5.5mM) glucose condition without and with stimulation, **A** and **B** respectively and high glucose (25mM) without and with stimulation **C** and **D** respectively. Scale bar 500µm.

3.2.3 Nitric oxide detected from nitrite accumulation in the absence and presence of stimulation

At the end of the real-time NO measurements, the media in the cell cultures was collected and assessed for nitrite accumulation using the triiodide assay [74]. The NO detected from the total nitrite accumulated in the media was compared to the integrated area under the curve for the real time NO detected from the cells (**Figure 3-5**). The cells cultured in normal glucose without stimulation showed absence of real time NO levels which was increased when stimulated (4.08±3.38nmol/10^5 cells). There was nitrite detected in normal glucose without stimulation, although lower compared to stimulated cell cultures (0.77±1.34 vs 1.52±2.64 nmol/10^5 cells). In high glucose conditions, both total NO and nitrite in the media could be detected in the absence of stimulation (0.61±1.06 vs 0.77±0.48 nmol/10^5 cells). However, with stimulation in high glucose conditions, there was no detectable accumulation of NO or nitrite after 24 hours. Overall there was no significant differences among all the treatment groups for 3 independent experiments.

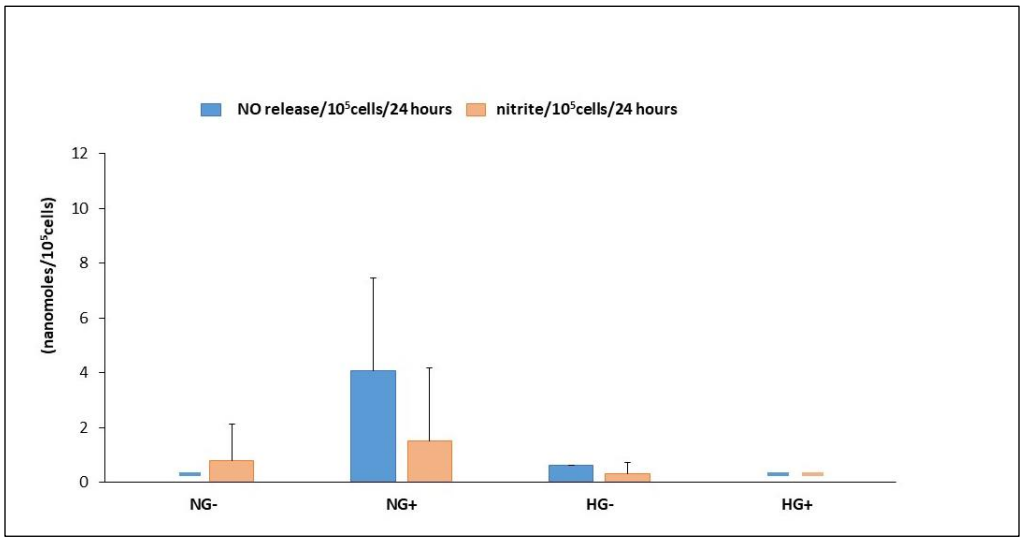

Figure 3-5. The total NO compared to nitrite accumulation in the cultured media determined for wound fibroblasts cultured under normal (**NG**) and high (**HG**) glucose conditions in the absence (-) and presence (+) of stimulation (n=3).

3.2.4 Western blot analysis for iNOS, eNOS and NF-κβ protein quantification

Wound fibroblasts at passages 2-4 were cultured in 100mm diameter dishes and at confluency were stimulated with 200U of IFN-Ɣ and 40 µg/ml of LPS for 72 hours. Western blot analysis showed absence of inducible NOS in all treatment groups (**Figure 3-6**). An independent experiment was run to determine the presence of constitutively expressed NOS isoforms (eNOS and nNOS) using a universal NOS antibody that can detect all three isoforms. RAW 264.7, human aortic endothelial cells were used as a positive control for iNOS and eNOS respectively. The results showed faint bands at the predicted molecular weight of eNOS and these bands were the same band size as the positive control (HAEC). Endothelial nitric oxide synthase levels were low in unstimulated wound fibroblasts cultured in normal and high glucose without stimulation compared to stimulated cells and in both cases the levels were higher in high glucose compared to normal glucose conditions (Figure **A1**). In addition, the protein levels of the transcription factor NF-κβ that is upstream in the pathway that leads to iNOS expression was determined and was found to be increased in stimulated wound fibroblasts cultured in normal and high glucose conditions compared to unstimulated cells. The levels were higher in high glucose with stimulation compared to normal glucose conditions (**Figure A2**).

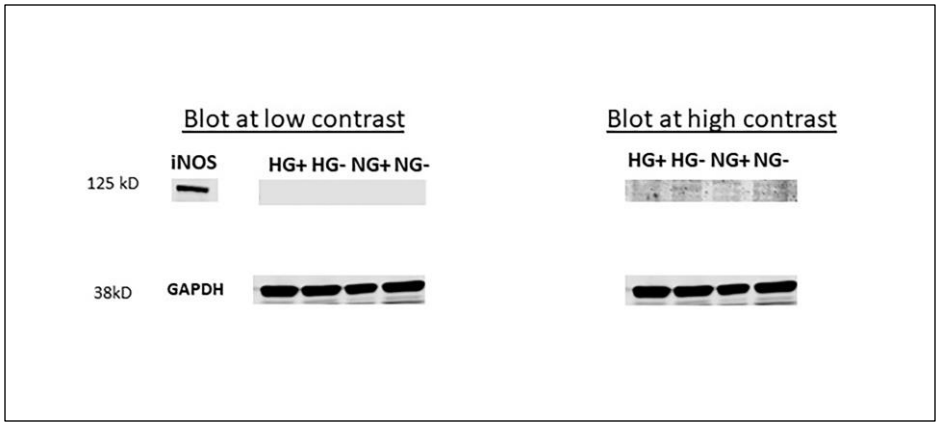

Figure 3-6 Western blot analysis to determine iNOS protein in wound fibroblasts cultured in normal glucose (**NG**) and high glucose (**HG**) in the absence (**-**) and presence (+) of stimulation (n=3). GAPDH was used as the housekeeping protein.

3.2.5 Nitrite and nitrate measurements from wound fluid

Nitrite and nitrate standard solutions were prepared with concentrations of 0-50 μM. The nitrate was converted to nitrite by the enzyme nitrate reductase and the NO released from the nitrite solutions was measured and used to obtain two calibration standard curves. **Figure 3-7** shows the linearity of the curves obtained. The results clearly indicate that the enzyme converted almost all the nitrate into nitrite. Chemiluminescence detection showed a minimum sensitivity level of 0.05-0.1μM of nitrite **(Figure A3)**. The enzyme converted nitrate concentrations of up to 150μM which was observed from the linearity and superposition of nitrite and nitrate curves of the same concentration. (**Figure A4**).

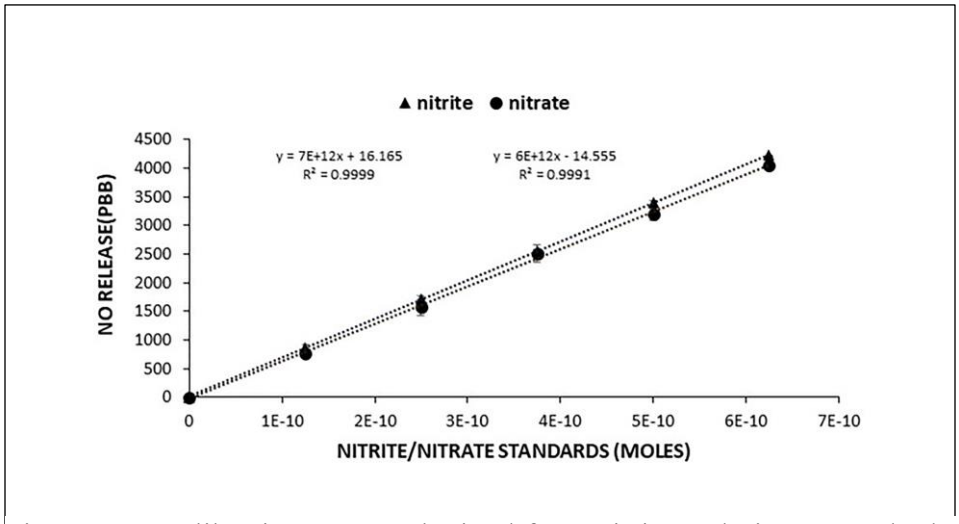

Figure 3-7. Calibration curves obtained from nitrite and nitrate standards for concentrations ranging from 0-50μM.

Three samples containing a combination of standard nitrite and nitrate concentrations were prepared and processed. The nitrate in the samples was converted into nitrite by the enzyme nitrate reductase and the nitrate was calculated by subtracting the total nitrite from the nitrite only preparations. The researcher was blinded to the concentrations in the samples during measurements. This was performed in order to determine the accuracy of our method to assess unknown levels of nitrite/nitrate present in clinical wound swab samples. Three ratios were prepared; 2:1 (**T19**), 1:1 (**T20**) and 1:2 (**T21**) of nitrite to nitrate concentrations. The analysis showed (**Figure 3-8**) that two of the samples (T20 and T21 maintained the theoretical ratio that was prepared before processing and taking measurements while T 21 showed a slight deviation of the ratio prepared (2.3:1 versus 2:1).

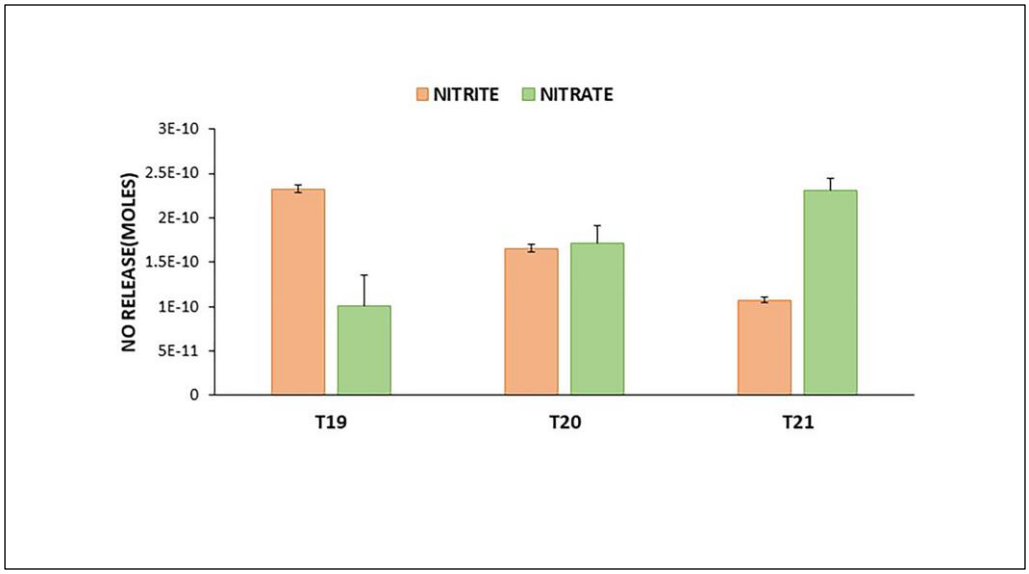

Figure 3-8. Samples containing combination of known standard nitrite and nitrate concentration. 2:1 (**T19**), 1:1 (**T20**) and 1:2 (**T21**) of nitrite to nitrate concentrations. For n=3

The data proves that it is reliable to use this method to determine nitrite and nitrate levels present in wound fluid. The swab with fluid that was obtained from the wound site from which the cells were isolated was analyzed for nitrite and nitrate using the method described above. The results (**Figure 3-9**) showed a higher nitrite concentration in the wound fluid compared to nitrate for 5 independent replicate measurements (60.25±1.79 µM vs 27.42±3.91 µM). Moreover, the NO detected was 1000-fold higher than the total direct NO measured in wound fibroblasts in both normal and high glucose conditions.

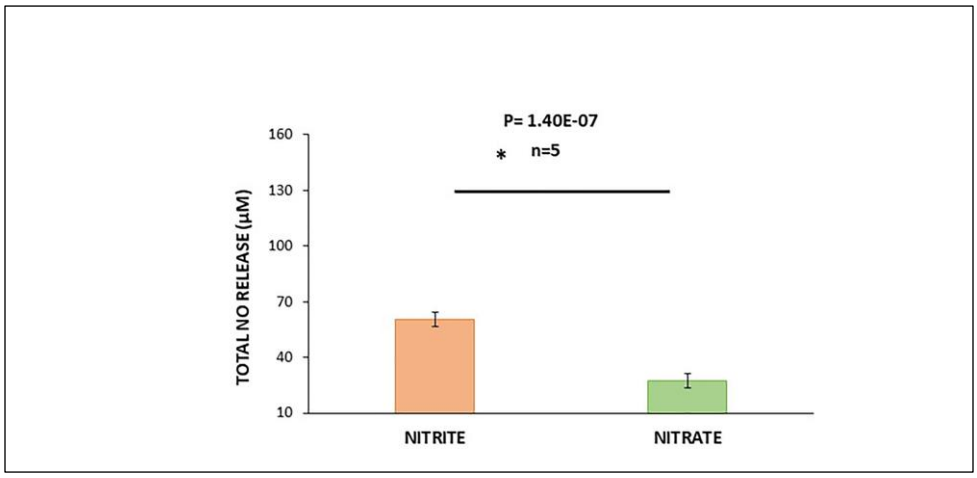

Figure 3-9. Total NO released from the nitrite and nitrate concentration measured from wound swab sample. For n=5 at $p< 0.05$ * represents statistical significance between the groups.

3.3 Discussion

The goal of this study, was to establish a protocol that can be used to assess the levels of NO produced by cells in the wounds of patients affected with DFU and compare the NO levels to the nitrite/nitrate present in the wound bed in order to clearly delineate the bioavailability of NO in the chronic wound. We were able to successfully isolate, expand and culture wound fibroblasts from a biopsy sample obtained from a patient with an ulcer. Establishing primary cultures from chronic wounds is challenging and, in some cases, the cells have a lower proliferative capacity and altered morphology compared to normal fibroblasts[199-202]. Overall, although the cell yield was lower than normal fibroblasts, the cells obtained in this study exhibited morphology and markers characteristic to fibroblasts and the cells maintained relatively uniform growth function through passage 5. Furthermore, the wound fibroblasts achieved greater than 95% viability in the NO measurement device (**Figure 3-4**). The real-time NO levels could be detected in the cells using this system. The cells cultured in normal glucose media without stimulation showed absence of NO detected which was similar to normal skin fibroblasts. When stimulated with inflammatory mediators, there was an increase in NO detected however the NO profile was markedly different (**Figure 3-3**) and lower compared to normal fibroblasts cultured under the same conditions (Figure **2-1**). The sample used in this chapter is part of an ongoing blinded clinical study (IRB 1146644-1) and therefore, it is interesting to note that the cells obtained were isolated from the biopsy of a non-diabetic patient with a chronic wound aged one year and 8 months. Studies have suggested that there is a deficiency or reduced availability of NO in chronic wounds both diabetic and non-diabetic[85, 161, 203]. In addition, chronic wounds have a common finding which is the persistent production of

reactive oxygen /nitrite species as well as a reduced antidefense mechanism[203]. This is the first study to report the levels of real-time NO produced from cells isolated from a human chronic wound and our preliminary data has shown a possible reduction of NO produced from wound fibroblasts obtained from chronic wound tissue. We also measured the change in the NO detected when the cells were cultured in high glucose conditions with and without stimulation and the results also showed suppressed NO levels compared to normal skin fibroblasts. The NO levels measured after 24 hours was compared to the nitrite present in the cell culture media. In normal glucose conditions, the trend remained consistent with normal skin fibroblasts with the data showing increased NO and nitrite levels for stimulated cells compared to unstimulated cells (**Figure 3-4**). A key finding was detectable nitrite (0.77 ± 1.34 nmols/10^5 cells) in normal glucose without stimulation and absence of real-time NO under the same treatment conditions. During the normal wound healing process, cells such as the immune cells, endothelial cells, fibroblasts and keratinocytes produce proportional amounts of ROS (superoxide)[203]. Superoxide reacts very rapidly with NO to produce the more toxic compound peroxynitrite that can be oxidized into nitrite/nitrate as well[129]. Fortunately, antioxidant mechanisms are present to modulate the production and levels of superoxide in order to increase the bioavailability of NO to the cells. For example, the enzyme superoxide dismutase present at the wound will convert superoxide into hydrogen peroxide and the enzyme catalase will then convert the hydrogen peroxide into oxygen and water[203]. Our finding suggests that there might be high levels of ROS that surpass the antioxidant mechanisms in chronic wound cells that leads to absence of NO detection and the presence of nitrite. High glucose conditions without stimulation showed low levels of nitrite similar to the real time NO measurements under the same conditions. However, there was neither nitrite nor total NO detected for the cells cultured in high glucose with stimulation (**Figure 3-5**). Western blot analysis was performed for the wound fibroblasts to assess the upregulation the NOS enzymes known to be responsible for NO production. The data showed absence of the inducible nitric oxide synthase enzyme (**Figure 3-6**). Although, the NF-κβ protein which is the principal transcription factor that activates the genes responsible for the production of iNOS was upregulated with increased levels in stimulated cells (**Figure A-2**). Whether this could be an indication of an interference in the pathway that leads to upregulation of the iNOS enzyme still needs to be determined. We also assesed protein levels of constitutively expressed NOS isoforms using a universal NOS antibody and faint bands were observed that corresponded to the molecular weight of eNOS. The results showed a trend for higher protein levels in stimulated compared to non-stimulated wound fibroblasts (Figure **A-1**). Endothelial nitric oxide synthase and its activity has been identified in cultured human skin fibroblast cells[43, 204]. It has also been proposed as a mechanism to increase ROS in diabetic and chronic wounds through its uncoupling from the NO pathway to produce superoxide instead[203]. Only one replicate measurement was run to determine the presence of constitutively expressed NOS isoform enzymes and we cannot draw a definitive conclusion with the results so far. However, it shows that further studies will need to performed to determine the role of eNOS in the dysregulation of chronic wounds. There was no statistical difference obtained within the groups for the real time/nitrite measurements and a large variation in NO and nitrite detected for 3 independent experiments was observed. This could be attributed to the altered state of the cells that

resided in a persistent chronic state for over a year. Caley et al[201] reported a reduced reproducibility in cells isolated from chronic wounds and the reason is that the cells take on a distinct phenotype in the chronic wound bed that is ultimately retained even in invitro cell culture. To support this hypothesis Schaffer et al [44] assessed NO/nitrite production in cells isolated from a wounded rat model. The cells isolated from the wound only produced NO in the first two passages. This phenomenon might also be observed in primary cells obtained from a chronic wound.

Experiments were performed to determine the nitrite/nitrate levels present in the wound bed. The studies in the literature analyze the NO levels by looking at the nitrite/nitrate present in the plasma/urine of the patient as well as the metabolites of the substrate arginine that is present in the wound fluid[205, 206] while others use the fluid obtained in animal wound models to predict the NO state and function .The data gives an overview of the NO levels in the pathological states and how it could possibly affect the healing wound but it does not give an accurate assessment of the NO levels or even nitrite/nitrate that is actually present in a clinically relevant wound model. Besides, the Griess assay was mainly used to determine these nitrite levels and it has been shown to have a low sensitivity (0.5μM) [207] and the presence of blood components such as hemoglobin could greatly interfere with the results obtained[208]. We established an effective method to analyze the nitrite/nitrate present in the fluid of chronic wounds. The protocol used was adopted from Gilliam et al[198] with some modifications. Nitrite and nitrate standard solutions with equal concentrations were prepared and the nitrate was converted to nitrite by the enzyme nitrate reductase. The nitrite was reduced to NO using the triiodide assay and the NO released was measured using the most highly sensitive method for NO detection (chemiluminescence). The results showed complete conversion of nitrate into nitrite (**Figure 3-6**). To determine the accuracy of the method, 3 blinded samples containing standard concentrations of both nitrite and nitrate were prepared and measured. The results showed that the theoretical ratio matched up the experimental ratio obtained with slight deviation in one of the samples (**Figure 3-7**) The detection limit was as low as 0.05-0.1μM and for the enzyme concentration used, a linear response was maintained up to 150μM (Figure **A 3**) validating that we can use this method to analyze low and high nitrite concentrations in wound fluid samples. We determined the nitrite/nitrate levels in the wound fluid obtained from a human chronic wound (**Figure 3-8)**. The nitrite in the wound bed was found to be in the micromolar range which is one thousand-fold higher than the NO that was detected in the cells (**Figure 3-5)**. This confirms that tracking nitrite/nitrate accumulation cannot be used to determine actual NO production during wound healing. The rate of nitrite/nitrate clearance from the wound fluid is unknown. As NO decomposes, nitrite and nitrate will accumulate in fluid, the wound bed will influence how quickly fluid and ions are removed and this removal rate will likely change during the course of wound healing. Additionally, the wound fluid is collected after the biopsy was obtained. This might have provoked the hemostatic phase of wound healing, consequently increasing NO production at the wound site. The data further proves that there are many factors that can result in increased nitrite levels when the sample is collected at a specific time point and it is precisely why it's not accurate to rely only on these NO metabolites to predict the NO role in a given pathology. The high nitrite concentration measured could also support a

possible reduction of NO bioavailability to cells in and surrounding the wound bed from high ROS levels and low antioxidants. There is also the possibility of other cells such as the immune cells that persist in the chronic wound that are responsible for the high nitrite levels measured. The levels of nitrite were significantly higher compared to the nitrate level (60.25±1.79 μM vs 27.42±3.91 μM). Hemoglobin is an effective scavenger of NO. It reduces NO concentration by oxidizing NO predominantly into nitrate. Therefore, in the event of an increased hemostatic response, it is expected that NO produced would oxidize primarily to nitrate but this was not the case. The toxic NO metabolite peroxynitrite oxidizes significantly to nitrite at a pH of 7.5[129]. At lower pH levels (pH 3) it is predominantly oxidized to nitrate. Chronic wounds have been reported to have pH values ranging from 7.19-8.5 that is also taken as an indicator of the delayed healing status of the wound[209]. The pH at the wound used in this chapter was not determined in our study and it's also not know whether higher pH values (>7.5) or other components in the wound environment will result in more decomposition of peroxynitrite into nitrite. However, our data shows that further study on the metabolic fate of peroxynitrite is warranted.

3.4 Conclusion

In this chapter, the real-time NO and nitrite levels detected in wound fibroblasts isolated from a chronic wound cultured in normal and high glucose conditions for a duration of 24 hours was assessed. The results show that the NO production is altered in fibroblasts isolated from a chronic wound tissue. In addition, we validated a method to determine the nitrite/nitrate levels present in wound fluid. The nitrite/nitrate levels in wound fluid was 1000-fold higher than the NO levels measured in the cells which suggests that there is a dysregulation in NO levels in chronic wounds that could explain the delayed healing in the patient. The work presented proves that we can determine the real-time NO levels from cells isolated from patients with chronic wounds as well as the nitrite/nitrate present at the wound site. Combining the data obtained from these two methods of analysis coupled with measuring protein levels of the different enzymes/factors that might affect the bioavailability of NO will indeed offer better insight on the exact timing, dose and duration of NO treatment that is required to restore the *milieu interieur* in the chronic wound and lead to complete healing for patients.

4 INVESTIGATIVE STUDY OF REAL-TIME NO MEASUREMENTS IN MOUSE MACROPHAGE CELLS (RAW 264.7) IN NORMAL AND HIGH GLUCOSE CONDITIONS[5]

Macrophages are one of the most important cell types during wound healing. They are the guardians of the innate immune system and are involved in initiating and resolving the inflammatory response. Macrophages also facilitate the transition of the wound from the inflammatory to the proliferative phase and have the capacity to influence all other phases of the wound healing process. This was demonstrated in macrophage deficient wound mice models. The wounds resulted in reduced collagen synthesis and granulation formation, insufficient secretion of growth factors, low levels of myofibroblast cells and ultimately delayed wound closure[210]. The multifunctional roles of macrophages are possible because they can take on different functional phenotypes during the progression of wound healing. The most commonly known phenotypes are the classical (M1) and alternative (M2) macrophages. The former being pro-inflammatory and the latter anti-inflammatory[211]. On activation by inflammatory cytokines and/or bacterial products, M1 secrete large amounts of reactive oxygen and nitrogen species as well as other inflammatory mediators which act to disinfect the wound and recruit cells to the wound site[31, 32]. The M1 are also phagocytic cells and act by clearing the wound bed of cell debris. When the wound bed is appropriately prepared, the M1 phenotype changes to an M2 phenotype that does not produce ROS /RNS. Instead, these cells resolve the inflammatory process and are mainly involved in promoting cell proliferation and tissue repair by producing growth factors VEGF, TGF-β and Insulin like growth factor-1[210] This change is critical for the transition of the wound from the inflammatory to the proliferative stage of wound healing. The alteration in the phenotypes of macrophages has been greatly linked to the development of DFU and it is reported that factors and mechanisms that regulate glucose and lipid metabolism facilitate the change from M1 to M2 [122] Moreover, paracrine factors produced from both M1 and M2 macrophages have been shown to influence the phenotype and function of fibroblast cells [212]. Human skin fibroblasts cultured in M1 conditioned media expressed more pro inflammatory genes and produced more ECM degrading enzymes compared to the fibroblasts cultured in conditioned M2 media which exhibited increased ECM production and proliferation potential. Chronic wounds are often stalled in the inflammatory phase of wound healing and the altered phenotype and function of macrophages could explain the persistence of DFU in this phase [213]. Nitric oxide is the principal compound produced from M1 macrophages. Previous studies from our lab have clearly elucidated the real- time NO profile from the macrophage cell line RAW 264.7[152]. The nitrite accumulation and protein levels in these macrophages has also been well characterized from these cells. Additionally, RAW 264.7 cells have been widely used in the literature as a positive control to validate NO production in cells[132, 214, 215]. However, the real-time NO profile of

[5] The work in this chapter will be submitted to a journal for future publication.

RAW 264.7 cells cultured in normal and high glucose conditions and how it compares with the nitrite has not been previously explored. In addition, RAW 264.7 is also phenotypically and functionally stable through 30 passages [215]. Therefore, it allows us to validate the results from the two previous chapters that have shown that high glucose suppresses NO produced from the cells. A detailed understanding of the dynamic changes of NO produced from macrophages cultured in normal and high glucose conditions might be the key that unlocks the door to accelerated healing in chronic wounds such as DFU.

4.1 Materials and Methods[6]

4.1.1 Cell culture and chemical supplies

Mouse macrophage cell line RAW 264.7 (ATCC TIB-71), penicillin streptomycin, fetal bovine serum (FBS), phosphate buffered saline (PBS), and Dulbecco's modified eagle medium (DMEM high glucose 4500mg/l) were all purchased from ATCC (Manassas, VA). DMEM (no glucose), sodium pyruvate and Hoescht dye were obtained from Fischersci (Hanover Park, IL). Lipopolysaccharide *pseudomonas aeroguinosa* (LPS), Calcein-AM, protease inhibitor cocktail and dopamine-HCl were purchased from Sigma-Aldrich (St. Louis, MO). Ethidium bromide was acquired from Invitrogen (Grand Island, NY). The 7.5% SDS polyacrylamide gels, GAPDH antibody (VPA00187) and gelatin were acquired from Bio-Rad (Hercules, CA). Nitric oxide synthase antibody (PAN) (2977) was purchased from cell signaling technology (Danvers, MA). The secondary antibodies; IR dye®680RD and 800CW goat anti-mouse and anti-rabbit, Odyssey blocking buffer, immobilon-FL transfer membrane and the chameleon duo pre-stained protein ladder were obtained from *LI-COR* (Lincoln, NE). Silicone elastomer base and curing agent (Dow Corning Sylgard®184) were obtained from ML Solar LLC (Campbell, California).

4.1.2 Real time NO measurements from macrophages cells RAW 264.7

RAW 264.7 at passage 15 were cultured and expanded in conventional cell culture plates (100mm) in DMEM (high or normal glucose levels), 10% FBS and 1 % penicillin/streptomycin (complete growth media). At confluency, the cells were reseeded in the CellNO trap devices at a density of 0.25-1 $\times 10^5$ cells/cm^2. The detailed fabrication and characterization of the device has been previously reported [152]. After 24-72hours, the cell culture media was changed and substituted with media containing 1µg/ml of LPS or complete growth media (control) with normal glucose (5.5mM) and high glucose

[6] The materials and methods were adopted from chapter 2 [42]. The rights to use the content is presented in appendix C and licensed under Creative Commons Attribution 4.0 International License

(25mM) concentrations. The device was placed in a standard incubator (37°C, 65% humidity, 5% CO_2) and was connected to a calibrated nitric oxide analyzer (NOA) and the real-time NO release profile was measured for 24 hours.

4.1.3 Cell viability assay in the CellNO trap device

After the real-time NO measurements, a live-dead assay was carried out using 2µM calcein AM, 2µg/ml ethidium bromide in PBS for 10-15 minutes. The cells were imaged and analyzed using an Olympus fluorescent microscope (model BX51) and Image J1 respectively[169].

4.1.4 Nitrite assay

After 24 hours of measurement in the CellNO trap device, the cell culture media from the cell samples under normal and high glucose conditions were collected. The triiodide assay was used to measure the nitrite accumulation in the media[74]. Briefly, 50µl of the media was added to a vial containing a stirring solution of 300µl of glacial acetic acid and 120µl of potassium iodide. The vial was connected to a calibrated Sievers Nitric Oxide Analyzer 280i (Zysense, LLC, Boulder, CO, USA) and the NO produced from the nitrite present in the media was measured and normalized to the number of live cells.

4.1.5 Western blot analysis

Confluent RAW 264.7 cells cultured in 100mm diameter tissue culture dishes were stimulated with 1µg/ml of LPS in normal and high glucose conditions and incubated for 24 hours. The cells were scraped, centrifuged and re-suspended in 200µl of RIPA buffer in the presence of protease cocktail inhibitors. The cell lysates were incubated for 30 minutes on ice on a plate shaker and centrifuged at 12,000 rpm for 20 minutes at 4°C. The supernatant was collected, and the protein concentration determined for each sample using Bradford assay[170]. An equal amount of loading buffer containing dithiothreitol was added to each sample, boiled at 100°C for 5 mins and immediately placed on ice for 2 mins. About 30 µg of protein was loaded in a 7.5% SDS-PAGE gel and separated by electrophoresis at 100V for approximately 70 minutes. The proteins were transferred to immobilon®-FL PVDF membrane using the Trans-Blot® Turbo™ Transfer System (Bio-Rad) for 7 minutes. The membrane was incubated in Odyssey blocking buffer (TBS) for 60 minutes to block nonspecific binding sites followed by incubation in TBS containing 0.2% of tween20 (TBS-T), GAPDH and the iNOS antibodies (1:1000 and 1:10000 dilution respectively) for 18 hours at 4°C. After that, the membrane was washed 4 times with TBS

(0.1% tween20) and incubated in TBS-T with the secondary antibody (1:20000 dilution) for 1 hour then extensively washed in TBS, visualized by *LI-COR* Odyssey infrared imager and analyzed using Image Studio Lite Software Version 5.2.

Statistical analysis was performed in Microsoft Excel using a student's t-test with statistical significance set at a 95% confidence level ($P<0.05$).

4.2 Results

4.2.1 Real-time NO measurements from the macrophage cell line RAW264.7

Raw 264.7 cells cultured in the CellNO trap device in normal and high glucose media showed absence of NO in unstimulated cells (Figure **4-1**). After stimulation by the bacterial product LPS (1µg/ml), there was a steady increase in NO detected after 3 hours in normal glucose conditions which peaked at 12.5 hours (9.737×10^{-12}(moles/(min·cm^2))/10^6cells) with a gradual reduction in NO detected at 24 hours (3.645×10^{-12} (moles/(min ·cm^2))/10^6cells). In high glucose conditions, NO was detected after 4 hours and it peaked at 14.5 hours (2.212×10^{-12} (moles/(min·cm^2))/10^6cells) and gradually decreased to (1.734×10^{-12} (moles/(min·cm^2))/10^6cells) at the end of 24 hours. The NO detected in normal glucose condition was significantly higher compared to high glucose conditions as observed in (**Figure 4-1**)

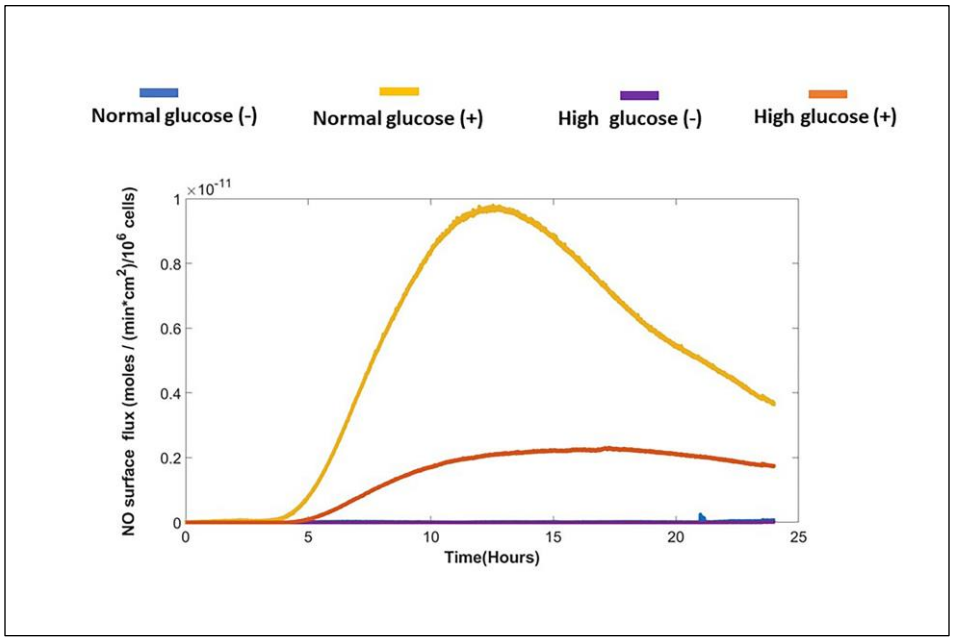

Figure 4-1. The average real- time NO surface flux from RAW 264.7 cultured in normal (5.5mM) and high glucose (25mM) media without (-) and with (+) stimulation by LPS (1µg/ml)

4.2.2 Nitric oxide detected from nitrite accumulation in the absence and presence of stimulation

The nitrite accumulated in the media at the end of the real-time NO measurements was analyzed using the triiodide assay[74]. In unstimulated cells, the levels of nitrite was very low compared to stimulated cells in normal and high glucose conditions (2.32±0.32 vs 1.22±1.19 nmol/10^6 cells for n=3). When stimulated, the nitrite detected in normal glucose conditions was slightly higher than the nitrite detected in high glucose but not statistically different (58±14.30 vs 36±10.72 nmol/10^6cells for n=3) (**Figure 4-2**).

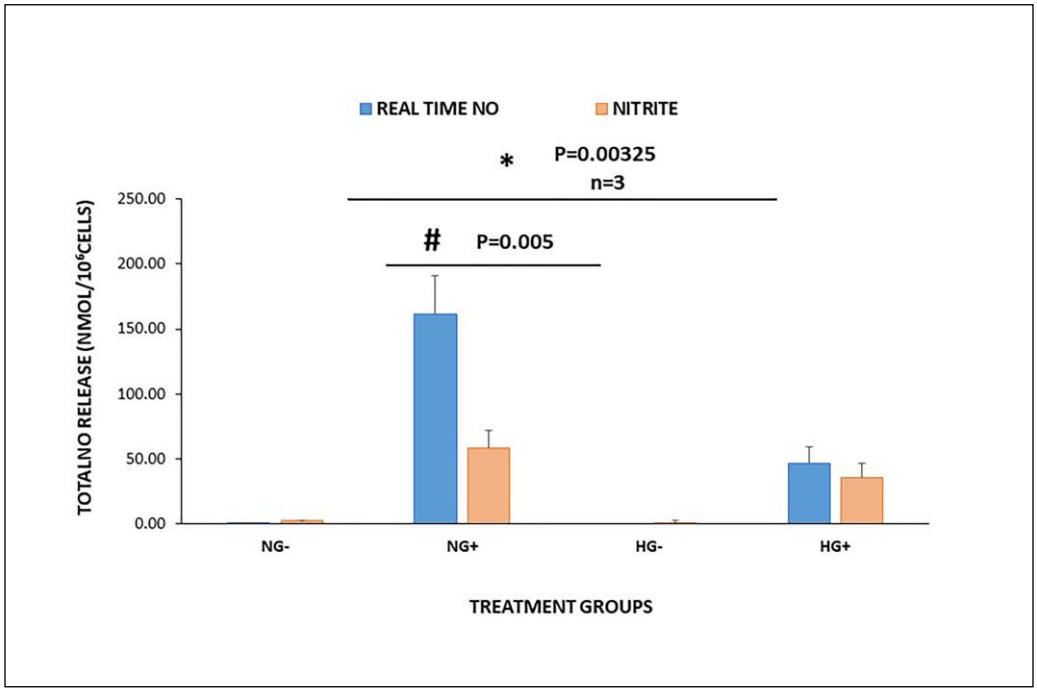

Figure 4-2 The comparison between the accumulated real-time NO and the nitrite measurements for normal (**NG**) and high (**HG**) glucose the absence (-) and presence (+) of stimulation. For n=3, * represents statistical difference in real time NO in **NG+** and **HG +**. # represents statistical difference in real-time and nitrite in **NG+**

4.2.3 The cell viability for RAW 264.7 cells cultured in normal and high glucose conditions in the absence and presence of stimulation

At the end of the real-time NO measurements, the cell viability was assessed using a live dead assay as previously described. Overall the cells maintained good viability in all treatment groups. Normal glucose conditions with stimulation had a lower cell viability compared to normal glucose without stimulation and high glucose without and with stimulation. (**Figure 4-3**). However, the difference was not statistically different.

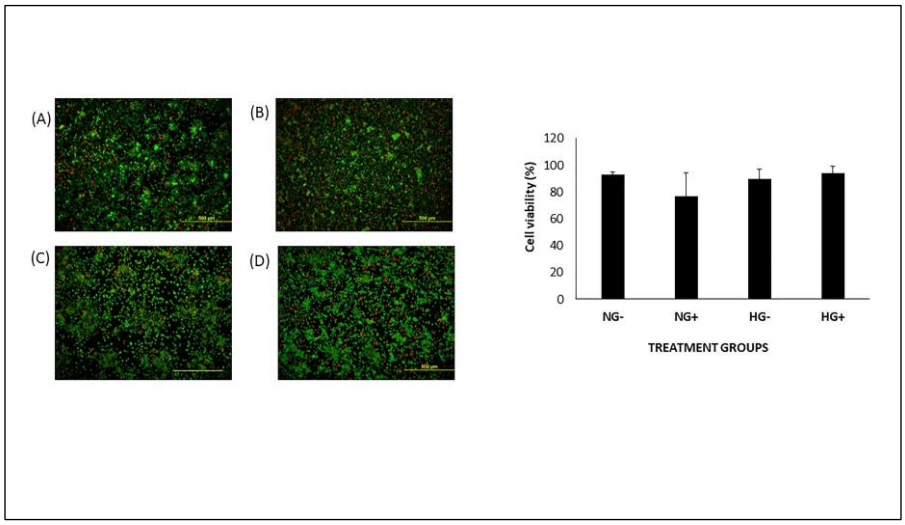

Figure 4-3 The cell viability detected by calcein AM and ethidium bromide for RAW 264.7 cultured in normal (**NG**) and high (**HG**) glucose media in the absence (-) and presence (+) of stimulation

4.2.4 The total real time-NO released compared to the nitrite accumulated in the media

The real-time NO detected was integrated to obtain the total NO released and it was compared to the nitrite detected in the cell culture media (**Figure 4-2**). The total NO released in normal glucose conditions with stimulation was significantly higher compared to the nitrite that was collected in the culture media (161.80±29.05 vs 58±14.30 nmol/10^6 cells n=3, p=0.005). High glucose followed a similar trend, the total real-time NO measured was higher compared to the nitrite although not statistically different (46.26±12.90 vs 36.05±10.72 nmol/10^6 cells). Interestingly, for the cells cultured in normal glucose conditions, the total real-time NO analyzed was significantly higher than total real-time NO measured in high glucose conditions when stimulated (161.80±29.05 vs 46.26±12.90 nmol/10^6cells n=3, p=0.00325). The nitrite measured was not statistically different in normal and high glucose conditions with stimulation.

4.2.5 Western blot analysis for iNOS protein levels in macrophages RAW 264.7 cultured in normal and high glucose conditions

RAW 264.7 cells seeded at the same cell density, were cultured in normal and high glucose conditions. At confluency, the cells were stimulated with 1ug/ml of LPS for 24 hours. The iNOS protein levels in the cells were analyzed using western blot. The results showed that the iNOS protein was not detected in the cells cultured in normal and high glucose in the absence of stimulation while the iNOS protein was upregulated in both normal and high glucose when the cells were stimulated (**Figure 4-4**) with the highest levels in macrophages cultured in normal glucose compared to high glucose conditions (23151.96 vs 7975.66, n=3 p=0.02)

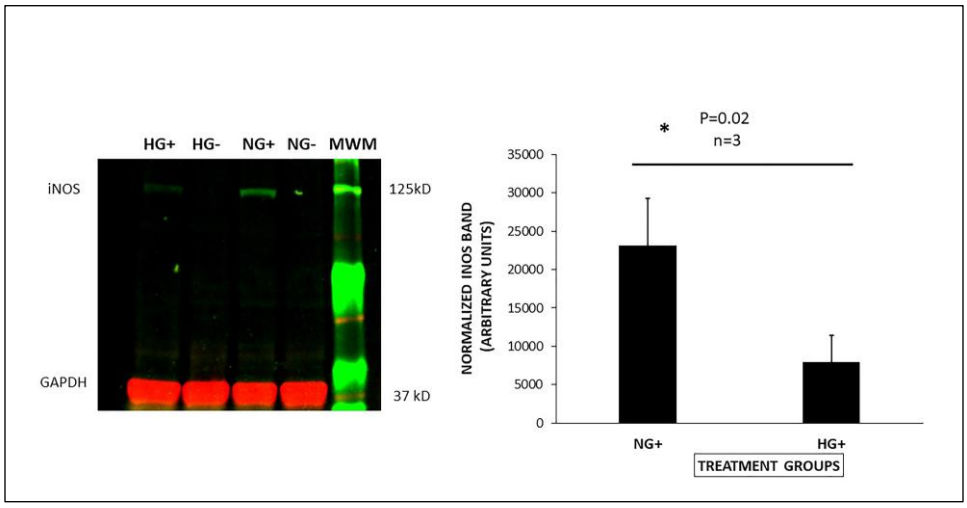

Figure 4-3. Western blot analysis for the detection of iNOS protein in normal (**NG**) and high glucose (**HG**) in the absence (-) and presence (+) of stimulation

4.3 Discussion

Diabetic foot ulcers remain stalled in the inflammatory stage of wound healing and it's suggested that the macrophages present in the wound retain their proinflammatory characteristics making it impossible for the wound to proceed to resolution. Nitric oxide is one of the key mediators produced by macrophages when faced with a hostile environment. Our lab has previously reported real-time NO levels from macrophage cells (RAW 264.7) cultured in high glucose conditions with stimulation by the inflammatory mediators LPS and IFN-ϒ[152]. Herein, we determined the real-time NO levels produced in RAW 264.7 cultured in normal and high glucose conditions with and without stimulation by the bacterial product LPS (1 µg/ml). In the absence of stimulation, NO was barely detectable in the cells cultured in normal and high glucose media (**Figure B-1)**. When the cells were stimulated by LPS, the real-time NO in normal glucose conditions was significantly higher compared to high glucose conditions (162± vs 46.25±1.29 nmols/10^6 cells). The results

presented in this chapter showed consistency with previous work under high glucose conditions[152]. Although slightly higher NO was detected in our study, it was still in the same order of magnitude (46.25±1.29 vs 35.37±2.90 nmol/10^6cells). Our work reports the first ever assessment of real-time NO produced from macrophage cells cultured in normal glucose conditions. There has been a lot of controversy in the literature in regards to the levels of NO in diabetic conditions (**Table 2**) and a similar trend is observed for macrophages cultured in normal and high glucose conditions. Tseng et al [216] showed that high glucose inhibited nitrite production and iNOS expression from macrophages while other studies show that the nitrite and iNOS protein levels are elevated in RAW 264.7 cultured in high glucose states[132, 217-220]. The evidence presented in these studies supports the results obtained by the authors. However, to base these findings purely on the metabolites of NO is not an accurate assessment. Nitric oxide reacts with a large number of oxidative molecules such as oxygen, transition metal ions, thiols to form other compounds, some of which metabolize to produce the same biproducts (nitrate and nitrite) as NO [203]. Moreover, depending on the surrounding environment, the NOS enzymes can also uncouple from its native NO metabolic pathway to generate the reactive oxygen species superoxide[96]. It is therefore critical to compare the actual levels of NO that the cells experience to the molecular pathways, protein levels and even culture environment that might affect the NO release or availability. The iNOS levels in our study strongly correlated with the real-time levels of NO observed in both treatment groups in the presence and absence of stimulation (**Figure 4-2 and 4-4**) with higher levels in normal glucose compared to high glucose conditions with stimulation (23151.96 vs 7975.66, n=3 p=0.02). Miao et al[35] showed reduced iNOS expression and levels in macrophages isolated from the wounds from diabetic mouse. The same group also observed increased arginase expression in the macrophages present in the wound suggesting a greater population of alternatively activated or altered macrophage function in the diabetic wound. Other researchers have reported iNOS deficiency from genetically diabetic mice. Furthermore, the administration of NOS inhibitors has also been shown to delay reepithelialization and collagen formation[221]. The nitrite that was accumulated in the culture media was compared in both treatment groups and it was found to be slightly higher in normal glucose compared to high glucose with stimulation but not statistically different. The total real-time NO was significantly higher in normal glucose compared to the nitrite inferred in the cell culture media of the same treatment group while the nitrite and total NO in high glucose conditions was not significantly different (**Figure 4-2)**. Macrophages produce both nitric oxide and superoxide when activated as part of the cell immune response[32]. Nitric oxide has a very strong affinity for superoxide and the reaction between the two species produces the more toxic compound peroxynitrite[58, 115]. Depending on the pH, peroxynitrite is oxidized to nitrite or nitrate[129]. In the presence of antioxidant molecules, the formation of this compound is modulated by scavengers of superoxide and nitric oxide [96]. High glucose levels alter the redox environment of the cells through various mechanisms[222]. One is through superoxide generation from the mitochondria which can activate the polyol pathway, increase consumption of NADPH a key cofactor required for NO synthesis and the activity of antioxidant molecules. The low NO levels in high glucose compared to normal glucose cell culture conditions that could be explained by this mechanism. The results strongly suggest a possible increase in

nitrosative stress for cells cultured under high glucose conditions. He and Frost[153] have shown that the generation of the reactive oxygen species such as superoxide greatly reduces the real-time NO levels produced from known NO donors and a similar mechanism might be observed in the cells. In addition, chronic wounds of patients have been found to have high levels of uncontrolled ROS and RNS with an insufficient antioxidant response[203]. consequently, the indirect effects of NO are observed instead of its biological role.

4.4 Conclusion

The macrophage cell line RAW 264.7 is widely used as a positive control for NO production and iNOS expression in tissue and cell culture. Moreover, previous work also validated the temporal and spatial NO released from these cells cultured in high glucose conditions. Therefore, it seemed fitting to use these cells to confirm the results obtained from normal and wound fibroblasts cultured in similar conditions. The work presented here proves that nitric oxide is significantly suppressed in cells cultured in high glucose conditions and that the nitrite levels do not correlate with the actual NO levels that cells experience in normal and high glucose cell culture conditions. The quantitative analysis of continuous real-time NO measurements is of utmost importance when understanding the role of NO especially in chronic pathological states and consequently can be used to develop treatments that will not only deliver the adequate dose of NO but also address the problem of increased oxidative and nitrosative stress, therefore increasing the bioavailability of NO in the wound.

5 CONCLUSION AND FUTURE WORK ON THE RELEVANCE OF REAL-TIME NO MEASUREMENTS

Diabetes Mellitus remains one of the most challenging and complex pathologies of the 21st century and individuals affected with DM are always at risk for the development of complications such as DFU. The risks of amputations and death are significantly higher in patients with DFU compared to patients without DFU. These wounds take a very long time to heal because of the underlying metabolic condition of the patient as well as persistent infections. Uncontrolled high glucose levels are characteristic for diabetic patients who develop DFU and downstream it triggers several metabolic pathways that interfere with the homeostatic environment that is necessary for the wound to heal. Nitric oxide is essential in the wound healing process. It is produced by cells that are actively present in the wound and is known to be involved in all the stages of wound healing. The effects of NO are like a double aged sword. At low concentrations it modulates blood flow, angiogenesis, cell proliferation, migration and activates various signaling pathways. While at high concentrations it acts as a microbial agent to fight off infections in the wound. The levels of NO need to be precisely controlled and this achieved by scavengers and antioxidant systems under physiological conditions. Additionally, the timing of delivery is of extreme importance in achieving normal physiological functioning. In diabetes, the high levels of glucose interfere with the metabolism of NO through a number of mechanisms; increased reactive oxygen species, reduced antioxidant levels, reduced co factors (NADPH, BH4). The result is reduced bioavailability of NO and ultimately NO function. The literature is vast on the effect of NO in the diabetic state however, the results reported are contradictory. The role of NO is clearly defined in physiological conditions and even in acute pathological states, the reported NO function is fairly consistent[190, 191, 223]. However, in regards to clinical application for chronic conditions such as DFU it still remains a challenge. Nitric oxide in the wound needs to maintain an extremely delicate balance when transitioning into different phases of the wound and this is achieved by a complex cascade of events involving cross talk between the cells and the surrounding matrix environment that act together to repair and restore the skin tissue barrier. Each of these events require different doses/durations of NO. Nitric oxide is very reactive and short lived. Understandably that makes it very difficult to measure and consequently the majority of studies in the literature rely on its oxidized products (nitrate and nitrite) to predict the NO function. This greatly under or over estimates the levels of NO that are actually needed because it does not give any information on the dynamic change of NO in specific conditions and how the NO levels change overtime. In addition, because of its reactivity NO generates reactive nitrogen species especially in conditions of oxidative stress as is the case of DFU. These RNS can also metabolize to produce nitrite/nitrate creating a confounding effect/misinterpretation of NO function. Its therefore why we emphasize the need to compare the actual levels of NO that cells produce and to see how well they correlate with the nitrite/nitrate levels observed so as to determine if the effect observed is primarily due to NO or other factors that interfere with its bioavailability and then proceed accordingly. The work presented in this dissertation assessed the real-time NO levels and nitrite produced from cells that are at the front line of the wound healing process under

normal and high glucose conditions. In Chapter two, the NO produced from normal human adult fibroblast cells was analyzed for normal and high glucose cell culture conditions in the absence and presence of stimulation. The NO levels were found to be higher in normal glucose compared to high glucose conditions when the cells were stimulated (8.42±1.16 and 3.26±0.79nmol/10^5 cells). The nitrite levels correlated to the real-time NO levels for the cells in normal glucose conditions with and without stimulation. However, in high glucose conditions, the NO levels were not statistically different in the absence and presence of stimulation. The nitrite levels appeared higher but did not reach statistical significance in high glucose with stimulation compared to cells without stimulation. The iNOS protein was upregulated in all treatment groups but not statistically different. Further studies would need to be performed to determine the mechanism involved in NO synthesis in fibroblast cells. After determining the NO levels expected in normal fibroblast cells, we adopted the same methodology to determine the NO produced from human adult wound fibroblasts isolated from a chronic non-healing wound (1 year and 8 months). The NO produced was slightly increased in normal glucose cells (4.08±3.38nmol/10^5) and yet suppressed in high glucose conditions and the NO profile was also markedly different compared to normal fibroblast cells. The nitrite/nitrate present in the wound bed was also analyzed and found to be significantly higher (micromolar compared to nanomolar range) compared to the NO levels produced from cells. The data suggests that there might be other cells responsible for the nitrite/nitrate levels observed or other factors present in the wound bed that interferes with NO function in the wound. The work from this chapter is part of an ongoing clinical study to determine how the NO levels differ in diabetic and non-diabetic patients with chronic wounds. The data from chapter 4 looks at the NO produced from the macrophage cell line RAW 264.7 which has been validated in previous studies and was used to confirm NO and nitrite measurements obtained from normal and wound fibroblasts cultured in normal and high glucose conditions. There was absence of NO detected from cells cultured in normal and high glucose in the absence of stimulation. When stimulated we observed a similar trend with normal glucose showing significantly higher levels of NO compared to cells cultured in high glucose conditions (162± vs 46.25±1.29 nmols/10^6 cells). There was no significant difference of nitrite levels in normal and high glucose with stimulation. The levels of the iNOS enzyme correlated with the real-time NO levels but not the nitrite. While the molecular pathways through which NO availability is altered in diabetic conditions deserves further investigation than we can offer in this dissertation, the conclusion can be drawn that in addition to analyzing NO metabolites and NOS protein expression/levels, it is also fundamental to assess the temporal and spatial aspects of NO in real-time to clearly and accurately define the NO function in DFU. In the long term, it will facilitate engineering of precisely controlled NO treatments that can model the physiological NO symphony in wound healing and repair the damaged skin tissue.

5.1 Future perspectives

We are at a precipice where the current research methodologies and treatment plans are mainly focused on either the positive or detrimental effects of NO and yet undermine the need for nitroso redox balance when treating chronic disease states. The use of real-time NO measurements addresses this limitation by monitoring the precise moment when NO affects different cell functions in a given experimental plan and then applying this knowledge to determine the causal factors or modify the treatment according to the changes observed.

5.1.1 The use of localized NO delivery systems to control the effect of NO

Now that we know the NO levels produced from normal wound fibroblasts and macrophages cells. The challenge at hand is to determine whether we can incorporate the NO levels measured in the cells into smart NO release wound dressings that can locally deliver the correct doses of NO required for each cell population in a given sight of the wound without altering the surrounding environment. Previously, an NO releasing polymer system that incorporates an S-nitrosothiol compound (S-nitroso acetyl penicillamine dimethyl siloxane (SNAP-PDMS)) was engineered in our lab that can be finely tuned to deliver controlled doses of NO by photoinitiation[224]. A gradient target of this polymer with varying concentrations of NO was prepared and applied to cells cultured in the upper chamber of the CellNO trap device to deliver NO to those cells (**Figure 5-1A).** The advantage of this system is that it allows us to deliver only NO to the cells so that when compared to the real-time NO or nitrite accumulation, the effect observed will be specific to either the dose of NO delivered or its bioavailability. Moreover, it can be modified to simultaneously track the changes in real-time. In our preliminary study we used this gradient as a localized NO treatment to assess the cell viability in the wound fibroblast cells used in chapter 3. The data showed that the viability of the cells exposed to the highest levels of NO was significantly reduced compared to cells exposed to lower doses of NO. In the same culture chamber an area of the cells was not exposed to the NO gradient target and these cells maintained over 95% cell viability (**Figure 5-1B).** The results clearly indicated that we can adopt this model to treat the cells with varying concentrations of NO that could have the potential to direct the migration and proliferation of cells from the wound edge into the wound bed and reestablish the skin integrity.

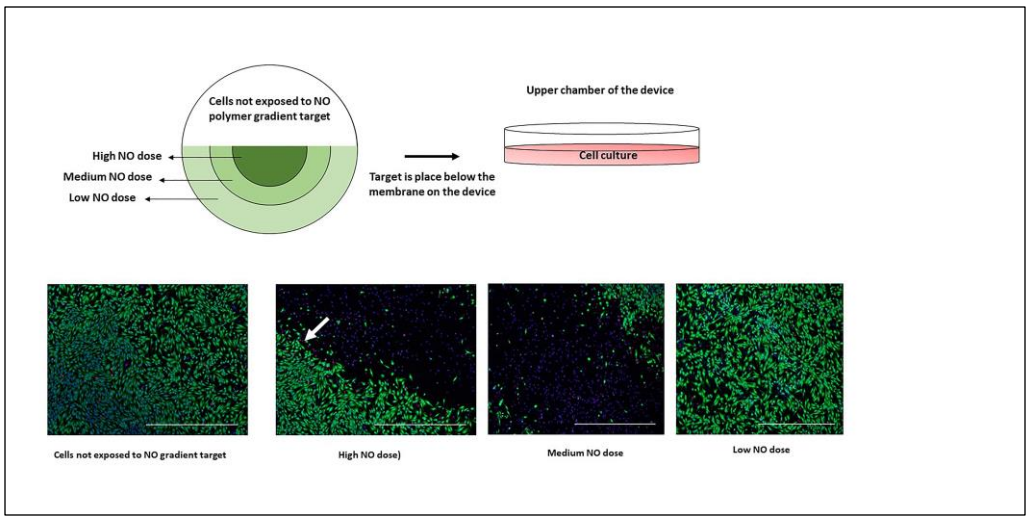

Figure 5-1 The treatment of wound fibroblasts with NO polymer gradient target. Green and red represents live and dead cells respectively. Blue represents the cell nuclei. The arrow represents the boundary between cells exposed and not exposed to the NO treatment.

5.1.2 Quantitative monitoring of NO exposed to vascular smooth muscle cell cultures for applications in cardiovascular calcification

Another application of the significance of real-time NO measurements is to determine the role of NO in cardiovascular calcification which has become a growing burden in westernized countries. Calcification has severe clinical consequences in diseases such as calcific aortic valve disease, atherosclerosis, diabetes and chronic kidney disease [225, 226]. In a meta-analytical study based on the presence or absence of calcification, the risk of any cardiovascular event, stroke and mortality in patients with heart disease, renal insufficiency and diabetes mellitus increased 3-4-fold in the presence of calcification after a 10 year follow up. The various treatment strategies that have been adopted to reduce the global burden of cardiovascular diseases do not address the problem of ectopic calcification. Nitric oxide has been proposed as a pharmaceutical option to halt the progress of ectopic calcification[227]. However, the effects of NO reported in the literature are controversial. Kanno et al [228] demonstrated that NO has an inhibitory role on vascular calcification by down regulating TGF beta signaling. In another study, the NO donor DETANO and valve endothelial cells had the same inhibitory effect on the calcification of a valve interstitial cell culture[229]. However, Alsabeelah [230] showed that NO aggravates vascular calcification through overexpression of iNOS enzyme. The drawback of all these studies is that they used soluble NO donors and recent work has shown the limitations of relying on the half-life of NO donors to investigate the biological role of NO[153]. In addition, the studies lacked real time measurements on the actual level of NO that cells experience at any given time in culture. The goal is to understand the role of NO in cardiovascular calcification by using the CellNO trap measuring device that will determine the actual level of NO that vascular smooth muscle cells are exposed to.

Primary vascular smooth muscle cells were isolated from the thoracic aorta of a rat. Immunofluorescent staining of the cell monolayers confirmed that the cell culture was mainly composed of smooth muscle cells by the presence of smooth muscle α actin in the cell cytoskeleton **(Figure 5-2)**.

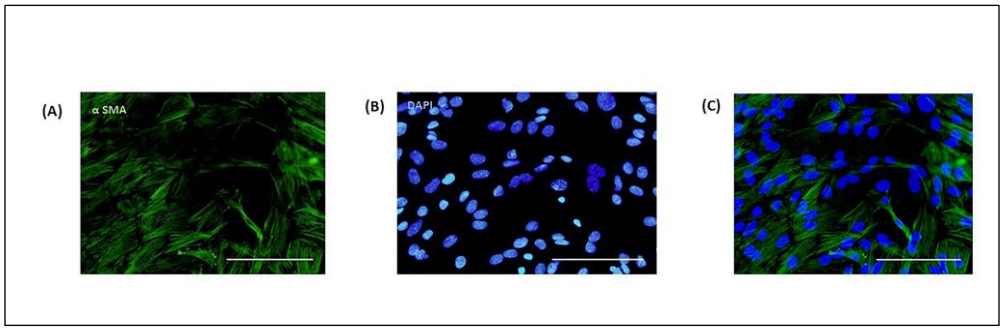

Figure 5-2 The characterization of primary smooth muscle cells. Green and blue represents smooth muscle α actin and cell nuclei respectively. Scale bar 100μM

The method from Kanno et al[228] was adopted to show that NO inhibits cardiovascular calcification when the cells are treated with 10μM of DETANO solution. The results showed that cell cultures in complete growth medium in the absence and presence of NO showed no signs of calcification. While the cells grown in osteogenic medium alone showed early signs of calcification. The cells cultured in osteogenic medium that contained the nitric oxide donor showed no signs of calcified nodule formation (**Figure 5-3**).

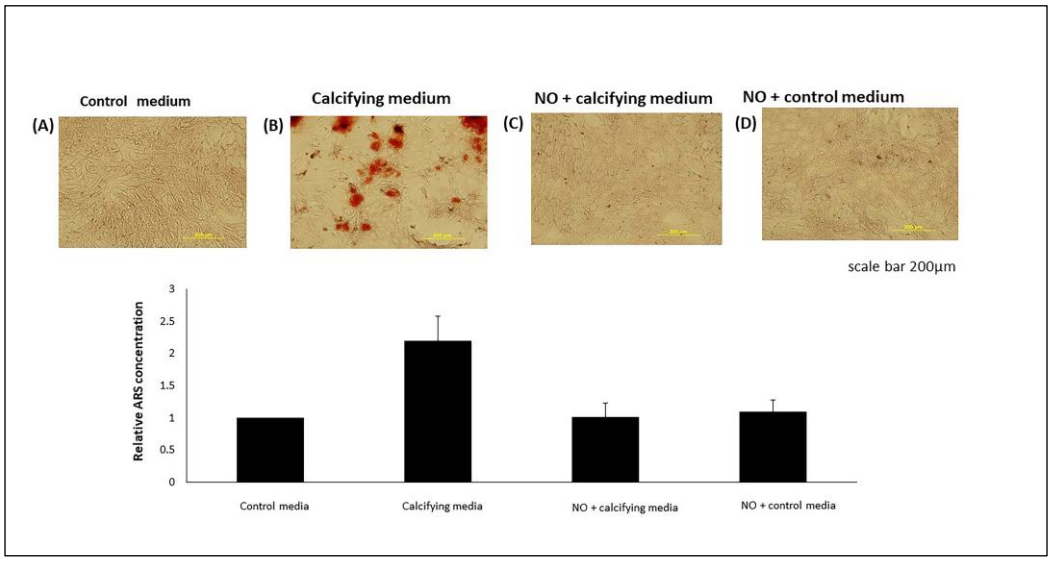

Figure 5-3 Alizarin red staining of primary rat aortic smooth muscle cells in culture for 14 days in (**A**) complete growth medium (control), (**B**) osteogenic medium, (**C**) complete growth medium and 10 µM DETANO, and (**D**) osteogenic medium and 10 µM DETANO. 20x magnification (scale bar 200 µm).

To determine the precise NO surface flux that the cells experience, we used the CellNO trap device that was previously developed [152, 231]. Cells were taken from passage 3-5 and seeded at a density of 2.1×10^5 cells per well. At confluency, the medium was changed and 10µM DETANO solution was added. The NO release was recorded for approximately 22 hours and cell viability in the device was confirmed by a live/dead assay using calcein acetoxymethyl ester (calcein AM) and ethidium bromide dye. The NO release profile of the NO donor alone in the device was recorded as well as the cells in the absence of the NO donor. Nitric oxide released in the cell culture increased gradually reaching a peak of approximately 0.05 picomoles /sec·cm^2 and then decreased for a duration of 14 hours and remained constant after 20 hours. The NO release profile of the NO donor in the absence of cells followed the same trend but the level of NO recorded was lower compared to the NO release in the presence of the cells. Interestingly, the cell culture in the absence of the NO donor produced NO but in a much smaller quantity, reaching a peak of 0.01 picomoles/sec·cm^2 (**Figure 5-4**). In previous studies, excess NO produced in vitro cell culture was assumed to be responsible for the adverse effects experienced by the cells due to the reaction of NO with reactive oxygen species[232, 233]. These data show how the NO release profile in donors could change when added to cell cultures.

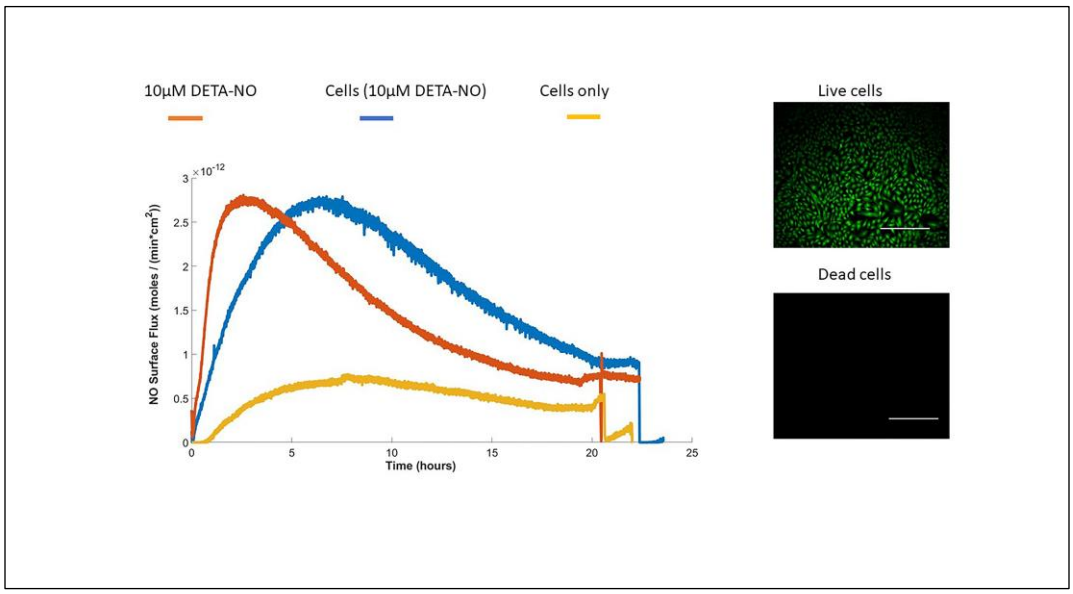

Figure 5-4 The real-time NO detected in primary smooth muscle cells cultured in media in the absence and presence of the NO donor DETANO

The ability to monitor this change in real time without altering the cell culture conditions would possibly explain the difference in observed effects of NO in calcification. This is the first study that has been able to achieve real time data on the actual level of NO that primary vascular smooth muscle cells require to inhibit matrix mineralization. Further investigation would involve assessing if the NO levels change in cells cultured in a calcifying media in the absence and presence of the NO donor. In addition, iNOS protein expression and the nitrite accumulation in the cell culture media needs to be analyzed and compared to the real time NO levels measured. It is highly possible that the results reported in the studies are consistent with the treatment delivered. However, the dose, duration and when in the cell cycle that NO is delivered maybe a key player to distinguish the observed effects of NO. The ability to determine this would require a highly controlled nitric oxide delivery system that can be modulated on demand. The SNAP-PDMS gradient strip with varying concentrations of the NO donor allows us to study dose effect simultaneously in the same cell culture to accurately determine the critical point when NO changes from an inhibitory to an aggravating effect on calcification. Real-time NO measurements will provide the armamentarium needed for custom designed drug delivery systems that can be applied to engineered constructs as well as pharmaceutical treatments to halt or slow down the progress of complications associated with chronic disease states.

6 REFERENCES

1. Atlas, D., *International Diabetes Federation (IDF). 2000.* Hallado en: http://www. diabetesatlas. org/resources/previous-editions. html, 2000.
2. Adeghate, E., P. Schattner, and E. Dunn, *An update on the etiology and epidemiology of diabetes mellitus.* Annals of the New York Academy of Sciences, 2006. **1084**(1): p. 1-29.
3. Federation., I.D., *IDF Diabetes Atlas, 8th edn. Brussels, Belgium:*

International Diabetes Federation

2017.
4. Inzucchi, S.E., *Diagnosis of diabetes.* New England Journal of Medicine, 2012. **367**(6): p. 542-550.
5. Deshpande, A.D., M. Harris-Hayes, and M. Schootman, *Epidemiology of diabetes and diabetes-related complications.* Physical therapy, 2008. **88**(11): p. 1254-1264.
6. Krolewski, A.S., et al., *Epidemiologic approach to the etiology of type I diabetes mellitus and its complications.* New England Journal of Medicine, 1987. **317**(22): p. 1390-1398.
7. Nolan, C.J., P. Damm, and M. Prentki, *Type 2 diabetes across generations: from pathophysiology to prevention and management.* The Lancet, 2011. **378**(9786): p. 169-181.
8. Reinehr, T., *Type 2 diabetes mellitus in children and adolescents.* World journal of diabetes, 2013. **4**(6): p. 270-281.
9. Baron, R., A. Binder, and G. Wasner, *Neuropathic pain: diagnosis, pathophysiological mechanisms, and treatment.* The Lancet Neurology, 2010. **9**(8): p. 807-819.
10. Ciulla, T.A., A.G. Amador, and B. Zinman, *Diabetic retinopathy and diabetic macular edema: pathophysiology, screening, and novel therapies.* Diabetes care, 2003. **26**(9): p. 2653-2664.
11. Dronavalli, S., I. Duka, and G.L. Bakris, *The pathogenesis of diabetic nephropathy.* Nature Reviews Endocrinology, 2008. **4**(8): p. 444.
12. Beckman, J.A., M.A. Creager, and P. Libby, *Diabetes and atherosclerosis: epidemiology, pathophysiology, and management.* Jama, 2002. **287**(19): p. 2570-2581.
13. Chen, R., B. Ovbiagele, and W. Feng, *Diabetes and stroke: epidemiology, pathophysiology, pharmaceuticals and outcomes.* The American journal of the medical sciences, 2016. **351**(4): p. 380-386.
14. Skrepnek, G.H., J.L. Mills Sr, and D.G. Armstrong, *A diabetic emergency one million feet long: Disparities and burdens of illness among diabetic foot ulcer cases within emergency departments in the United States, 2006–2010.* PLoS One, 2015. **10**(8): p. e0134914.
15. Kirsner, R.S., et al., *Advanced biological therapies for diabetic foot ulcers.* Archives of dermatology, 2010. **146**(8): p. 857-862.

16. Armstrong, D.G., A.J.M. Boulton, and S.A. Bus, *Diabetic Foot Ulcers and Their Recurrence.* New England Journal of Medicine, 2017. **376**(24): p. 2367-2375.
17. Taylor, M., *When Wounds Won't Heal, Therapies Spread-To The Tune of $5 Billion* 2017.
18. Falanga, V., *Wound healing and its impairment in the diabetic foot.* The Lancet, 2005. **366**(9498): p. 1736-1743.
19. Frykberg, R.G. and J. Banks, *Challenges in the Treatment of Chronic Wounds.* Adv Wound Care (New Rochelle), 2015. **4**(9): p. 560-582.
20. Velnar, T., T. Bailey, and V. Smrkolj, *The wound healing process: an overview of the cellular and molecular mechanisms.* Journal of International Medical Research, 2009. **37**(5): p. 1528-1542.
21. Guo, S.a. and L.A. DiPietro, *Factors affecting wound healing.* Journal of dental research, 2010. **89**(3): p. 219-229.
22. Li, J., J. Chen, and R. Kirsner, *Pathophysiology of acute wound healing.* Clinics in dermatology, 2007. **25**(1): p. 9-18.
23. Schultz, G.S., et al., *Wound bed preparation: a systematic approach to wound management.* Wound repair and regeneration, 2003. **11**: p. S1-S28.
24. Sattar, H.A., *Fundamentals of pathology.* Chicago: Pathoma. com, 2011.
25. Janis, J. and C. Attinger, *The basic science of wound healing.* Plastic and reconstructive surgery, 2006. **117**(7 Suppl): p. 12S-34S.
26. George Broughton, I., J.E. Janis, and C.E. Attinger, *The basic science of wound healing.* Plastic and reconstructive surgery, 2006. **117**(7S): p. 12S-34S.
27. Serhan, C.N., *Lipoxins and aspirin-triggered 15-epi-lipoxin biosynthesis: an update and role in anti-inflammation and pro-resolution.* Prostaglandins & other lipid mediators, 2002. **68**: p. 433-455.
28. Mosser, D.M. and J.P. Edwards, *Exploring the full spectrum of macrophage activation.* Nature reviews immunology, 2008. **8**(12): p. 958.
29. Mills, C.D., L.L. Lenz, and K. Ley, *Macrophages at the fork in the road to health or disease.* Frontiers in immunology, 2015. **6**: p. 59.
30. Martinez, F.O., et al., *Macrophage activation and polarization.* Front Biosci, 2008. **13**(1): p. 453-461.
31. Rizk, M., M.B. Witte, and A. Barbul, *Nitric oxide and wound healing.* World J Surg, 2004. **28**(3): p. 301-6.
32. Assreuy, J., et al., *Production of nitric oxide and superoxide by activated macrophages and killing of Leishmania major.* European Journal of Immunology, 1994. **24**(3): p. 672-676.
33. Martinez, F.O. and S. Gordon, *The M1 and M2 paradigm of macrophage activation: time for reassessment.* F1000prime reports, 2014. **6**.
34. Berger, A., *Th1 and Th2 responses: what are they?* Bmj, 2000. **321**(7258): p. 424.
35. Miao, M., et al., *Diabetes-impaired wound healing and altered macrophage activation: A possible pathophysiologic correlation.* Wound Repair and Regeneration, 2012. **20**(2): p. 203-213.
36. Loots, M.A.M., et al., *Differences in Cellular Infiltrate and Extracellular Matrix of Chronic Diabetic and Venous Ulcers Versus Acute Wounds.* Journal of Investigative Dermatology, 1998. **111**(5): p. 850-857.

37. Clark, R.A., et al., *Fibronectin and fibrin provide a provisional matrix for epidermal cell migration during wound reepithelialization.* 1982. **79**(5): p. 264-269.
38. Kanno, S. and Y.J.P.i. Fukuda, *Fibronectin and tenascin in rat tracheal wound healing and their relation to cell proliferation.* 1994. **44**(2): p. 96-106.
39. Ploeger, D.T.A., et al., *Cell plasticity in wound healing: paracrine factors of M1/ M2 polarized macrophages influence the phenotypical state of dermal fibroblasts.* Cell Communication and Signaling, 2013. **11**(1): p. 29.
40. Singer, A.J. and R.A.J.N.E.j.o.m. Clark, *Cutaneous wound healing.* 1999. **341**(10): p. 738-746.
41. Gill, S.E. and W.C. Parks, *Metalloproteinases and their inhibitors: regulators of wound healing.* The international journal of biochemistry & cell biology, 2008. **40**(6-7): p. 1334-1347.
42. P Kwesiga, M., et al., *Investigative Study on Nitric Oxide Production in Human Dermal Fibroblast Cells under Normal and High Glucose Conditions.* Medical Sciences, 2018. **6**(4): p. 99.
43. Wang, R., et al., *Human Dermal Fibroblasts Produce Nitric Oxide and Express Both Constitutive and Inducible Nitric Oxide Synthase Isoforms.* Journal of Investigative Dermatology, 1996. **106**(3): p. 419-427.
44. Schäffer, M., et al., *Nitric oxide, an autocrine regulator of wound fibroblast synthetic function.* The Journal of Immunology, 1997. **158**(5): p. 2375-2381.
45. Goldman, R., *Growth factors and chronic wound healing: past, present, and future.* Advances in skin & wound care, 2004. **17**(1): p. 24-35.
46. Yang, C.-C., S.-D. Lin, and H.-S.J.J.o.d.s. Yu, *Effect of growth factors on dermal fibroblast contraction in normal skin and hypertrophic scar.* 1997. **14**(2): p. 162-169.
47. Almine, J.F., et al., *Elastin sequences trigger transient proinflammatory responses by human dermal fibroblasts.* The FASEB Journal, 2013. **27**(9): p. 3455-3465.
48. Pastar, I., et al., *Epithelialization in wound healing: a comprehensive review.* Advances in wound care, 2014. **3**(7): p. 445-464.
49. Freedberg, I.M., et al., *Keratins and the Keratinocyte Activation Cycle.* Journal of Investigative Dermatology, 2001. **116**(5): p. 633-640.
50. Gniadecki, R., *Regulation of Keratinocyte Proliferation.* General Pharmacology: The Vascular System, 1998. **30**(5): p. 619-622.
51. Gantwerker, E.A. and D.B. Hom, *Skin: histology and physiology of wound healing.* Clinics in plastic surgery, 2012. **39**(1): p. 85-97.
52. Candi, E., R. Schmidt, and G. Melino, *The cornified envelope: a model of cell death in the skin.* Nature Reviews Molecular Cell Biology, 2005. **6**: p. 328.
53. Mejia, A.J., et al., *Intracellular signaling pathways involved in the release of IL-4 and VEGF from human keratinocytes by activation of kinin B 1 receptor: functional relevance to angiogenesis.* Archives of dermatological research, 2015. **307**(9): p. 803-817.
54. Pendsey, S.P., *Understanding diabetic foot.* International journal of diabetes in developing countries, 2010. **30**(2): p. 75.

55. Allan Boike, D., Michael Maier,Daniel Logan, DPM, *Prevention and Treatment of Leg and Foot Ulcers in Diabetes Mellitus.* Cleveland Clinic 2010.
56. Masters, K.S.B., et al., *Effects of nitric oxide releasing poly (vinyl alcohol) hydrogel dressings on dermal wound healing in diabetic mice.* Wound Repair and regeneration, 2002. **10**(5): p. 286-294.
57. Brownlee, M., *Biochemistry and molecular cell biology of diabetic complications.* Nature, 2001. **414**(6865): p. 813.
58. Pacher, P., J.S. Beckman, and L. Liaudet, *Nitric oxide and peroxynitrite in health and disease.* Physiol Rev, 2007. **87**(1): p. 315-424.
59. Morgan, M.J. and Z.-g.J.C.r. Liu, *Crosstalk of reactive oxygen species and NF-κB signaling.* 2011. **21**(1): p. 103.
60. Liu, T., et al., *NF-κB signaling in inflammation.* 2017. **2**: p. 17023.
61. Patel, S. and D. Santani, *Role of NF-κB in the pathogenesis of diabetes and its associated complications.* Pharmacological Reports, 2009. **61**(4): p. 595-603.
62. Schmidt, A.M., et al., *Activation of receptor for advanced glycation end products: a mechanism for chronic vascular dysfunction in diabetic vasculopathy and atherosclerosis.* Circulation research, 1999. **84**(5): p. 489-497.
63. Bierhaus, A., et al., *Diabetes-associated sustained activation of the transcription factor nuclear factor-κB.* Diabetes, 2001. **50**(12): p. 2792-2808.
64. Singh, V.P., et al., *Advanced glycation end products and diabetic complications.* The Korean Journal of Physiology & Pharmacology, 2014. **18**(1): p. 1-14.
65. Schramm, J.C., T. Dinh, and A. Veves, *Microvascular changes in the diabetic foot.* The international journal of lower extremity wounds, 2006. **5**(3): p. 149-159.
66. Blakytny, R. and E. Jude, *The molecular biology of chronic wounds and delayed healing in diabetes.* Diabetic Medicine, 2006. **23**(6): p. 594-608.
67. Barnea, Y., J. Weiss, and E. Gur, *A review of the applications of the hydrofiber dressing with silver (Aquacel Ag) in wound care.* Therapeutics and clinical risk management, 2010. **6**: p. 21-27.
68. Biglari, B., et al., *Multicentre prospective observational study on professional wound care using honey (Medihoney™).* International Wound Journal, 2013. **10**(3): p. 252-259.
69. Dhivya, S., V.V. Padma, and E. Santhini, *Wound dressings - a review.* BioMedicine, 2015. **5**(4): p. 22-22.
70. Brett, D., *A review of collagen and collagen-based wound dressings.* Wounds, 2008. **20**(12): p. 347-356.
71. Kavitha, K.V., et al., *Choice of wound care in diabetic foot ulcer: A practical approach.* World journal of diabetes, 2014. **5**(4): p. 546-556.
72. Marisa, T., *When Wounds Won't Heal, Therapies Spread-To The Tune of $5 Billion 2017.* 2017.
73. Murad, F., *Nitric oxide and cyclic GMP in cell signaling and drug development.* New England Journal of Medicine, 2006. **355**(19): p. 2003-2011.
74. Feelisch, M. and J. Stamler, *Methods in nitric oxide research*. 1996: Wiley-Blackwell.

75. Arnold, W.P., R. Aldred, and F. Murad, *Cigarette smoke activates guanylate cyclase and increases guanosine 3',5'-monophosphate in tissues.* Science, 1977. **198**(4320): p. 934.
76. Ignarro, L.J., *Nitric Oxide: A Unique Endogenous Signaling Molecule in Vascular Biology (Nobel Lecture).* Angewandte Chemie International Edition, 1999. **38**(13-14): p. 1882-1892.
77. Cho, H.J., et al., *Calmodulin is a subunit of nitric oxide synthase from macrophages.* The Journal of Experimental Medicine, 1992. **176**(2): p. 599-604.
78. Förstermann, U. and W.C. Sessa, *Nitric oxide synthases: regulation and function.* European heart journal, 2012. **33**(7): p. 829-837d.
79. Heck, D.E., et al., *Epidermal growth factor suppresses nitric oxide and hydrogen peroxide production by keratinocytes. Potential role for nitric oxide in the regulation of wound healing.* Journal of Biological Chemistry, 1992. **267**(30): p. 21277-21280.
80. Cals-Grierson, M.-M. and A. Ormerod, *Nitric oxide function in the skin.* Nitric oxide, 2004. **10**(4): p. 179-193.
81. Frank, S., et al., *Induction of inducible nitric oxide synthase and its corresponding tetrahydrobiopterin-cofactor-synthesizing enzyme GTP-cyclohydrolase I during cutaneous wound repair.* Journal of investigative dermatology, 1998. **111**(6): p. 1058-1064.
82. Sirsjö, A., et al., *Increased expression of inducible nitric oxide synthase in psoriatic skin and cytokine-stimulated cultured keratinocytes.* British Journal of Dermatology, 1996. **134**(4): p. 643-648.
83. Stallmeyer, B., et al., *The Function of Nitric Oxide in Wound Repair: Inhibition of Inducible Nitric Oxide-Synthase Severely Impairs Wound Reepithelialization.* Journal of Investigative Dermatology, 1999. **113**(6): p. 1090-1098.
84. Dhaunsi, G.S. and P.T. Ozand, *Nitric oxide promotes mitogen-induced dna synthesis in human dermal fibroblasts through cGMP.* Clinical and Experimental Pharmacology and Physiology, 2004. **31**(1-2): p. 46-49.
85. Witte, M.B. and A. Barbul, *Role of nitric oxide in wound repair.* The American Journal of Surgery, 2002. **183**(4): p. 406-412.
86. Marshall, H.E. and J.S. Stamler, *Inhibition of NF-κB by S-Nitrosylation.* Biochemistry, 2001. **40**(6): p. 1688-1693.
87. Ridnour, L.A., et al., *Nitric oxide regulates matrix metalloproteinase-9 activity by guanylyl-cyclase-dependent and -independent pathways.* Proceedings of the National Academy of Sciences of the United States of America, 2007. **104**(43): p. 16898-16903.
88. Soneja, A., M. Drews, and T.J.P.R. Malinski, *Role of nitric oxide, nitroxidative and oxidative stress in wound healing.* 2005. **57**: p. 108.
89. FRANK, S., et al., *Nitric oxide triggers enhanced induction of vascular endothelial growth factor expression in cultured keratinocytes (HaCaT) and during cutaneous wound repair.* The FASEB Journal, 1999. **13**(14): p. 2002-2014.
90. Thomas, D.D., et al., *Hypoxic inducible factor 1alpha, extracellular signal-regulated kinase, and p53 are regulated by distinct threshold concentrations of nitric oxide.* Proc Natl Acad Sci U S A, 2004. **101**(24): p. 8894-9.

91. Weller, R., *Nitric oxide: a key mediator in cutaneous physiology.* Clinical and Experimental Dermatology, 2003. **28**(5): p. 511-514.
92. Stancic, A., et al., *The role of nitric oxide in diabetic skin (patho)physiology.* Mechanisms of Ageing and Development, 2018. **172**: p. 21-29.
93. Ikeyama, K., et al., *Neuronal Nitric Oxide Synthase in Epidermis Is Involved in Cutaneous Circulatory Response to Mechanical Stimulation.* Journal of Investigative Dermatology, 2010. **130**(4): p. 1158-1166.
94. Roméro-Graillet, C., et al., *Ultraviolet B radiation acts through the nitric oxide and cGMP signal transduction pathway to stimulate melanogenesis in human melanocytes.* Journal of Biological Chemistry, 1996. **271**(45): p. 28052-28056.
95. Roméro-Graillet, C., et al., *Nitric oxide produced by ultraviolet-irradiated keratinocytes stimulates melanogenesis.* The Journal of clinical investigation, 1997. **99**(4): p. 635-642.
96. He, W., et al., *Nitric Oxide and Oxidative Stress-Mediated Cardiovascular Functionality: From Molecular Mechanism to Cardiovascular Disease*, in *Vascular Biology*. 2019, IntechOpen.
97. Shao, D., et al., *Redox modification of cell signaling in the cardiovascular system.* Journal of molecular and cellular cardiology, 2012. **52**(3): p. 550-558.
98. Bedard, K. and K.-H. Krause, *The NOX family of ROS-generating NADPH oxidases: physiology and pathophysiology.* Physiological reviews, 2007. **87**(1): p. 245-313.
99. Veal, E.A., A.M. Day, and B.A. Morgan, *Hydrogen Peroxide Sensing and Signaling.* Molecular Cell, 2007. **26**(1): p. 1-14.
100. Kanta, J., *The role of hydrogen peroxide and other reactive oxygen species in wound healing.* Acta Medica (Hradec Kralove), 2011. **54**(3): p. 97-101.
101. Reth, M., *Hydrogen peroxide as second messenger in lymphocyte activation.* Nature immunology, 2002. **3**(12): p. 1129.
102. Cohen, G. and R.E. Heikkila, *The generation of hydrogen peroxide, superoxide radical, and hydroxyl radical by 6-hydroxydopamine, dialuric acid, and related cytotoxic agents.* Journal of Biological Chemistry, 1974. **249**(8): p. 2447-2452.
103. Phaniendra, A., D.B. Jestadi, and L. Periyasamy, *Free Radicals: Properties, Sources, Targets, and Their Implication in Various Diseases.* Indian Journal of Clinical Biochemistry, 2015. **30**(1): p. 11-26.
104. Arisawa, S., et al., *EFFECT OF THE HYDROXYL RADICAL ON FIBROBLAST-MEDIATED COLLAGEN REMODELLING IN VITRO.* Clinical and Experimental Pharmacology and Physiology, 1996. **23**(3): p. 222-228.
105. Bergendi, L., et al., *Chemistry, physiology and pathology of free radicals.* Life Sciences, 1999. **65**(18): p. 1865-1874.
106. Russwurm, M. and D. Koesling, *NO activation of guanylyl cyclase.* The EMBO journal, 2004. **23**(22): p. 4443-4450.
107. Lai, T.S., et al., *Calcium Regulates S-Nitrosylation, Denitrosylation, and Activity of Tissue Transglutaminase.* Biochemistry, 2001. **40**(16): p. 4904-4910.
108. Friederich, M., P. Hansell, and F. Palm, *Diabetes, Oxidative Stress, Nitric Oxide and Mitochondria Function.* Current Diabetes Reviews, 2009. **5**(2): p. 120-144.

109. Jiang, Z.L., et al., *S-nitrosylation of caspase-3 is the mechanism by which adhesion fibroblasts manifest lower apoptosis.* Wound repair and regeneration : official publication of the Wound Healing Society [and] the European Tissue Repair Society, 2009. **17**(2): p. 224-229.
110. Van der Veen, B.S., M.P. de Winther, and P. Heeringa, *Myeloperoxidase: molecular mechanisms of action and their relevance to human health and disease.* Antioxidants & redox signaling, 2009. **11**(11): p. 2899-2937.
111. Sies, H., et al., *Glutathione peroxidase protects against peroxynitrite-mediated oxidations a new function for selenoproteins as peroxynitrite reductase.* Journal of Biological Chemistry, 1997. **272**(44): p. 27812-27817.
112. Pacher, P., J.S. Beckman, and L. Liaudet, *Nitric oxide and peroxynitrite in health and disease.* Physiological reviews, 2007. **87**(1): p. 315-424.
113. Eich, R.F., et al., *Mechanism of NO-induced oxidation of myoglobin and hemoglobin.* 1996. **35**(22): p. 6976-6983.
114. Ignarro, L.J., et al., *Oxidation of nitric oxide in aqueous solution to nitrite but not nitrate: comparison with enzymatically formed nitric oxide from L-arginine.* Proceedings of the National Academy of Sciences of the United States of America, 1993. **90**(17): p. 8103-8107.
115. Pacher, P., et al., *Role of nitrosative stress and peroxynitrite in the pathogenesis of diabetic complications. Emerging new therapeutical strategies.* Current medicinal chemistry, 2005. **12**(3): p. 267-275.
116. Xu, J., et al., *Proteasome-Dependent Degradation of Guanosine 5′-Triphosphate Cyclohydrolase I Causes Tetrahydrobiopterin Deficiency in Diabetes Mellitus.* Circulation, 2007. **116**(8): p. 944-953.
117. Roustit, M., et al., *Microvascular Changes in the Diabetic Foot*, in *The Diabetic Foot: Medical and Surgical Management*, A. Veves, J.M. Giurini, and R.J. Guzman, Editors. 2018, Springer International Publishing: Cham. p. 173-188.
118. Alavi, A., et al., *Diabetic foot ulcers: Part I. Pathophysiology and prevention.* Journal of the American Academy of Dermatology, 2014. **70**(1): p. 1.e1-1.e18.
119. Castilla, D.M., Z.-J. Liu, and O.C. Velazquez, *Oxygen: Implications for Wound Healing.* Advances in wound care, 2012. **1**(6): p. 225-230.
120. Olson, N. and A. van der Vliet, *Interactions between nitric oxide and hypoxia-inducible factor signaling pathways in inflammatory disease.* Nitric oxide : biology and chemistry, 2011. **25**(2): p. 125-137.
121. Brüne, B. and J. Zhou, *Nitric oxide and superoxide: interference with hypoxic signaling.* Cardiovascular research, 2007. **75**(2): p. 275-282.
122. Galván-Peña, S. and L.A. O'Neill, *Metabolic reprograming in macrophage polarization.* Frontiers in immunology, 2014. **5**: p. 420.
123. Catrina, S.-B., et al., *Hyperglycemia regulates hypoxia-inducible factor-1α protein stability and function.* Diabetes, 2004. **53**(12): p. 3226-3232.
124. Jazayeri, L., et al., *Diabetes increases p53-mediated apoptosis following ischemia.* Plastic and reconstructive surgery, 2008. **121**(4): p. 1135-1143.
125. Agani, F.H., et al., *Role of nitric oxide in the regulation of HIF-1α expression during hypoxia.* American Journal of Physiology-Cell Physiology, 2002. **283**(1): p. C178-C186.

126. Ceriello, A., et al., *Detection of nitrotyrosine in the diabetic plasma: evidence of oxidative stress.* Diabetologia, 2001. **44**(7): p. 834-838.
127. Jankovic, A., et al., *Targeting the superoxide/nitric oxide ratio by L-arginine and SOD mimic in diabetic rat skin.* Free radical research, 2016. **50**(sup1): p. S51-S63.
128. Tie, L., et al., *Ganoderma lucidum polysaccharide accelerates refractory wound healing by inhibition of mitochondrial oxidative stress in type 1 diabetes.* Cellular Physiology and Biochemistry, 2012. **29**(3-4): p. 583-594.
129. Pfeiffer, S., et al., *Metabolic fate of peroxynitrite in aqueous solution Reaction with nitric oxide and pH-dependent decomposition to nitrite and oxygen in a 2: 1 stoichiometry.* Journal of Biological Chemistry, 1997. **272**(6): p. 3465-3470.
130. Cosentino, F., et al., *High glucose increases nitric oxide synthase expression and superoxide anion generation in human aortic endothelial cells.* Circulation, 1997. **96**(1): p. 25-8.
131. Hoshiyama, M., et al., *Effect of high glucose on nitric oxide production and endothelial nitric oxide synthase protein expression in human glomerular endothelial cells.* Nephron Experimental Nephrology, 2003. **95**(2): p. e62-e68.
132. Hwang, J.-S., et al., *Lipopolysaccharide (LPS)-stimulated iNOS induction is increased by glucosamine under normal glucose conditions but is inhibited by glucosamine under high glucose conditions in macrophage cells.* Journal of Biological Chemistry, 2017. **292**(5): p. 1724-1736.
133. Houreld, N.N., P.R. Sekhejane, and H. Abrahamse, *Irradiation at 830 nm stimulates nitric oxide production and inhibits pro-inflammatory cytokines in diabetic wounded fibroblast cells.* Lasers in surgery and medicine, 2010. **42**(6): p. 494-502.
134. Wadham, C., et al., *High glucose attenuates protein S-nitrosylation in endothelial cells: role of oxidative stress.* Diabetes, 2007. **56**(11): p. 2715-2721.
135. Lee, P.C., et al., *Impaired wound healing and angiogenesis in eNOS-deficient mice.* American Journal of Physiology-Heart and Circulatory Physiology, 1999. **277**(4): p. H1600-H1608.
136. Adela, R., et al., *Hyperglycaemia enhances nitric oxide production in diabetes: a study from South Indian patients.* PloS one, 2015. **10**(4): p. e0125270.
137. Yang, Y., et al., *In situ eNOS/NO up-regulation—a simple and effective therapeutic strategy for diabetic skin ulcer.* Scientific Reports, 2016. **6**: p. 30326.
138. Saidian, M., et al., *Characterisation of impaired wound healing in a preclinical model of induced diabetes using wide-field imaging and conventional immunohistochemistry assays.* International Wound Journal, 2019. **16**(1): p. 144-152.
139. EARLE, K.A., et al., *Defective Nitric Oxide Production and Functional Renal Reserve in Patients with Type 2 Diabetes Who Have Microalbuminuria of African and Asian Compared with White Origin.* Journal of the American Society of Nephrology, 2001. **12**(10): p. 2125-2130.
140. Suarez-Pinzon, W.L., et al., *An inhibitor of inducible nitric oxide synthase and scavenger of peroxynitrite prevents diabetes development in NOD mice.* Journal of autoimmunity, 2001. **16**(4): p. 449-455.

141. Zhan, R., et al., *Nitric oxide enhances keratinocyte cell migration by regulating Rho GTPase via cGMP-PKG signalling.* PloS one, 2015. **10**(3): p. e0121551.
142. Zhan, R., et al., *Nitric oxide promotes epidermal stem cell migration via cGMP-Rho GTPase signalling.* Scientific reports, 2016. **6**: p. 30687.
143. La Torre, C., et al., *Nitric Oxide Chemical Donor Affects the Early Phases of In Vitro Wound Healing Process.* Journal of Cellular Physiology, 2016. **231**(10): p. 2185-2195.
144. Masters, K.S.B., et al., *Effects of nitric oxide releasing poly(vinyl alcohol) hydrogel dressings on dermal wound healing in diabetic mice.* Wound Repair and Regeneration, 2002. **10**(5): p. 286-294.
145. Han, G., et al., *Nitric Oxide–Releasing Nanoparticles Accelerate Wound Healing by Promoting Fibroblast Migration and Collagen Deposition.* The American Journal of Pathology, 2012. **180**(4): p. 1465-1473.
146. Kang, Y., et al., *Nitric oxide-releasing polymer incorporated ointment for cutaneous wound healing.* Journal of Controlled Release, 2015. **220**: p. 624-630.
147. Zhou, X., et al., *Functional poly (ε-caprolactone)/chitosan dressings with nitric oxide-releasing property improve wound healing.* Acta biomaterialia, 2017. **54**: p. 128-137.
148. Blecher, K., et al., *Nitric oxide-releasing nanoparticles accelerate wound healing in NOD-SCID mice.* Nanomedicine: Nanotechnology, Biology and Medicine, 2012. **8**(8): p. 1364-1371.
149. Edmonds, M.E., et al., *Multicenter, randomized controlled, observer-blinded study of a nitric oxide generating treatment in foot ulcers of patients with diabetes—ProNOx1 study.* Wound Repair and Regeneration, 2018. **26**(2): p. 228-237.
150. Silva, S.Y., et al., *Double blind, randomized, placebo controlled clinical trial for the treatment of diabetic foot ulcers, using a nitric oxide releasing patch: PATHON.* Trials, 2007. **8**(1): p. 26.
151. Hunter, R.A., et al., *Inaccuracies of nitric oxide measurement methods in biological media.* Anal Chem, 2013. **85**(3): p. 1957-63.
152. He, W. and M.C. Frost, *CellNO trap: Novel device for quantitative, real-time, direct measurement of nitric oxide from cultured RAW 267.4 macrophages.* Redox Biol, 2016. **8**: p. 383-97.
153. He, W. and M.C. Frost, *Direct measurement of actual levels of nitric oxide (NO) in cell culture conditions using soluble NO donors.* Redox biology, 2016. **9**: p. 1-14.
154. Shukla, V., et al., *Evaluation of pH measurement as a method of wound assessment.* Journal of wound care, 2007. **16**(7): p. 291-294.
155. Yuen, K.C., N.R. Baker, and G. Rayman, *Treatment of chronic painful diabetic neuropathy with isosorbide dinitrate spray: a double-blind placebo-controlled cross-over study.* Diabetes care, 2002. **25**(10): p. 1699-1703.
156. Taylor, A.L., et al., *Combination of Isosorbide Dinitrate and Hydralazine in Blacks with Heart Failure.* New England Journal of Medicine, 2004. **351**(20): p. 2049-2057.
157. García-Álvarez, Y., J.L. Lázaro-Martínez, and R.J. Molines-Barroso, *Reflections on the effects of nitric oxide produced by a new dressing in the local management*

of diabetic foot ulcers. Annals of translational medicine, 2018. **6**(Suppl 2): p. S101-S101.
158. Tracy, L.E., R.A. Minasian, and E.J. Caterson, *Extracellular Matrix and Dermal Fibroblast Function in the Healing Wound.* Advances in wound care, 2016. **5**(3): p. 119-136.
159. Baum, C.L. and C.J. Arpey, *Normal cutaneous wound healing: clinical correlation with cellular and molecular events.* Dermatologic surgery, 2005. **31**(6): p. 674-686.
160. Chen, M., et al., *Effect of UVA irradiation on proliferation and NO/iNOS system of human skin fibroblast.* Zhong nan da xue xue bao. Yi xue ban= Journal of Central South University. Medical sciences, 2009. **34**(8): p. 705-711.
161. Schäffer, M.R., et al., *Diabetes-impaired healing and reduced wound nitric oxide synthesis: A possible pathophysiologic correlation.* Surgery, 1997. **121**(5): p. 513-519.
162. Houreld, N. and H. Abrahamse, *Low-Intensity Laser Irradiation Stimulates Wound Healing in Diabetic Wounded Fibroblast Cells (WS1).* Diabetes Technology & Therapeutics, 2010. **12**(12): p. 971-978.
163. Enoch, S. and D.J. Leaper, *Basic science of wound healing.* Surgery (Oxford), 2008. **26**(2): p. 31-37.
164. Quan, T., et al., *CCN1 contributes to skin connective tissue aging by inducing age-associated secretory phenotype in human skin dermal fibroblasts.* Journal of cell communication and signaling, 2011. **5**(3): p. 201-207.
165. Quan, T., et al., *Cysteine-rich protein 61 (CCN1) mediates replicative senescence-associated aberrant collagen homeostasis in human skin fibroblasts.* Journal of cellular biochemistry, 2012. **113**(9): p. 3011-3018.
166. Tsou, P.-S., D. Khanna, and A.H. Sawalha, *Identification of Cysteine-Rich Angiogenic Inducer 61 as a Potential Antifibrotic and Proangiogenic Mediator in Scleroderma.* Arthritis & Rheumatology. **0**(0).
167. Chen, C.-C., N. Chen, and L.F. Lau, *The angiogenic factors Cyr61 and connective tissue growth factor induce adhesive signaling in primary human skin fibroblasts.* Journal of Biological Chemistry, 2001. **276**(13): p. 10443-10452.
168. Mansbridge, J.N., et al., *Growth factors secreted by fibroblasts: role in healing diabetic foot ulcers.* Diabetes, Obesity and Metabolism, 1999. **1**(5): p. 265-279.
169. Schneider, C.A., W.S. Rasband, and K.W. Eliceiri, *NIH Image to ImageJ: 25 years of image analysis.* Nature methods, 2012. **9**(7): p. 671.
170. Bradford, M.M., *A rapid and sensitive method for the quantitation of microgram quantities of protein utilizing the principle of protein-dye binding.* Analytical biochemistry, 1976. **72**(1-2): p. 248-254.
171. Kisselbach, L., et al., *CD90 Expression on human primary cells and elimination of contaminating fibroblasts from cell cultures.* Cytotechnology, 2009. **59**(1): p. 31-44.
172. Mosmann, T., *Rapid colorimetric assay for cellular growth and survival: application to proliferation and cytotoxicity assays.* Journal of immunological methods, 1983. **65**(1-2): p. 55-63.

173. Loots, M., *Fibroblasts derived from chronic diabetic ulcers differ in their response to stimulation with EGF, IGF-I, bFGF and PDGF-AB compared to controls.* European Journal of Cell Biology, 2002. **81**(3): p. 153-160.
174. Tracy, L.E., R.A. Minasian, and E. Caterson, *Extracellular matrix and dermal fibroblast function in the healing wound.* Advances in wound care, 2016. **5**(3): p. 119-136.
175. Brecher, P., *The fibroblast and nitric oxide*, in *Nitric Oxide and the Cardiovascular System*. 2000, Springer. p. 177-189.
176. Luo, J.D. and A.F. Chen, *Nitric oxide: a newly discovered function on wound healing.* Acta Pharmacol Sin, 2005. **26**(3): p. 259-64.
177. Grisham, M.B., D. Jourd'Heuil, and D.A. Wink, *I. Physiological chemistry of nitric oxide and its metabolites: implications in inflammation.* American Journal of Physiology-Gastrointestinal and Liver Physiology, 1999. **276**(2): p. G315-G321.
178. Thomas, D.D., et al., *The chemical biology of nitric oxide: implications in cellular signaling.* Free Radic Biol Med, 2008. **45**(1): p. 18-31.
179. Jorens, P.G., et al., *Synergism between interleukin-1ß and interferon-γ, an inducer of nitric oxide synthase, in rat lung fibroblasts.* European journal of pharmacology, 1992. **224**(1): p. 7-12.
180. Walton, D.M., S.D. Minton, and A.D. Cook, *The potential of transdermal nitric oxide treatment for diabetic peripheral neuropathy and diabetic foot ulcers.* Diabetes & Metabolic Syndrome: Clinical Research & Reviews, 2018.
181. Cosentino, F., et al., *High glucose increases nitric oxide synthase expression and superoxide anion generation in human aortic endothelial cells.* Circulation, 1997. **96**(1): p. 25-28.
182. Ii, M., et al., *Neuronal nitric oxide synthase mediates statin-induced restoration of vasa nervorum and reversal of diabetic neuropathy.* Circulation, 2005. **112**(1): p. 93-102.
183. Halliwell, B., *Cell culture, oxidative stress, and antioxidants: avoiding pitfalls.* Biomedical journal, 2014. **37**(3): p. 99.
184. Kopincová, J., A. Púzserová, and I. Bernátová, *Biochemical aspects of nitric oxide synthase feedback regulation by nitric oxide.* Interdisciplinary toxicology, 2011. **4**(2): p. 63-68.
185. Guzik, T., R. Korbut, and T. Adamek-Guzik, *Nitric oxide and superoxide in inflammation.* J physiol pharmacol, 2003. **54**(4): p. 469-487.
186. Schwentker, A., et al., *Nitric oxide and wound repair: role of cytokines?* Nitric oxide, 2002. **7**(1): p. 1-10.
187. Villalobo, A., *Nitric oxide and cell proliferation.* The FEBS journal, 2006. **273**(11): p. 2329-2344.
188. Xuan, Y.H., et al., *High-glucose inhibits human fibroblast cell migration in wound healing via repression of bFGF-regulating JNK phosphorylation.* PloS one, 2014. **9**(9): p. e108182.
189. Shi, H.P., et al., *The role of iNOS in wound healing.* Surgery, 2001. **130**(2): p. 225-229.

190. Coriat, P., et al., *Prévention de l'ischémie myocardique per-opératoire Emploi d'une perfusion continue de trinitrine.* Annales Françaises d'Anesthésie et de Réanimation, 1982. **1**(1): p. 47-51.
191. Payne, D.N.R., et al., *Relationship between Exhaled Nitric Oxide and Mucosal Eosinophilic Inflammation in Children with Difficult Asthma, after Treatment with Oral Prednisolone.* American Journal of Respiratory and Critical Care Medicine, 2001. **164**(8): p. 1376-1381.
192. Houreld, N.N., P.R. Sekhejane, and H. Abrahamse, *Irradiation at 830 nm stimulates nitric oxide production and inhibits pro-inflammatory cytokines in diabetic wounded fibroblast cells.* Lasers in Surgery and Medicine, 2010. **42**(6): p. 494-502.
193. García-Álvarez, Y., J.L. Lázaro-Martínez, and R.J. Molines-Barroso, *Reflections on the effects of nitric oxide produced by a new dressing in the local management of diabetic foot ulcers.* Annals of translational medicine, 2018. **6**(Suppl 2).
194. Bernatchez, S.F., et al., *Nitric oxide levels in wound fluid may reflect the healing trajectory.* Wound Repair and Regeneration, 2013. **21**(3): p. 410-417.
195. Lee, R.H., et al., *Nitric Oxide in the Healing Wound: A Time-Course Study.* Journal of Surgical Research, 2001. **101**(1): p. 104-108.
196. Zandifar, E., et al., *The effect of captopril on impaired wound healing in experimental diabetes.* International journal of endocrinology, 2012. **2012**.
197. Vangipuram, M., et al., *Skin punch biopsy explant culture for derivation of primary human fibroblasts.* JoVE (Journal of Visualized Experiments), 2013(77): p. e3779.
198. Gilliam, M.B., et al., *A spectrophotometric assay for nitrate using NADPH oxidation by Aspergillus nitrate reductase.* Analytical biochemistry, 1993. **212**(2): p. 359-365.
199. Stanley, A.C., et al., *Reduced growth of dermal fibroblasts from chronic venous ulcers can be stimulated with growth factors.* Journal of vascular surgery, 1997. **26**(6): p. 994-1001.
200. Mendez, M.V., et al., *Fibroblasts cultured from venous ulcers display cellular characteristics of senescence.* Journal of vascular surgery, 1998. **28**(5): p. 876-883.
201. Caley, M., et al., *Development and Characterisation of a Human Chronic Skin Wound Cell Line—Towards an Alternative for Animal Experimentation.* International journal of molecular sciences, 2018. **19**(4): p. 1001.
202. Loots, M.A., et al., *Fibroblasts derived from chronic diabetic ulcers differ in their response to stimulation with EGF, IGF-I, bFGF and PDGF-AB compared to controls.* European journal of cell biology, 2002. **81**(3): p. 153-160.
203. Soneja, A., M. Drews, and T. Malinski, *Role of nitric oxide, nitroxidative and oxidative stress in wound healing.* Pharmacological reports, 2005. **57**: p. 108.
204. Wang, R., et al., *Nitric oxide synthase expression and nitric oxide production are reduced in hypertrophic scar tissue and fibroblasts.* Journal of investigative dermatology, 1997. **108**(4): p. 438-444.
205. Boykin Jr, J., *Prediction of diabetes impaired wound healing by urinary nitrate assay*. 2002, Google Patents.

206. Debats, I.B.J.G., et al., *Infected Chronic Wounds Show Different Local and Systemic Arginine Conversion Compared With Acute Wounds.* Journal of Surgical Research, 2006. **134**(2): p. 205-214.
207. Hunter, R.A., et al., *Inaccuracies of nitric oxide measurement methods in biological media.* Analytical chemistry, 2013. **85**(3): p. 1957-1963.
208. Bryan, N.S. and M.B. Grisham, *Methods to detect nitric oxide and its metabolites in biological samples.* Free Radical Biology and Medicine, 2007. **43**(5): p. 645-657.
209. Kumar, P. and T.M. Honnegowda, *Effect of limited access dressing on surface pH of chronic wounds.* Plast. Aesthet. Res, 2015. **2**: p. 257-260.
210. Lucas, T., et al., *Differential roles of macrophages in diverse phases of skin repair.* The Journal of Immunology, 2010. **184**(7): p. 3964-3977.
211. Krzyszczyk, P., et al., *The Role of Macrophages in Acute and Chronic Wound Healing and Interventions to Promote Pro-wound Healing Phenotypes.* Frontiers in physiology, 2018. **9**: p. 419-419.
212. Ploeger, D.T., et al., *Cell plasticity in wound healing: paracrine factors of M1/M2 polarized macrophages influence the phenotypical state of dermal fibroblasts.* Cell Communication and Signaling, 2013. **11**(1): p. 29.
213. Hu, M.S., et al., *Delivery of monocyte lineage cells in a biomimetic scaffold enhances tissue repair.* JCI insight, 2017. **2**(19): p. e96260.
214. Noda, T. and F. Amano, *Differences in nitric oxide synthase activity in a macrophage-like cell line, RAW264. 7 cells, treated with lipopolysaccharide (LPS) in the presence or absence of interferon-γ (IFN-γ): possible heterogeneity of iNOS activity.* The Journal of Biochemistry, 1997. **121**(1): p. 38-46.
215. Taciak, B., et al., *Evaluation of phenotypic and functional stability of RAW 264.7 cell line through serial passages.* PloS one, 2018. **13**(6): p. e0198943-e0198943.
216. Tseng, C.-C., et al., *Decreased production of nitric oxide by lps-treated J774 macrophages in high-glucose medium.* Life Sciences, 1997. **60**(7): p. PL99-PL106.
217. Hill, J.R., et al., *Hyperglycemic levels of glucose inhibit interleukin 1 release from RAW 264.7 murine macrophages by activation of protein kinase C.* Journal of Biological Chemistry, 1998. **273**(6): p. 3308-3313.
218. Sharma, K., et al., *Enhanced expression of inducible nitric oxide synthase in murine macrophages and glomerular mesangial cells by elevated glucose levels: possible mediation via protein kinase C.* Biochemical and biophysical research communications, 1995. **207**(1): p. 80-88.
219. Lu, C.-P., et al., *Improvement of hyperglycemia in a murine model of insulin resistance and high glucose- and inflammasome-mediated IL-1β expressions in macrophages by silymarin.* Chemico-Biological Interactions, 2018. **290**: p. 12-18.
220. Hua, K.-F., et al., *High glucose increases nitric oxide generation in lipopolysaccharide-activated macrophages by enhancing activity of protein kinase C-α/δ and NF-κB.* Inflammation Research, 2012. **61**(10): p. 1107-1116.
221. Frank, S., et al., *Nitric oxide drives skin repair: novel functions of an established mediator.* Kidney international, 2002. **61**(3): p. 882-888.

222. Srinivasan, S., et al., *Hyperglycaemia-induced superoxide production decreases eNOS expression via AP-1 activation in aortic endothelial cells.* Diabetologia, 2004. **47**(10): p. 1727-1734.
223. Bice, J.S., et al., *Nitric oxide treatments as adjuncts to reperfusion in acute myocardial infarction: a systematic review of experimental and clinical studies.* Basic research in cardiology, 2016. **111**(2): p. 23-23.
224. Gierke, G.E., M. Nielsen, and M.C. Frost, *S-Nitroso-N-acetyl-D-penicillamine covalently linked to polydimethylsiloxane (SNAP-PDMS) for use as a controlled photoinitiated nitric oxide release polymer.* Science and technology of advanced materials, 2011. **12**(5): p. 055007-055007.
225. Ruiz, J.L., J.D. Hutcheson, and E. Aikawa, *Cardiovascular calcification: current controversies and novel concepts.* Cardiovascular Pathology, 2015. **24**(4): p. 207-212.
226. Leopold, J.A., *Vascular calcification: mechanisms of vascular smooth muscle cell calcification.* Trends in cardiovascular medicine, 2015. **25**(4): p. 267-274.
227. Furukawa, K.-I., *Recent advances in research on human aortic valve calcification.* Journal of pharmacological sciences, 2014. **124**(2): p. 129-137.
228. Kanno, Y., et al., *Nitric oxide regulates vascular calcification by interfering with TGF-β signalling.* Cardiovascular research, 2007. **77**(1): p. 221-230.
229. Kennedy, J.A., et al., *Inhibition of calcifying nodule formation in cultured porcine aortic valve cells by nitric oxide donors.* European journal of pharmacology, 2009. **602**(1): p. 28-35.
230. Alsabeelah, N.F.N., *Vascular Calcification in Rat Cultured Smooth Muscle Cells: a Role for Nitric Oxide.* 2016.
231. He, W., *Systematic study of the biological effects of nitric oxide (NO) using innovative NO measurement and delivery systems.* 2015.
232. Änggård, E., *Nitric oxide: mediator, murderer, and medicine.* The Lancet, 1994. **343**(8907): p. 1199-1206.
233. Beckman, J.S. and W.H. Koppenol, *Nitric oxide, superoxide, and peroxynitrite: the good, the bad, and ugly.* American Journal of Physiology-Cell Physiology, 1996. **271**(5): p. C1424-C1437.

A Supplementary figures from Chapter 3

A.1 Western blot analysis

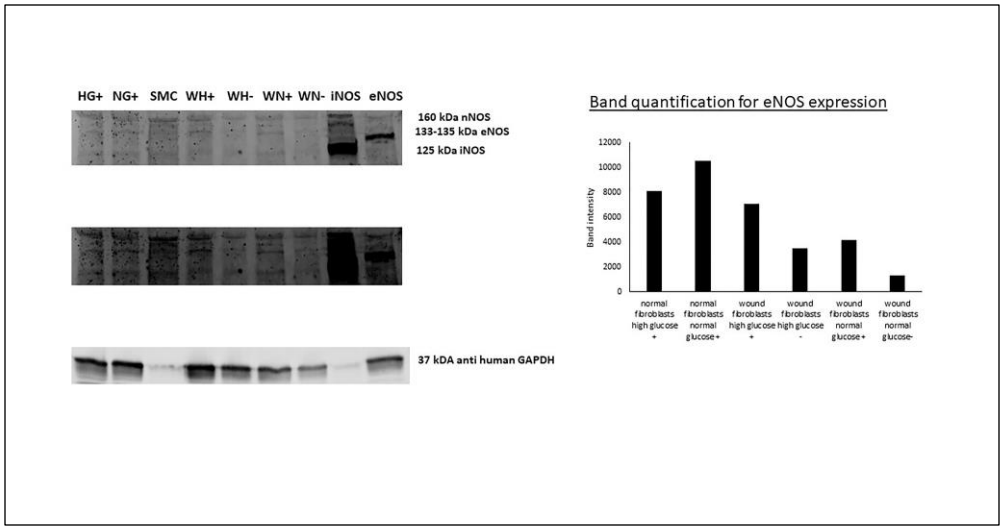

Figure A-1. Western blot analysis for eNOS protein in normal (**NG** and **HG**) and wound fibroblasts cultured in normal (**WN**) and high glucose (**WH**)in the absence (**-**) and presence (+) of stimulation. RAW 264.7 and human endothelial cells were used as positive controls for iNOS and eNOS respectively. MOVAS cell line was used as a negative control for eNOS. GAPDH was used as the housekeeping protein

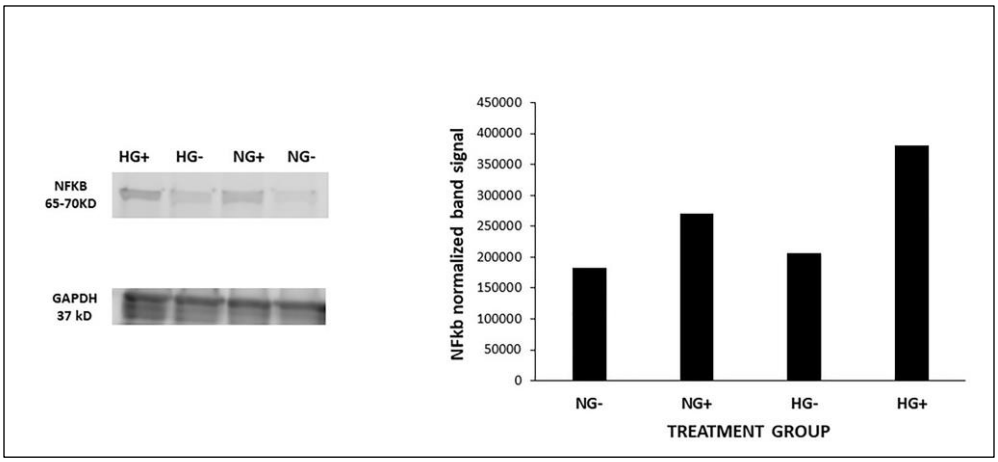

Figure A-2. Western blot analysis to determine NF-κβ protein in wound fibroblasts cultured in normal (**NG**) and high glucose (**HG**) in the absence (-) and presence (+) of stimulation

A.2 Supplementary figures for nitrate and nitrite measurements

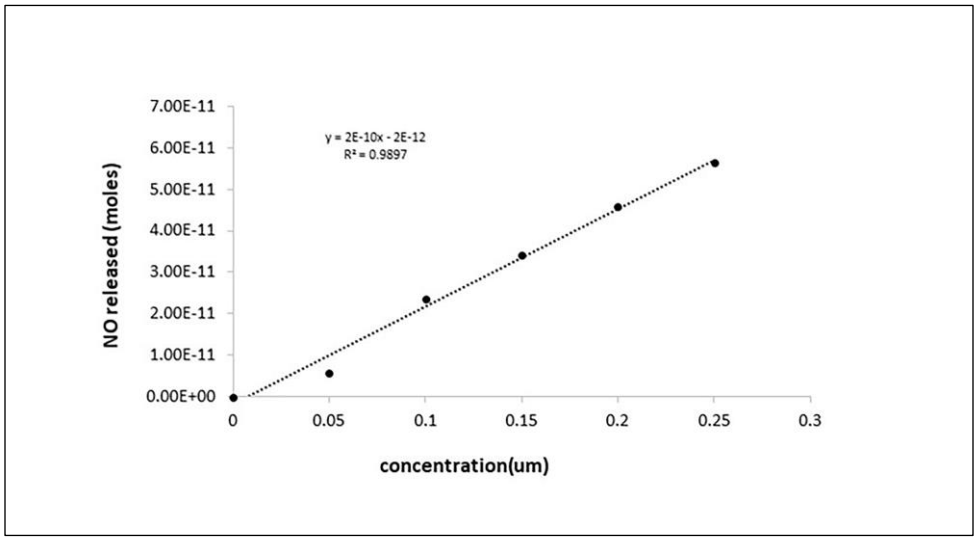

Figure A-3 Minimum sensitivity for the nitrite/nitrate measurements

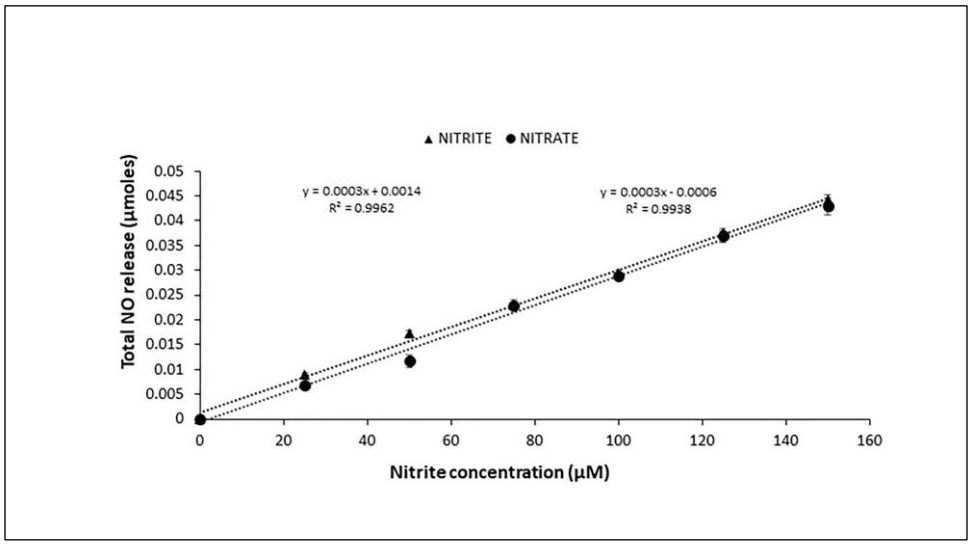

Figure A-4 Maximum sensitivity for the nitrite/nitrate measurements

B Copyright documentation

The document presented below shows that I obtained the rights to use the material presented in chapter 2

MDPI
Academic Open Access Publishing
since 1996

MDPI AG
Postfach
CH–4020 Basel
Switzerland

Tel. +41 61 683 77 34
Fax +41 61 302 89 18
www.mdpi.com

Terms of Use

§ 1 These Terms of Use govern the use of the MDPI websites or any other MDPI online services you access. This includes any updates or releases thereof. By using our online services, you are legally bound by and hereby consent to our Terms of Use and Privacy Policy. These Terms of Use form a contract between MDPI AG, registered at St. Alban-Anlage 66, 4052 Basel, Switzerland ("MDPI") and you as the user ("User"). These Terms of Use shall be governed by and construed in accordance with Swiss Law, applicable at the place of jurisdiction of MDPI in Basel, Switzerland.

§ 2 Unless otherwise stated, the website and affiliated online services are the property of MDPI and the copyright of the website belongs to MDPI or its licensors. You may not copy, hack or modify the website or online services, or falsely claim that some other site is associated with MDPI. MDPI is a registered brand protected by the Swiss Federal Institute of Intellectual Property.

§ 3 Unless otherwise stated, articles published on the MDPI websites are labeled as "Open Access" and licensed by the respective authors in accordance with the Creative Commons Attribution (CC-BY) license. Within the limitations mentioned in §4 of these Terms of Use, the "Open Access" license allows for unlimited distribution and reuse as long as appropriate credit is given to the original source and any changes made compared to the original are indicated.

§ 4 Some articles published on this website (especially articles labeled as "Review" or similar) may make use of copyrighted material for which the author(s) have obtained a reprint permission from the copyright holder. Usually such reprint permissions do not allow author(s) and/or MDPI to further license the copyrighted material. The licensing described in §3 of these terms and conditions are therefore not applicable to such kind of material enclosed within articles. It is the User's responsibility to identify reusability of material provided on this website, for which he may take direct contact with the authors of the article.

§ 5 You may register or otherwise create a user account, user name or password (your "Registration") that allows you to access or receive certain content and/or to participate or utilize certain features of our online service, including features in which you interact with us or other users. You represent and warrant that the information provided in your Registration is accurate to the best of your knowledge. You are responsible for the use of any password you create as part of your Registration and for maintaining its confidentiality, and you agree that MDPI may use this password to identify you. We reserve the right to deny, terminate or restrict your access to any content or feature reached via such Registration process for any reason, at our sole discretion. MDPI reserves the right to block or to terminate the User's access to the website at any time and without prior notice.

§ 6 The MDPI website and online services may provide links to other websites or external resources. As part of these Terms of Use, you acknowledge that MDPI is in not responsible for the availability of such external sites or resources, and that MDPI is not liable for any content, services, advertising, or materials available from such external sites or resources.